Inaugural Dissertation

submitted to the

Combined Faculties for the Natural Sciences and for Mathematics

of the Ruperto-Carola University of Heidelberg, Germany

for the degree of

Doctor of Natural Sciences

Presented by

BSc, BSc (Hons), MSc Reinhard Kai Liebers

Born in: Cologne, Germany

Oral-examination: December 11th, 2015

Dnmt2 in RNA methylation, RNA inheritance, and environmental responses in the mouse

Referees:
Prof. Dr. Frank Lyko
Dr. Brian Luke

Abstract

Dnmt2 is a highly conserved RNA methyltransferase that is responsible for cytosine-C5 methylation of C38 in the anticodon-loop of $tRNA^{AspGUC}$, $tRNA^{ValAAC}$, and $tRNA^{GlyGCC}$. This modification has been shown to contribute to tRNA integrity and function. Additionally, it was demonstrated that RNA-mediated inheritance in mice depends on the presence of Dnmt2.

Since the mechanistic role of Dnmt2 in many biological processes remains elusive, the aim of this thesis was to further functionally characterize Dnmt2 in the mouse. A special focus was set on tissues and cells which had a published $Dnmt2^{-/-}$ phenotype. Dnmt2 characterization thus concentrated on tissues and cells involved in inheritance, i.e. sperm as the transmitting cells and early embryos as the target.

Phenotypic characterization showed that relevant $Dnmt2^{-/-}$ tissues were morphologically indistinguishable from those of wild type mice. Sperm, testis, and embryonic tissues showed proper differentiation and tissue characteristics. However, high Dnmt2 expression in testis and sperm supported its role in inheritance. Due to Dnmt2's known role in RNA methylation, RNAs were analysed in depth in the relevant tissues. RNA-Seq experiments illustrated that RNA expression levels in sperm, testis, and embryonic samples showed only minor differences between wild type and $Dnmt2^{-/-}$. For RNAs that were further investigated, the potential differences did not appear to have an immediate effect on processes associated with these RNAs. Importantly, targeted bisulfite sequencing and Northern blots showed that Dnmt2 is responsible for tRNA methylation and stability in the male germline. Furthermore, a whole-transcriptome bisulfite sequencing approach confirmed that Dnmt2 specifically methylates $tRNA^{AspGUC}$, $tRNA^{ValAAC}$, and $tRNA^{GlyGCC}$, and most likely no other RNAs. The methylation and assurance of integrity of these tRNAs is thus suspected to play a pivotal role in RNA-mediated inheritance. For further functional characterization of Dnmt2, a screen of different physiological as well as non-physiological conditions in cell culture and live mice was carried out to define factors that regulate Dnmt2 activity. It was found that depriving cell cultures and live mice of the micronutrient queuine decreases C38 methylation of $tRNA^{AspGUC}$.

In conclusion, this thesis shows that Dnmt2 is a highly specific tRNA methyltransferase, which confers stability to tRNAs in sperm, and responds to environmental stimuli in mice.

Zusammenfassung

Dnmt2 is eine hochkonservierte RNA-Methyltransferase, welche Cytosin-C5 Methylierung an C38 der Anticodon-Loops von $tRNA^{AspGUC}$, $tRNA^{ValAAC}$ und $tRNA^{GlyGCC}$ vornimmt. Es wurde gezeigt, dass diese Modifikation zur Funktion und Integrität von tRNAs beiträgt. Des Weiteren wurde nachgewiesen, dass RNA-vermittelte Vererbung in Mäusen abhängig vom Vorhandensein von Dnmt2 ist.

Da die Funktion von Dnmt2 in verschiedenen biologischen Prozessen unklar ist, war das Ziel dieser Arbeit eine umfassende Charakterisierung von Dnmt2 in der Maus. Der Fokus der Analysen wurde auf Gewebe gelegt bei welchen bereits gezeigt wurde, dass ein Knockout von Dnmt2 zu einer phänotypischen Ausprägung führt. In der Dnmt2-abhängigen Vererbung von RNA spielen Spermien als Informationsträger und frühe Embryos als Informationsempfänger wichtige Rollen.

Die phänotypische Charakterisierung zeigte, dass die relevanten $Dnmt2^{-/-}$ Gewebe morphologisch nicht vom Wildtyp zu unterscheiden sind. Spermien, Hoden und embryonisches Gewebe zeigten normale Differenzierung und Gewebscharakteristiken. Die gezeigte hohe Expression von Dnmt2 in Hoden und Spermien spricht für die Beteiligung von Dnmt2 an Vererbungsvorgängen. Da bekannt ist, dass Dnmt2 bei RNA-Methylierungen eine Rolle spielt, wurden in den relevanten Geweben detaillierte RNA-Analysen durchgeführt. Die Ergebnisse der RNA-Sequenzierungen zeigten, dass sich die Expressionsmuster in Spermien, Hoden und Embryos zwischen Wildtyp und $Dnmt2^{-/-}$ nur marginal unterscheiden. Diese Unterschiede scheinen zudem keinen unmittelbaren Einfluss auf mit diesen RNAs assoziierte Prozesse zu haben. Interessanterweise zeigten gezielte Bisulfitsequenzierungen und Northern Blots, dass Dnmt2 für tRNA-Methylierung und -Stabilität in der männlichen Keimbahn verantwortlich ist. Zusätzlich bestätigte eine Transkriptom-weite Bisulfitsequenzierung, dass Dnmt2 spezifisch $tRNA^{AspGUC}$, $tRNA^{ValAAC}$ und $tRNA^{GlyGCC}$ methyliert und höchstwahrscheinlich keine weiteren Substrate hat. Die tRNA-methylierende und -stabilisierende Funktion von Dnmt2 spielt demnach eventuell eine Rolle in RNA-vermittelter Vererbung. Für eine tiefergehende Charakterisierung von Dnmt2 wurden in Zellkultur und in Mäusen diverse physiologische und nicht-physiologische Bedingungen überprüft, um Faktoren zu bestimmen, welche möglicherweise die Aktivität von

Dnmt2 regulieren. Es zeigte sich *in vitro* und *in vivo*, dass der Entzug des Nährstoffes Queuin zu einer verringerten Methylierung von $tRNA^{AspGUC}$ führt.

Zusammenfassend zeigt diese Arbeit, dass Dnmt2 eine hochspezifische tRNA-Methyltransferase ist, welche für tRNA-Stabilität in Spermien sorgt und auf äußere Einflüsse, wie die Abwesenheit bestimmter Nährstoffe, reagiert.

Table of Contents

1. List of abbreviations

µg	microgram
µL	microliter
µM	micromolar
A	adenosine
AdoHcy	S-Adenosyl-Homocystein
AdoMet	S-adenosyl-L-methionine
APB	acryloyl aminophenylboronic acid
APS	ammonium persulfate
Asp	aspartate
C	cytosine
CpG	cytosine guanosine dinucleotide
D. melanogaster	*Drosophila melanogaster*
DMEM	Dulbecco's Modified Eagle Medium
DNA	deoxyribonucleic acid
DNase	deoxyribonuclease
Dnmt	DNA methyltransferase
dNTP	deoxynucleotide triphosphate
EDTA	ethylendiamine tetraacetate
FCS	fetal calf serum
G	guanine
Gly	glycine
IAP	intracisternal A particle
IMDM	Iscove's Modified Dulbecco's Medium
Leu	leucine
LTR	long terminal repeat
m^5C	5-methylcytosine
m^6A	6-methylcytosine
mRNA	messenger RNA
NSun2	NOP2/Sun domain protein 2

ncRNA	non-coding RNA
nt	nucleotide
ORF	open reading frame
P/S	penicillin/streptomycin
piRNA	Piwi-interacting RNA
PNK	polynucleotide kinase
Q	queuosine
qRT-PCR	quantitative reverse transcriptase PCR
RNA	ribonucleic acid
rpm	revolutions per minute
RT	room temperature
SAH	S-Adenosyl-Homocystein
SAM	S-adenosyl-L-methionine
SCF	Stem Cell Factor
SDS-PAGE	sodium dodecyl sulfate polyacrylamide gel electrophoresis
T	thymin
TAE	tris acetate EDTA
TBE	tris borate EDTA
TEI	transgenerational epigenetic inheritance
TEMED	tetramethyl ethylenediamine
TPO	thrombopoietin
tRNA	transfer ribonucleic acid
tRF	tRNA-derived fragment
U	uridine
UTR	untranslated region
UV	ultra violet
Val	valine
x g	times earth gravitational force
rRNA	ribosomal RNA
WTBS	whole transcriptome bisulfite sequencing

2. Introduction

The complexity of mammalian development and the high level of plasticity of mammalian cells require an accordingly dynamic regulatory system. This sophisticated gene regulation is governed by different processes, many of which fall into the category of epigenetics. Epigenetics describes gene functions that are mitotically and/or meiotically heritable, however are reversible and thus do not modify the underlying genetic code (Waddington 1942). The proof of covalent nucleotide modifications on DNA, in the form of cytosine-5 methylation (Hotchkiss 1948) marked the beginning of defining the molecular mechanisms behind epigenetics.

2.1 RNA modifications are important epigenetic marks

Cytosine-C5 methylation on DNA and RNA is a major hallmark of epigenetics and plays an important role in a plethora of biological processes, including mammalian development (Guo et al. 2014), transposon repression (Zemach et al. 2010), cancer (Kulis and Esteller 2010), and translation (Motorin, Lyko, and Helm 2010). Epigenetically active molecules exist in many different forms, ranging from nucleic acids to proteins and chemical modifications on these. These molecules essentially allow a cell to modify a biological process in response to intrinsic or extrinsic signals. Possibly the most prominent epigenetic modification is cytosine-C5 methylation of DNA at gene promoters. This addition to the DNA generally leads to transcriptional repression of the respective gene by rendering these regions less accessible to transcriptional machinery. RNAs have been shown to influence gene expression through both transcriptional and translational modulation, and RNA modifications contribute to the maturation, stability, and integrity of these regulatory RNAs (Alarcón, Lee, et al. 2015; Ivanov et al. 2011; Hussain, Sajini, et al. 2013).

Posttranscriptional modifications exist on all bases of RNA (adenine, guanine, cytosine, uridine) and come in a variety of chemical structures, such as methylation, hydroxylation, acetylation, and ribosylation (Motorin and Helm 2011). There are over 100 known RNA modifications that have impacts on a wide variety of biological processes, many of which are only beginning to be explored (Motorin, Lyko, and Helm 2010).

Adenine-6 methylation (m6A) is the most prominent modification on mammalian RNAs. The availability of high quality m6A-specific antibodies allowed immunoprecipitation of methylated RNAs followed by sequencing, which revealed thousands of m6A marks on mRNAs (Dominissini, Moshitch-Moshkovitz, et al. 2012). The marks were especially frequent in the vicinity of stop codons and in internal exons, and are suggested to play a role in RNA splicing and miRNA binding (Dominissini, Moshitch-moshkovitz, et al. 2012; Meyer et al. 2012). More recent publications have shown that m6A regulates miRNA processing (Alarcón, Lee, et al. 2015; Alarcón, Goodarzi, et al. 2015), plays pivotal roles in pluripotency (Chen et al. 2015; Geula et al. 2015), and controls RNA-protein interactions (Liu et al. 2015).

Cytosine-5 methylation (m5C) is another prominent modification of RNA. Early attempts to decipher the m5C modification in a transcriptome-wide fashion confirmed that it is mostly found on rRNAs and tRNAs, however also occurs in other RNA classes (Squires et al. 2012). Subsequently, another approach further exposed the prevalence of m5C in tRNAs (Khoddami and Cairns 2013). Cytosine-5 methylation of tRNAs is thus a major part of the RNA m5C methylome and must have biological implications.

2.2 tRNA m5C modification

m5C is present on a number of tRNA molecules. The transfer of a methyl group from a methyl donor to the 5-carbon atom on the pyrimidine ring of a target cytosine is catalyzed by methyltransferases. A variety of methyltransferases exist for RNA, DNA, and protein methylation and can transfer methyl groups to carbon, oxygen, or nitrogen atoms. The methyltransferase Dnmt2 employs a mechanism in which a methyl-donor, generally SAM (S-adenosyl-L-methionine, also abbreviated as AdoMet) is converted to SAH (S-Adenosyl-Homocystein, also abbreviated as AdoHcy) and the methyl group is transferred to the pyrimidine ring of C38 (Motorin, Lyko, and Helm 2010) (**Fig. 1A+B**). Mechanistic details and biological functions of the modifications are being discovered frequently, and less than a decade ago Dnmt2 was discovered to methylate tRNA (Goll et al. 2006).

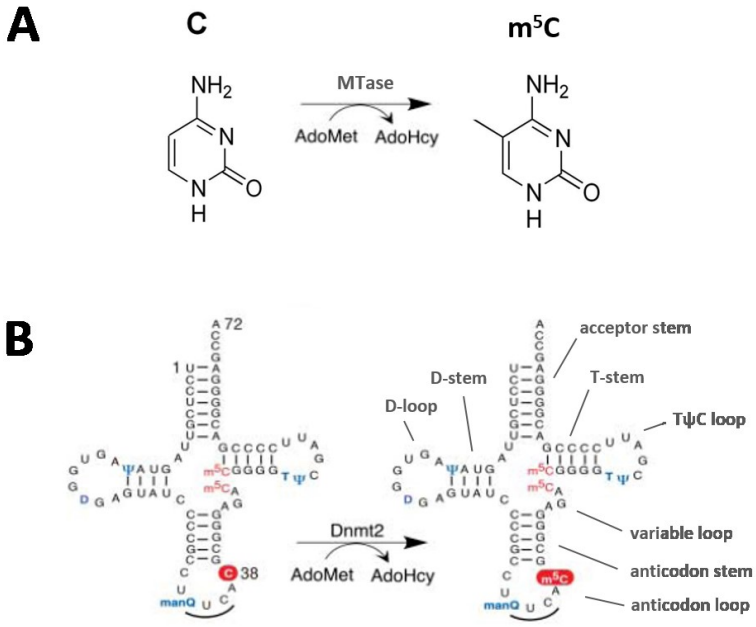

Figure 1. Cytosine-C5 methylation. A. Schematic of carbon-5 cytosine methylation by a methyltransferase (MTase). (AdoMet - SAM/S-adenosyl-L-methionine; AdoHcy - SAH/S-Adenosyl-Homocystein). **B.** Simplified illustration of $tRNA^{Asp}$ C38 (red C) methylation by Dnmt2. General structural features of tRNAs are labelled (right) and the anticodon is underlined in black. (Image modified from Goll et al., 2006).

2.3 tRNA m5C-transferases

There are two known tRNA m5C-transferases in animals, Dnmt2 and NSun2.

The methyltransferase NSun2 (NOP2/Sun domain protein 2) catalyzes cytosine-C5 methylation at positions 34, 40, 48, and 49 on different tRNAs (Auxilien and Virus 2012; Brzezicha et al. 2006) and additionally methylates a selection of mRNAs and non-coding RNAs (ncRNAs) (Squires et al. 2012; Hussain, Sajini, et al. 2013). NSun2 has implications in tRNA stability, protein synthesis (Tuorto et al. 2012), mitotic spindle stability (Hussain et al. 2009), and regulation of ncRNA processing (Hussain, Sajini, et al. 2013). Direct phenotypic effects of NSun2 mutations are arrested sperm development and sterility in mice (Hussain, Tuorto, et al. 2013; Blanco et al. 2011) and neurodevelopmental phenotypes in humans (Komara et al. 2015; Martinez et al. 2012; Abbasi-Moheb et al. 2012). We previously showed that in conjunction with NSun2, Dnmt2 maintains physiological tRNA levels and protein synthesis in mice, and double mutants show a synthetic lethal interaction (Tuorto et al. 2012).

The RNA methyltransferase Dnmt2 is closely related to the DNA methyltransferases Dnmt2 and Dnmt3 and the catalytic motifs show strong sequence conservation (Dong et al. 2001). The name Dnmt2 (DNA methyltransferase 2) was thus originally given to this enzyme due to its structure, however it has been shown that Dnmt2 does not methylate DNA (Raddatz et al. 2013), but prefers RNA as a substrate (Goll et al. 2006; Khoddami and Cairns 2013; Schaefer et al. 2010). Evolutionary studies have suggested that Dnmt2 has switched substrate activity from DNA to RNA, and the RNA specificity has been suggested to be caused by certain residues within the catalytic motif that differ from other Dnmts (Schaefer and Lyko 2010b; Goll and Bestor 2005; Jurkowski et al. 2012). Dnmt2 is a highly conserved enzyme, with orthologs in 65 different species, including protists, plants, fungi, and animals (**Fig. 2**) (Schaefer and Lyko 2010b). Being the most broadly conserved of the Dnmts, its role is suspected to be of substantial importance.

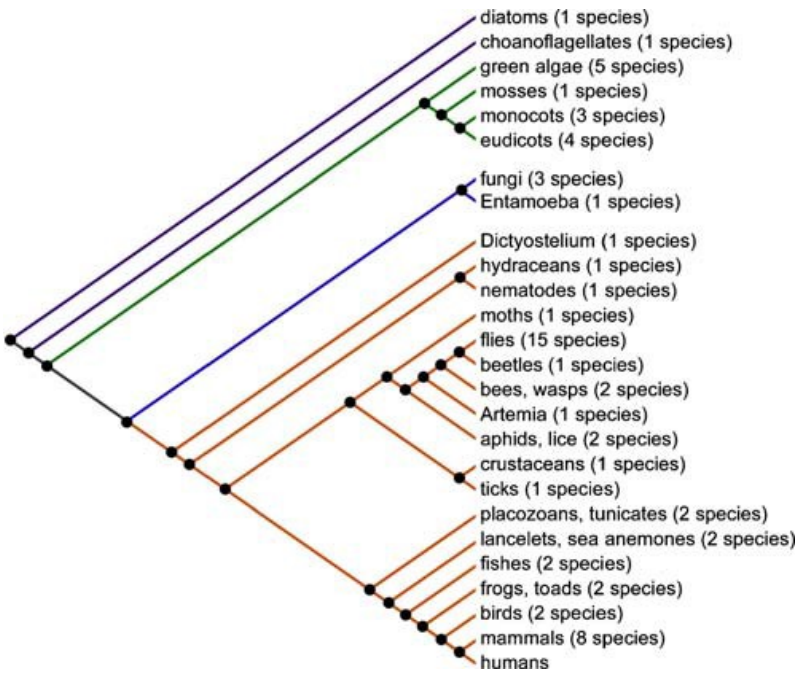

Figure 2. Dnmt2 is a highly conserved enzyme. BLAST (Basic Local Alignment Search Tool) analysis of mammalian Dnmt2 protein showed orthologs in 65 different species in protists, plants, fungi, and animals. (Taken from Schaefer & Lyko, 2010).

2.4 Known functions of Dnmt2

The highly conserved methyltransferase Dnmt2 methylates C38 of $tRNA^{AspGUC}$, $tRNA^{ValAAC}$, and $tRNA^{GlyGCC}$. Research on Dnmt2 has given insight into the regulatory functions of RNA methylation and has shown that C38 methylation protects tRNAs against stress-induced endonucleolytic cleavage and is thus a key player in the generation of tRNA-derived fragments (tRFs) (Schaefer et al. 2010), which can influence and act in small RNA silencing pathways (Haussecker et al. 2010; Durdevic, Mobin, et al. 2013). In fact, both Dnmt2 and NSun2 work together to assure tRNA integrity and function. Upon deletion of both enzymes, the lack of m5C on several tRNAs leads to decreased tRNA levels and a significant reduction in protein translation rates (Tuorto et al. 2012). Dnmt2 function has further implications in proper proteome homeostasis, as the lack of C38 methylation, especially on $tRNA^{AspGUC}$ has been demonstrated to lead to a decrease in translation of proteins that contain poly-aspartate stretches and are involved in transcriptional regulation and gene expression (Shanmugam et al. 2015).

Importantly, we recently detected a phenotype in $Dnmt2^{-/-}$ mice and discovered a possible mechanism behind this. Defects in haematopoietic stem cell differentiation in $Dnmt2^{-/-}$ mice are suggested to be caused by amino acid misincorporations, leading to improper polypeptide synthesis during haematopoiesis (Tuorto, Herbst, Alerasool, Bender, Popp, Federico, Reitter, Liebers, Stoecklin, Gröne, Dittmar, Glimm, and Lyko 2015). This is likely due to the inability of translational machinery to discriminate C38-unmethylated $tRNA^{AspGUC}$ from its near-cognate $tRNA^{GluGUG}$.

In addition to this differentiation phenotype, knockdown of Dnmt2 in zebrafish leads to differentiation defects in the retina, liver, and brain (Rai et al. 2007). The liver appears to fail to complete late differentiation, a developmental arrest of the retina was likely caused by a differentiation defect of retinal progenitors or derived neuroepithelial precursors, and abnormal neurogenesis in the brain was detected. tRNA methylation was strongly decreased in the Dnmt2 morphant, however further insights into mechanisms were not described. Based on the recent publication on haematopoietic stem cell differentiation defects as a result of improper protein synthesis in mice (Tuorto, Herbst, Alerasool, Bender, Popp, Federico, Reitter, Liebers, Stoecklin, Gröne, Dittmar, Glimm, and Lyko 2015), a link between proteome homeostasis and development is also conceivable for zebrafish.

Notably, in addition to Dnmt2's role in protein homeostasis and proper haematopoiesis, only one additional direct biological role has been shown for Dnmt2 in mice. It was demonstrated that the inheritance of paramutant mouse phenotypes is Dnmt2-dependent (Kiani et al. 2013). A paramutation describes an inheritance pattern in which a mutant phenotype, which is initially caused by a mutated allele, also appears in genotypically wild-type offspring. This uncoupling of genotype and phenotype is termed paramutation and it has been shown that sperm RNA is the carrier of the paramutation across generations (Rassoulzadegan et al. 2006). The dependence of the paramutation on Dnmt2 suggested that tRNA methylation may play a role in RNA-mediated inheritance.

Dnmt2 has also been shown to play a role in host defense, where an efficient innate immune response to viral infection in *Drosophila* required Dnmt2 (Durdevic, Hanna, et al. 2013). Dnmt2 binds to the viral DNA, however further details on the mechanism are currently unknown. Finally, mutations in *Dnmt2* strongly correlate with spina bifida risk in humans (Franke et al. 2009). Folate levels and related metabolic pathways have been linked to these neural tube defects, however no details on a mechanistic role of Dnmt2 have been published.

It has become clear that Dnmt2 has a number of functions, especially in response to environmental insults (stress, viral infection) or in conjunction with other mutations (NSun2). Direct phenotypes of Dnmt2-deficient organisms remain scarce, however mechanisms appear to be related to Dnmt2's tRNA methylating function and are slowly being exposed.

2.5 Methods for the detection of m5C in RNA

Multiple methodologies have been developed to detect m5C in RNA, many of which are based on bisulfite conversion (Schaefer et al. 2009). The methodologies each have pros and cons, ranging from resolution, i.e. precise position of the m5C, to width and depth, i.e. the amount of RNAs analyzed. Protocols employing chromatographic and mass spectrometric or differential enzymatic reactions have been applied, however are generally not suitable for high-throughput position-precise determination of m5C (reviewed in Motorin et al., 2010). The most promising approach with respect to throughput and precision is based on bisulfite conversion followed by deep sequencing. In this procedure, a nucleophilic bisulfite reagent causes deamination and conversion of unmethylated cytosines to uridine, which are then paired with adenine during cDNA synthesis, and thus subsequently read as thymins during

sequencing of the amplified libraries. Methylated cytosines, however, are not converted by the bisulfite reagents. Thus, known C positions can be analyzed whether they are methylated or not.

In 2012, one of the first approaches for transcriptome-wide methylation detection applied an oligo-dT mRNA enrichment, followed by rRNA-depletion technologies and bisulfite sequencing (Squires et al. 2012). In this study, prior to bisulfite conversion, a small fraction of total RNA was spiked into the rRNA-depleted and mRNA-enriched RNA in order to sequence known non-mRNA targets, for example tRNAs (4ng total RNA in 4µg processed RNA). This makes a quantitative comparison of the known tRNA methylation targets with potential new hits impossible and makes the detection of unknown methylation sites in other ncRNAs unlikely, as they are represented in very low numbers. Another approach utilized targeted bisulfite sequencing of RNAs that are bound by the known methyltransferase NSun2 (Hussain, Sajini, et al. 2013). This iCLIP (individual-nucleotide-resolution crosslinking and immunoprecipitation) approach however will only give information on methylation sites of this specifically tagged methyltransferase, and an antibody-mediated enrichment step is necessary. A third approach is called Aza-IP and relies on the incorporation of the cytidine analog 5-aza-Cytidine (5-aza-C) into RNA during transcription. 5-aza-C has the capability of trapping m5C-methyltransferases covalently on the RNA, allowing immunoprecipitation of tagged methyltransferases along with target RNAs. Another protocol simply bisulfite converted total RNA, without any additional rRNA depletion steps. This however significantly reduces the sequencing depth of non-rRNA reads, as rRNA quantities are high and dilute all other RNAs significantly (Edelheit et al. 2013). In the same publication, the protocol was optimized and re-applied to a set of samples, however small RNAs were fragmented in the same fashion as long RNAs, which produces very short reads and may render them unmappable. The endeavor to create a deeper and simpler, antibody-free, transcriptome-wide methylation analysis protocol for single-base resolution and applicable to any given sample was thus followed (unpublished internal protocol by Mark Hartmann and Matthias Schaefer). The newly established bisulfite protocol consists of rRNA depletion of total RNA, followed by specific fractionation and fragmentation steps to assure deep sequencing of all lengths and types of RNAs. Detailed information on this novel technique will be given within this thesis (**Fig. M1** as part of section **6.15 Whole transcriptome bisulfite sequencing – lab**).

2.6 RNA-mediated non-Mendelian inheritance

Classical genetics is based on the principle that phenotypes arise from the expression of genetic variants. However, non-Mendelian inheritance patterns have challenged this rigid view and called for alternative mechanisms of inheritance. Research in animal models has shown that RNAs as well as the RNA methyltransferase Dnmt2 can control the transmission and expression of modified phenotypes across generations (for a review along these lines, see Liebers, Rassoulzadegan, & Lyko, 2014).

The understanding of transgenerational inheritance is formed by Gregor Mendel's studies of pea plant crosses and breeding in the 1860s and has been confirmed and expanded by decades of research to show that DNA is the canonical carrier of genetic information from one generation to the next. Not only simple traits, but also highly complex inheritance patterns have been approached by analyzing interactions between multiple genetic variants within a single genome. In large-scale genome-wide association studies (GWAS), millions of identified genetic variants such as single nucleotide polymorphisms are analyzed in an effort to explain complex disorders (Hardy, Ph, and Singleton 2009). However, additional extragenomic molecules associate with DNA and can also be transmitted through the germline. This includes epigenetic factors such as proteins, RNAs, and specific modifications on these (Grossniklaus et al. 2013). Epigenetic modifications, such as DNA methylation can dynamically alter an organisms' phenotype and are thus an attractive process to consider for complex inheritance patterns. As part of studies on environmental and nutritional influences, DNA methylation has also been suggested to have adaptive functions (Lillycrop et al. 2008; Weaver et al. 2004). However, with only very few exceptions, DNA methylation patterns are robustly and globally erased in primordial germ cells and preimplantation embryos (Seisenberger, Peat, and Reik 2013), and are thus not the most suitable factor for inheritance mechanisms of adaptive phenotypic changes.

The importance of RNA in non-Mendelian inheritance is nicely demonstrated by paramutation phenotypes in mice. A paramutation describes a mutated allele with the capacity to cause a heritable change on the other allele of that locus. The *Kit* mouse model is the first example of a mammalian paramutation. *Kit* encodes a tyrosine kinase receptor that plays a role in developmental processes, including hematopoiesis, germ cell differentiation,

and melanogenesis. A homozygous deletion of *Kit* is lethal, however a heterozygous deletion by a *LacZ* insertion ($Kit^{tm1Alf/+}$) shows a white-tail phenotype (Rassoulzadegan et al. 2006). In this mouse model, a number of wild type offspring of heterozygous parents retain the white-tail phenotype, and are referred to as *Kit* paramutants (Kit*) (**Fig. 3A**). In this paramutant, *Kit* gene expression is altered and this change is stably inherited over several generations through the male or female germline (Rassoulzadegan et al. 2006). Another publication presented reproducibility of paramutability of the *Kit* locus by disruption of *Kit* via an insertion of a copGFP gene cassette (Yuan et al. 2015). Further research evinced that microinjection of parental RNA or synthetic oligoribonucleotides into pronuclei of fertilized eggs could elicit a white-tail Kit* phenotype (Rassoulzadegan et al. 2006). By injection of a *Kit*-derived RNA fragment or of sperm RNA from the heterozygous parents, a heritable epigenetic change was induced and a considerable fraction of mice showed the Kit* phenotype. Additionally, injection of microRNAs (miRNAs) that targeted kit mRNA also induced the Kit* phenotype (Rassoulzadegan et al. 2006). Importantly, while injection of *Kit* RNA fragments into fertilized wild-type eggs led to upregulation and possibly also methylation of the Kit transcript, the Kit genomic DNA remained unmethylated in all genotypes and in Kit* mice (Kiani et al. 2013). A similar phenomenon could be observed for microinjection of miR-124 or of fragments of its target transcript *Sox9*, which caused heritable paramutation of *Sox9*. The paramutation caused overexpression during the first embryonic stages, increased proliferation of embryonic stem cells, body sizes during postnatal development, and twin pregnancies (Kiani et al. 2013). In both paramutation cases, the paramutation phenotype was associated with an increased rate of transcription of the respective locus, suggesting a long-term induction of transcription, either through miRNAs or fragments of the transcript itself. The experimentally injected RNAs are all present in the male germline, i.e. sperm, and are thus paternally heritable. All three elucidated paramutants share three characteristics that clearly distinguish them from genetic mutations that would be transmitted in a Mendelian fashion: (1) paramutants were induced and inherited at far greater frequencies and not according to Mendelian ratios; (2) although stably heritable for three or more generations, they were eventually reversed; (3) paternal inheritance was associated with the presence of sperm RNAs originating from, or targeting, the respective gene.

These publications show that RNAs are necessary for the inheritance of the paramutant phenotypes, however do not prove that RNAs are the sole factor acting in this

process. The possibility of sequence specificity playing a role, and the maintenance over several generations allow to assume that additional players that regulate these mechanism, such as small RNA machinery or epigenetic modulators, may be involved. Small RNAs are a proven regulator of gene expression in the mouse (Watanabe et al. 2008; Tam et al. 2008; Watanabe et al. 2011), however it is not clear how small RNAs can be inherited over several generations, and why such paramutations appear to only occur at a few loci.

Importantly, the inheritance of both the *Kit* and *Sox9* paramutant phenotypes were found to be dependent on the presence of Dnmt2 (Kiani et al. 2013). As part of this publication, I showed that Dnmt2 was active in the male germline by 454 sequencing of $tRNA^{AspGUC}$ and $tRNA^{GlyGCC}$, and methylation was substantially decreased in $Dnmt2^{-/-}$ sperm. Consequently, Dnmt2 function in the germline is suggested to play a pivotal role in RNA transgenerational epigenetic inheritance (TEI).

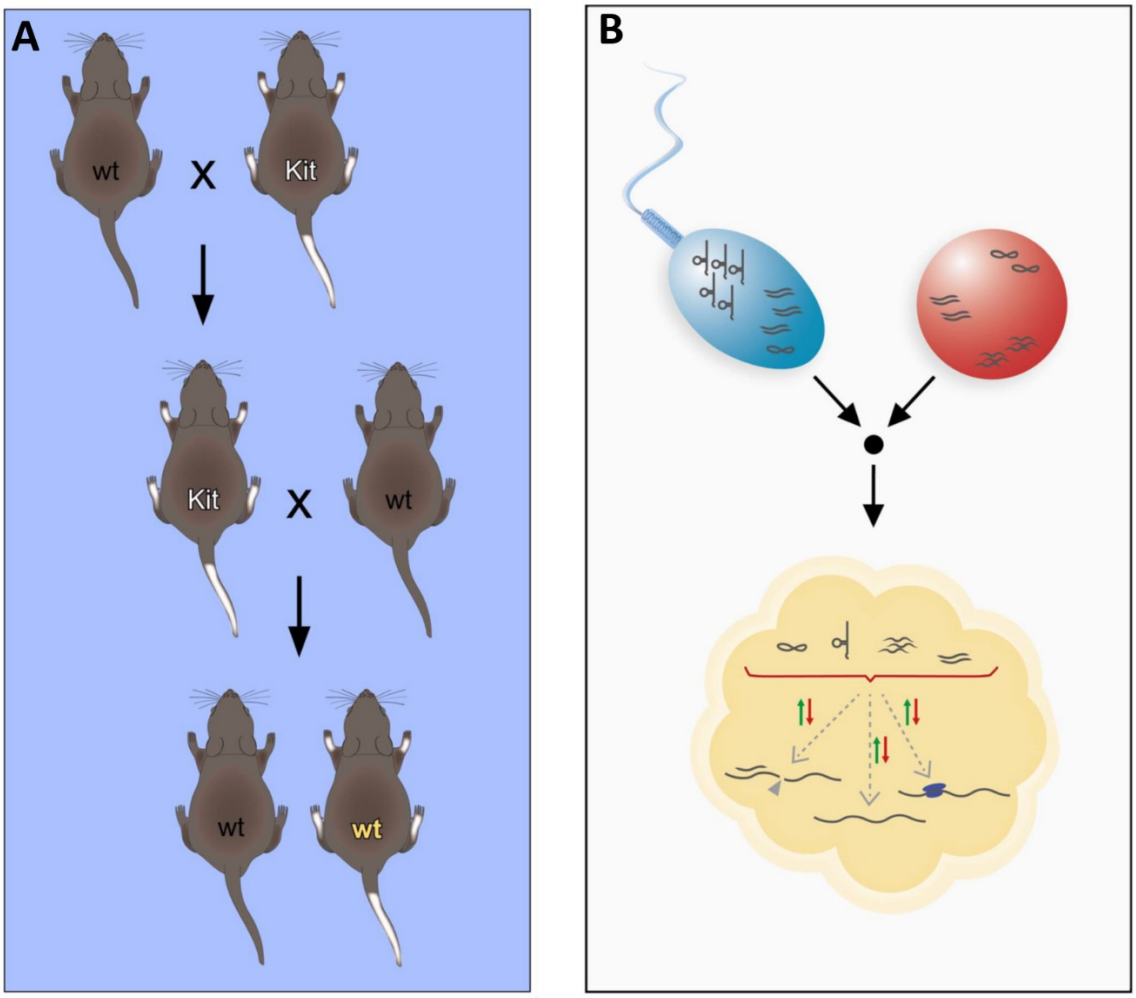

Figure 3. Non-Mendelian inheritance of RNA. A. Inheritance of the Kit paramutation. The white tail and feet phenotype in $Kit^{tm1Alf/+}$ mice provides an important paradigm for RNA-mediated non-Mendelian inheritance. Mating of heterozygous $Kit^{tm1Alf/+}$ (labelled 'Kit') mice with wild type (labelled

'wt') mice results in $Kit^{tm1Alf/+}$ (Kit) offspring with characteristic white tails and feet. When these mice are again mated with wild type mice, a fraction of the offspring retains the white phenotype, even with a wild-type genotype. This paramutant phenotype is also inducible by microinjection of RNA into fertilized oocytes, which suggests that RNA plays an important role in the mechanism of inheritance. **B.** RNA inheritance pathways. Sperm and ovum contribute diverse classes of RNAs to the developing embryo. Small regulatory RNAs, mRNAs, and tRFs are a part of these. The regulatory processes in which these RNAs might act remain enigmatic. (Figures taken from Liebers et al., 2014.)

2.7 Heritability of RNAs

The presence of RNAs within gametes is a prerequisite for their heritability. Research has shown that sperm as well as oocytes contain a diverse set of RNAs (Krawetz 2005; Walser and Lipshitz 2011; Ostermeier et al. 2002). Importantly, it has also been shown that sperm RNAs are delivered into oocytes upon fertilization (Avendaño et al. 2009; Ostermeier et al. 2004). These findings illustrate that a fertilized ovum is initially equipped with a diverse and complex RNA cache composed of both maternal and paternal RNAs (**Fig. 3B**).

2.8 Inheritance of regulatory RNAs

As gametes are transcriptionally quiescent, the lifetime of heritable RNAs must match that of a gamete. Several oocytic as well as zygotic RNAs indeed contain specific sequence motifs for regulation of stability (Evsikov et al. 2006), which led to the assumption that additional RNA-binding proteins or antisense RNAs may play a role in inheritance. Supporting this notion, published data shows that microRNAs (miRNAs) are heritable (Lim and Brunet 2013). Intriguingly, miRNAs are established regulators of developmental gene expression (Ebert and Sharp 2012; Abd El Naby et al. 2013) and even a single sperm-borne miRNA can be necessary for embryogenesis (Liu et al. 2012). Recently, miRNAs have been suggested to mediate transgenerational inheritance of the effects of obesity (Fullston et al. 2013) and stress in mice (Gapp et al. 2014; Rodgers et al. 2013). Furthermore, siRNAs are present in female and male mouse germ cells (Watanabe et al. 2008; Tam et al. 2008; Song et al. 2011) and have the capacity to regulate gene expression. Similarly, tRFs are present in mouse germ cells of both sexes (García-López et al. 2014) and can act as siRNA-mimics to regulate gene expression (Haussecker et al. 2010). Additionally, such heritable tRFs have also been proven to alter

translation (Sobala and Hutvagner 2013; Ivanov et al. 2011). Taken together, it is conceivable that regulatory RNAs are deposited in gametes and inherited for a biological purpose.

2.9 RNA-mediated inheritance in human disease

GWAS studies have been applied to identify complex combinations of genomic variants as causes for diseases. Compilation and analysis of data from a variety of sources and acquired through modern technologies such as arrays and deep sequencing has helped in identifying links between combinations of SNPs with phenotypes. However, because it still has not been possible to define major risk factors for many complex diseases (Manolio et al. 2009), the term missing heritability has been used to describe these gaps. Importantly, ncRNAs are often omitted in GWAS and present an intriguing mechanism to explain some of the missing heritability, namely by RNA-mediated inheritance.

Two well-known examples of unresolved complex inheritance patterns in humans are based on the influence of nutritional factors on health across multiple generations. Studies on the Dutch Hunger Winter Families cohort exposed a relationship between malnutrition during pregnancy and poor health of daughters and granddaughters (Lumey et al. 2007; Lumey et al. 2009; Painter et al. 2008). Subsequent studies have implied the involvement of DNA methylation changes in the IGF2 gene, however the effect sizes for this as well as other environment-related DNA methylation studies in mammals appear to be very small (Ferguson-Smith and Patti 2011; Tobi et al. 2012; Ng et al. 2010; Carone et al. 2010; Sen et al. 2015; Heijmans et al. 2008). Another example of complex inheritance can be seen in epidemiological studies of the Överkalix parish in northern Sweden, in which a strong increase in food supplies during early male adolescence led to decreased health and life span of grandchildren (Kaati et al. 2007; Kaati, Bygren, and Edvinsson 2002; Bygren, Kaati, and Edvinsson 2001). RNA-mediated inheritance may be an attractive candidate mechanism to explain these inheritance patterns. Taken together, resolving RNA-mediated inheritance mechanisms may allow to fill some of the missing heritability gaps for complex disorders.

3. Aims of the Thesis

The aim was to functionally characterize the RNA-methyltransferase Dnmt2 in the mouse, especially with respect to the known Dnmt2-knockout mouse phenotypes.

1) The published function of Dnmt2 in the germline and its involvement in inheritance implied that the male germline may show phenotypic aberrations. This was addressed by phenotypic characterization with histological and viability assays.
2) The known role of Dnmt2 in tRNA methylation and tRNA stabilization and its roles in inheritance suggested that RNAs in Dnmt2$^{-/-}$ sperm or early embryos may be deregulated. The question of RNA expression differences was addressed by different approaches, including RNA-Seq and Northern blotting.
3) A role of Dnmt2 was considered to be the methylation of unknown RNA targets. A whole-transcriptome bisulfite sequencing approach was employed to clarify whether Dnmt2 methylates RNAs other than the three known tRNA targets.
4) A fourth goal was to define which factors, be it stress, differentiation, or nutrition, are capable of regulating Dnmt2 function in mammals. This was done via a screening of various conditions.

4. Results

4.1 Dnmt2-dependent RNA inheritance: Characterization of the target tissue

RNA transgenerational epigenetic inheritance (TEI) describes the delivery of parental RNAs to their offspring. The transmitting cells are sperm and oocytes, and the target tissue the developing embryo. To detect any gene expression or phenotypic differences elicited by Dnmt2 deletion in the target tissue, wild type (wt) and Dnmt2$^{-/-}$ early embryos were characterized.

4.1.1 Dnmt2$^{-/-}$ E7.5 show no phenotypic aberrations

As mammalian RNA TEI from the male germline into the zygote must employ a currently unknown mechanism to elicit the Dnmt2-dependent phenotypes (Kiani et al. 2013), the search for this mechanism began at the macro level, i.e. the morphology of the involved tissues. Dnmt2$^{-/-}$ E7.5 embryos (embryonic day 7.5 post-fertilization) showed no phenotypic aberrations when examined microscopically (**Fig. 4**). Sizes were comparable to controls and no defects could be detected in the mutant. These results were expected as Dnmt2$^{-/-}$ mice are viable, fertile, and have no obvious morphological phenotype (Goll et al. 2006). This prompted the question whether molecular effects not visible externally, such as RNA deregulation, may play a role in Dnmt2-dependent RNA-mediated TEI.

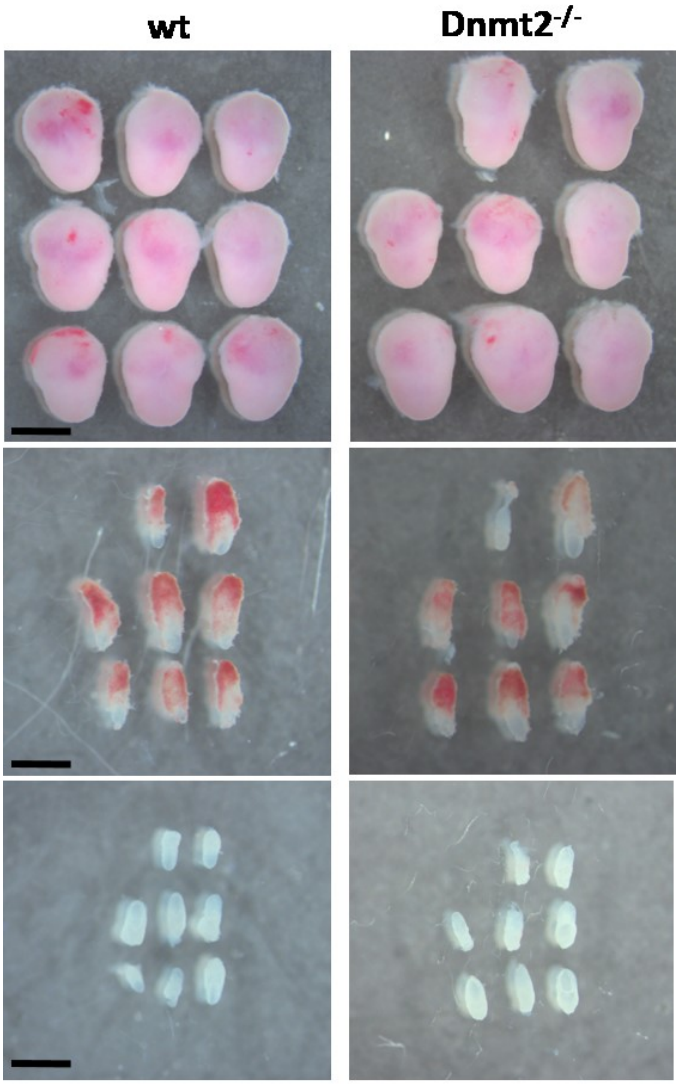

Figure 4. Wild type and Dnmt2$^{-/-}$ E7.5 embryos are phenotypically indistinguishable. Top row shows embryos isolated from the uterus, including decidua and placenta (scale bar = 2mm). Second row shows embryos with extraembryonic tissue, including the ectoplacental cone (one of the 9 wt embryos was lost during dissection) (scale bar = 1mm). Bottom row depicts isolated embryos (scale bar = 1mm).

4.1.2 Dnmt2 deficiency in embryonic cells has only subtle effects on the transcriptome

To discover possible transcriptome changes that could play a role in RNA-mediated TEI, RNA-Seq of wild type and Dnmt2$^{-/-}$ E7.5 embryos was carried out. An rRNA depletion protocol was applied in order to sequence mRNAs as well as ncRNAs in sufficient depth. In addition, as an *ex vivo* model to the E7.5 samples, wild type and Dnmt2$^{-/-}$ embryonic stem cells (ESCs) were cultured and sequenced in parallel.

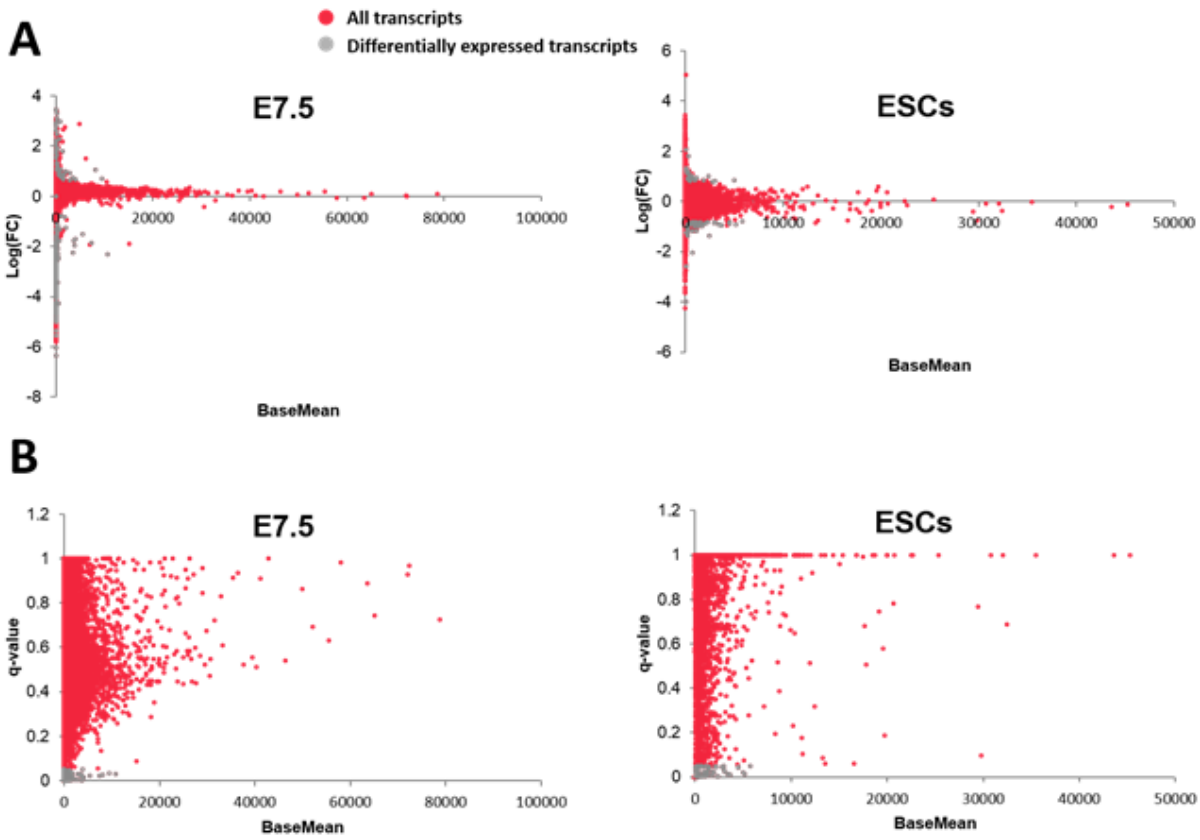

Figure 5. DESeq analyses show limited RNA expression changes in Dnmt2$^{-/-}$ embryonic cells. A. MA-plots show RNA-Seq data as logarhithmic fold change (y-axis/M) versus BaseMean (mean average) (x-axis/A) of both E7.5 (left) and ESCs (right). The BaseMean for each transcript is calculated by counting the reads that map to the respective gene, normalizing these to all reads of the sample, and then taking the average between the two compared samples (wt and Dnmt2$^{-/-}$). Differentially expressed transcripts (gray dots) can be seen to generally show a low BaseMean (normalized read count), when compared to all other transcripts (red dots). **B.** Correlation of BaseMean to q-value of DESeq output. Differentially expressed transcripts with a low q-value (higher significance) show relatively low BaseMean values. For both **A.** and **B.**, some non-differentially expressed outliers were removed for ease of display: for ESCs; RN45s (BaseMean 1414640; log(FC) 0.93) and Malat1 (BaseMean 78710; log(FC) 0.97). For E7.5; RN45s (BaseMean 607445; log(FC) 0.83). (DESeq analysis of these data was carried out by Günter Raddatz, results provided in numerical form, and were then further processed).

Differential expression analyses (DESeq) revealed that a lack of Dnmt2 has only minor effects on either of the analyzed samples. In embryos, 323 genes were classified as differentially expressed (by a q-value<0.05; 59 up- and 264 downregulated), however most of the significantly deregulated transcripts with a high fold change (**Fig. 5A**) and low q-value (**Fig. 5B**) had low BaseMeans (normalized read counts) in both wild type and Dnmt2$^{-/-}$ samples, making them more prone to physiological variation. Normalized read counts were further normalized to the length of each transcript, i.e. converted to FPKM (fragments per kilobase

per million reads) values, which reflects gene expression more precisely. Following this, a subset of down- as well as upregulated transcripts with high and low FPKM values were selected for validation by qRT-PCR. The qRT-PCR results confirmed the FPKM values only in very few cases; the transcripts that showed the same direction of change for both methods only did so in 3 out of 8 cases (Ass1, Nampt, Sgk1) (**Fig. 6A**).

The ESC RNA-Seq results that were run in parallel indicated 65 differentially regulated genes by DESeq (43 down- and 21 upregulated). Similar to E7.5, most of the significantly deregulated transcripts with a high fold change (**Fig. 5A**) and low q-value (**Fig. 5B**) had low BaseMeans (normalized read counts) in both wild type and Dnmt2$^{-/-}$ samples. A subset was selected for qRT-PCR validation by the same criteria as for E7.5. The expression levels and also the magnitudes of expression changes were more subtle for the qRT-PCR results and could not clearly validate the RNA-Seq results (**Fig. 6B**). For example, Rps3a1 was expressed at around 200 units, both for FPKM and % actin values, however the expression change between the genotypes was not as clear in % actin as in FPKM. Other transcripts, such as Itgb1, Mbtps1, Fgfr1, and Atp13a1 showed expression levels between 50 and 200 FPKM (by RNA-Seq), and significantly lower values, between 1 and 4, for % actin (by qRT-PCR).

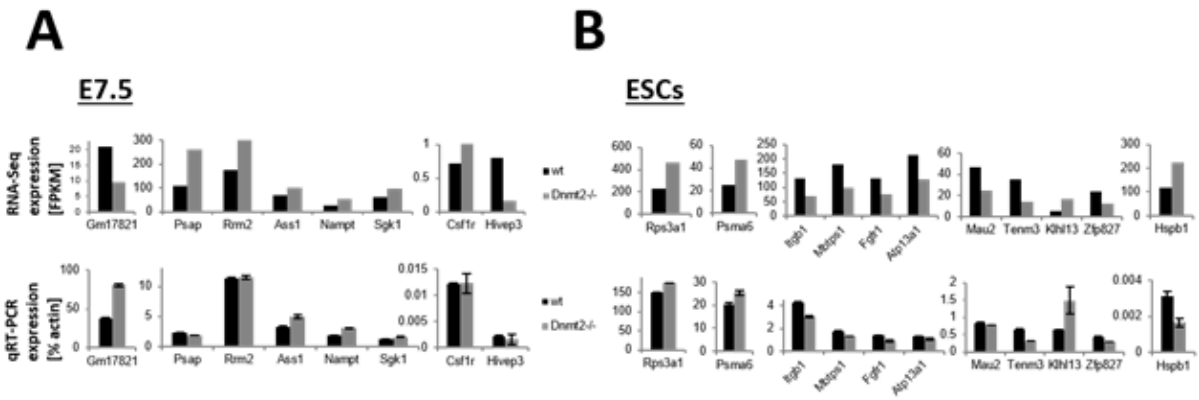

Figure 6. Differential expression in RNA-Seq data can only be partially validated. A subset of down- and upregulated transcripts from RNA-Seq data with high as well as low FPKM (fragments per kilobase per million reads) values were quantified by qRT-PCR (% actin). Due to abundance differences, separate graphs with different ranges of FPKM and %actin are given for ease of display. **A.** E7.5 transcripts. **B.** ESC transcripts.

The RNA-Seq differentially expressed transcripts for both E7.5 and ESCs were mostly subtly deregulated and only very few appeared similar in both RNA-Seq and qRT-PCR. This

may be a result of the fact that many differentially expressed RNAs show low expression and in many cases borderline significant q-values (**Fig. 5A+B**). Additionally, the precise age in hours of embryos from different mothers, i.e. wild type versus Dnmt2$^{-/-}$, may vary slightly and cause variation. Thus, detection of differentially expressed RNAs is likely caused by physiological fluctuation and is not related to the Dnmt2 mutation. These results are in agreement with previously published data on Dnmt2 mutant cells and tissues (mouse embryonic fibroblast cell lines, liver, bone marrow), where no or only minor gene expression deregulation could be detected (Tuorto et al. 2012; Tuorto et al. 2015). Thus, Dnmt2 appeared to play no or only a minor role in RNA expression.

4.1.3 Contribution of Dnmt2 to the RNA methylome: Whole-transcriptome bisulfite sequencing (WTBS)

To determine whether Dnmt2 methylates cytosines outside of tRNAs, the RNA methylome of wild type and mutant cells was sequenced. For this purpose, a whole transcriptome bisulfite sequencing protocol (unpublished internal protocol provided by Mark Hartmann) was applied on wild type and Dnmt2$^{-/-}$ ESCs. ESCs were used, as the protocol requires a considerable amount of starting material (20-30µg), which would have required up to 100x E7.5 embryos per genotype. Abiding to humane experimental techniques by the 3R principles (replacement, reduction, refinement), ESCs were thus used (Russell WMS 1992). Briefly, total RNA was rRNA depleted, fragmented, bisulfite converted, and sequenced (for details, see **Figure M1** as part of section **6.15 Whole transcriptome bisulfite sequencing – lab**). An m5C-antibody approach for enriching methylated RNAs was not pursued, as the currently available m5C antibodies did not pass initial quality controls (data not shown). The resulting reads were mapped transcriptome-wide to call potential methylation sites, using an internal analysis pipeline (provided by Sebastian Bender & Mark Hartmann).

4.1.4 Dnmt2 is a three-tRNA-specific methyltransferase

As a first step of resolving the mouse RNA methylome, known Dnmt2 target RNAs were analyzed. The results confirmed the three known tRNA targets, tRNA^{AspGUC}, tRNA^{GlyGCC}, and tRNA^{ValAAC} being methylated at C38 in the wild type and unmethylated in the Dnmt2$^{-/-}$ sample (**Fig. 7A**). Analysis of the remaining tRNAs identified a single further potential Dnmt2-target

site, on $tRNA^{ValCAC}$ (**Fig. 7B**). The aligments of this candidate were carefully checked and revealed that this was a false positive. False positives were an important topic during the establishment and optimization of the analyses. The nature of bisulfite sequencing causes Cs in RNAs to be virtually eradicated, which leads to reduced complexity of the reads (3 instead of 4 bases) and can lead to ambiguous mapping of short reads. $tRNA^{ValCAC}$ C38-methylated reads were short and the regions of $tRNA^{ValCAC}$ to which the reads mapped differed to $tRNA^{ValAAC}$ merely in a few Cs versus Ts. However, after bisulfite conversion, these Cs were converted to Ts and thus the reads were mappable to either $tRNA^{ValCAC}$ or $tRNA^{ValAAC}$ (**Fig. 7C**). All methylated reads actually originated from $tRNA^{ValAAC}$, as became evident by the following mechanism. The natural editing of A34 to I34 (inosine) on $tRNA^{ValAAC}$ by deamination (of the first A of AAC) (Torres et al. 2014), causes the I34 to be read as a G during sequencing (Nigita, Veneziano, and Ferro 2015). This in turn leads to a single G-C mismatch in the reads that incorrectly mapped to $tRNA^{ValCAC}$, and a single G-A mismatch if these reads were correctly mapped to $tRNA^{ValAAC}$ (**Fig. 7C**). Another reference sequence for such edited tRNAs may need to be implemented into the developing WTBS pipeline for improved mapping. Thus, the three known tRNA targets were confirmed, with no additional targets within the set of tRNAs in mouse. However, a number of potential Dnmt2-dependent methylation sites were called on ncRNA as well as mRNAs (**Supplementary Table S1**).

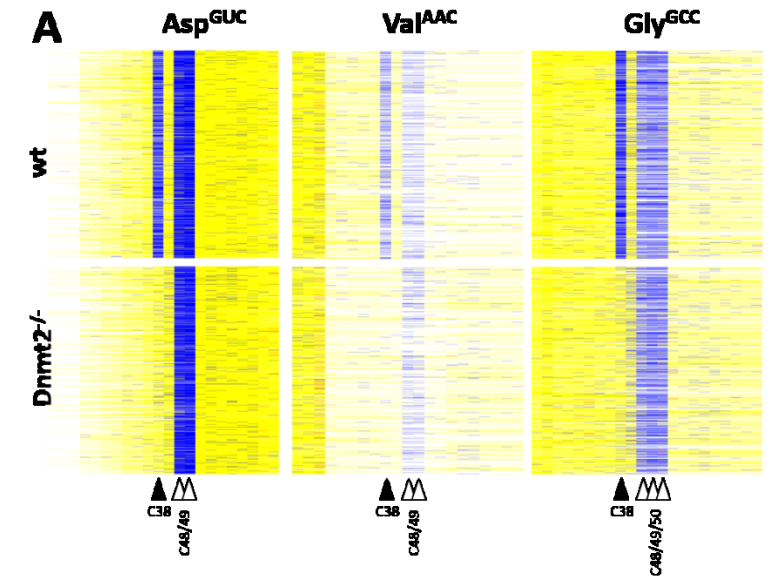
A
Asp^GUC
Val^AAC
Gly^GCC
wt
Dnmt2-/-
C38
C48/49
C38
C48/49
C38
C48/49/50

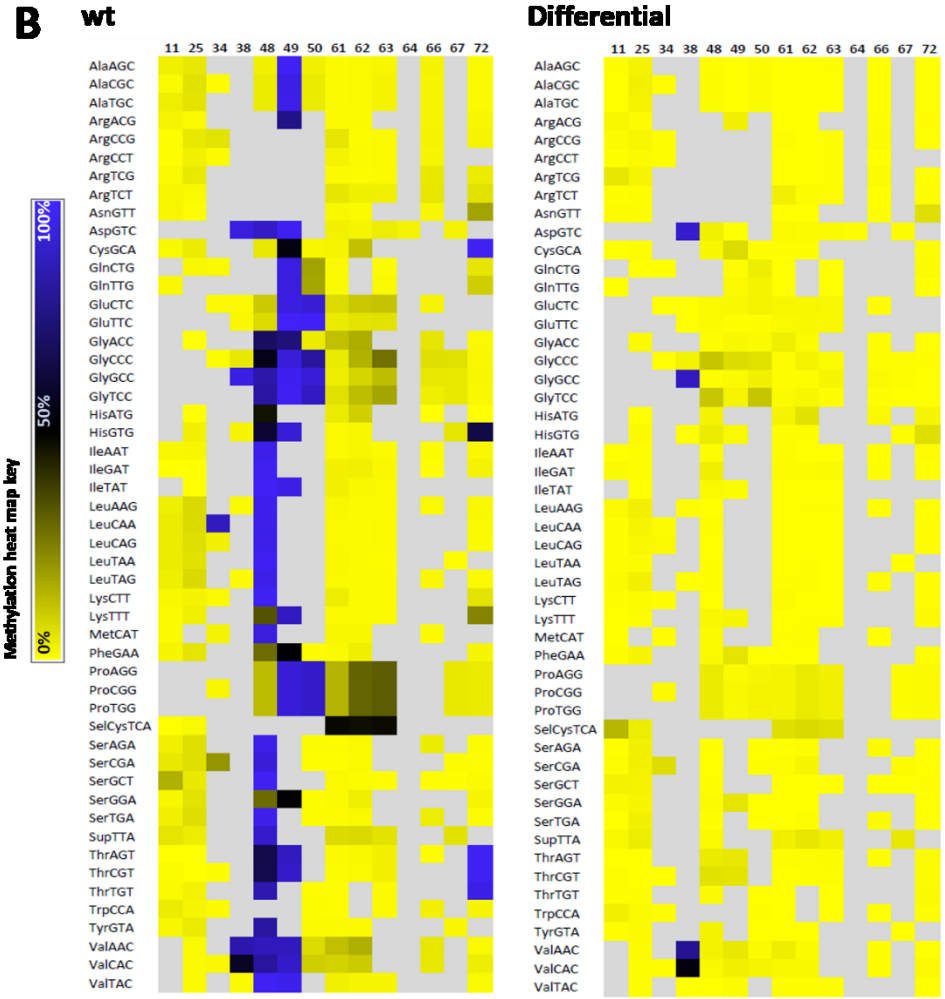
B
wt
Differential
11 25 34 38 48 49 50 61 62 63 64 66 67 72
AlaAGC
AlaCGC
AlaTGC
ArgACG
ArgCCG
ArgCCT
ArgTCG
ArgTCT
AsnGTT
AspGTC
CysGCA
GlnCTG
GlnTTG
GluCTC
GluTTC
GlyACC
GlyCCC
GlyGCC
GlyTCC
HisATG
HisGTG
IleAAT
IleGAT
IleTAT
LeuAAG
LeuCAA
LeuCAG
LeuTAA
LeuTAG
LysCTT
LysTTT
MetCAT
PheGAA
ProAGG
ProCGG
ProTGG
SelCysTCA
SerAGA
SerCGA
SerGCT
SerGGA
SerTGA
SupTTA
ThrAGT
ThrCGT
ThrTGT
TrpCCA
TyrGTA
ValAAC
ValCAC
ValTAC
Methylation heat map key
100%
50%
0%


C
Reference tRNA^ValCAC GTTTCCGTAGTGTAGTGGTCATCACGCTCGCCTCACACGCGA...
Short bisulfite read GTTTttGTAGTGTAGTGGTtATtAtGtTtGttTGAtACGtGA
Reference tRNA^ValAAC GTTTCCGTAGTGTAGTGGTtATCACGTTCGCCTAACACGCGA...
Anticodon
C38

Figure 7. Whole transcriptome bisulfite sequencing of ESCs confirms that Dnmt2 has three substrates within tRNAs. A. Methylation status of cytosines in the three known Dnmt2 target tRNAs ($tRNA^{AspGUC}$, $tRNA^{GlyGCC}$, $tRNA^{ValAAC}$) are depicted. Each row represents one read and each column one cytosine, with positions given at the bottom. Yellow boxes indicate unmethylated cytosines, blue boxes methylated cytosines. Sequencing gaps are shown in white, mismatches in red. **B.** Left panel: A global heat map of tRNAs (in rows) shows methylation states of individual cytosines (in columns) from 0% (yellow) to 100% (blue) in wild type ESCs. Cytosine positions are given at the top. Right panel: Heat map showing the difference in methylation between wt and $Dnmt2^{-/-}$ cells. Blue is indicative of a strong loss of methylation in the mutant. (The analysis pipeline for WTBS data was designed and carried out by Sebastian Bender and Mark Hartmann). **C.** The first 42 nucleotides of highly similar $tRNA^{ValCAC}$ and $tRNA^{ValAAC}$ are shown, with an exemplary sequencing read in between. Bisulfite converted positions in the read are indicated by lower case ‚t', differences between the two references are highlighted in green, and the G which allows to distinguish which tRNA the origin of the read is, is highlighted in red.

Candidate Dnmt2-methylated cytosine residues were quantified (**Fig. 8A+B**) and grouped according to the type of RNA, i.e. tRNA or non-tRNA. This revealed that 99.1% of the detected methylated cytosines belonged to the three known tRNAs (**Fig. 8B**), and merely 0.9% of methylated cytosines were on non-tRNAs. These remaining 128 candidate cytosines on 42 non-tRNA transcripts were ranked by methylation levels and by coverage. All candidate targets were compared to E7.5 and ESC RNA-Seq data for potential overlap with DESeq-deregulated transcripts. Indeed, a single transcript, Vax2os (ventral anterior homeobox 2, opposite strand) was called as deregulated by DESeq in E7.5 and was a WTBS candidate. However, the potential methylation sites were located in midst of a stretch of 215 nucleotides composed exclusively of Cs and Ts. This enrichment of C and T was a first hint that this may be an artifact. The three known Dnmt2 target cytosines are in CpG context and Dnmt2 methylates RNA via a catalytic mechanism similar to DNA methyltransferases (Jurkowski et al. 2012; Jurkowski et al. 2008; Schaefer and Lyko 2010), which in mammals almost exclusively methylate in a CpG context (Raddatz et al. 2013; Feng et al. 2010; Zemach et al. 2010). Furthermore, after bisulfite conversion, a C/T-rich stretch becomes a homopolymeric repeat (exclusively Ts) and not amplifiable (Hommelsheim et al. 2014) or sequenceable reliably via targeted Sanger- (ABI 3730xl) or pyrosequencing (454) approaches (Metzker 2010). Finally, the likelihood of these highly repetitive reads from WTBS having mapped incorrectly is very high, as a sequence consisting solely of Ts (with only a few candidate Cs) is indistinguishable from other regions with low complexity. Therefore, another, promising candidate transcript (mouse predicted rRNA gene Gm26391) with over 1200 reads for wild type as well as

Dnmt2$^{-/-}$ ESCs and a methylation ratio of 70% versus 2%, respectively, was used for validation by an independent and targeted sequencing approach (454 pyrosequencing). The candidate methylation site was not confirmed, merely showing 1.29% methylation in the wild type, which can be considered background (**Fig. 8C**). This result is in line with previous experiments in Dnmt2-deficient *Drosophila melanogaster*, where all tested WTBS candidate RNA methylation sites proved to be false positives (Hartmann et al., unpublished). False positives may be generated by biochemical and bioinformatic issues alike. Incomplete bisulfite conversion of sites with strong secondary structures, incorrect mapping (especially of short) reads due to sequence similarities, or too sensitive methylation calling are potential causes. Thus both conversion efficiency and methylation calling will require optimization.

In summary, the three known Dnmt2-mediated tRNA methylation sites were clearly confirmed. These sites represent 99.1% of all called methylation sites, and the remaining 0.9% were demonstrated to likely be false positives. The data leads to conclude that Dnmt2 is a tRNA-specific methyltransferase, selective for tRNA^{AspGUC}, tRNA^{GlyGCC}, and tRNA^{ValAAC}.

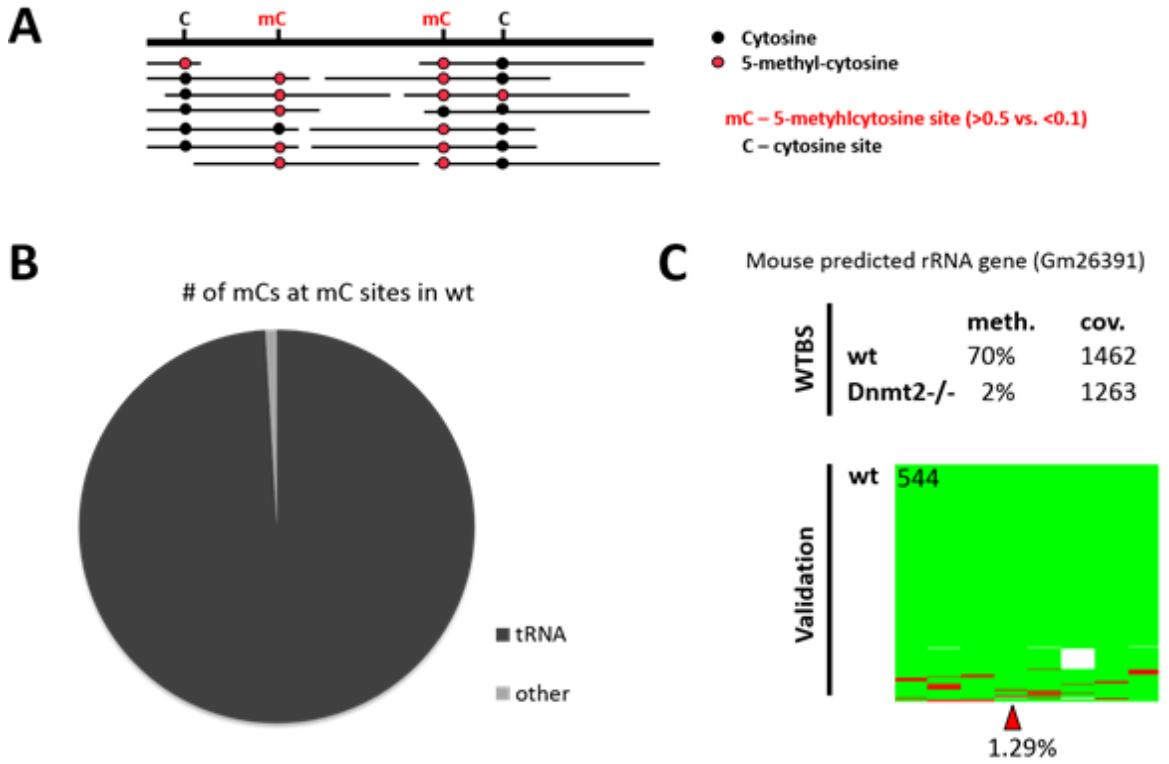

Figure 8. Analysis of WTBS data shows that Dnmt2 is a three-tRNA-specific methyltransferase. A. Candidate Dnmt2 methylation sites (red mC) were defined by having a methylation ratio of >0.5 in the wt and <0.1 in the mutant. At each of these candidate sites, the methylated reads (red dots) were counted. The counts were grouped according to whether they were located on tRNAs or on non-tRNAs

(other), and graphed in **B.** 99.1% of Dnmt2-methylated cytosines come from known Dnmt2 substrates, 0.9% are located elsewhere. (Conceptual contributions to calculations by Mark Hartmann, Cassandra Falckenhayn, and Frank Lyko). **C.** The high-confidence candidate Gm26391 with high coverage (cov.) and methylation ratios (meth.) high above the thresholds for candidate calling was 454-bisulfite sequenced. Each row represents one read and each column one cytosine, with the candidate cytosine marked with a red arrowhead and labelled with the actual methylation level in wildtype as determined by 454-bisulfite sequencing. Green boxes indicate unmethylated cytosines, red boxes methylated cytosines, sequencing gaps are shown in white. Read count is stated top left.

4.2 Dnmt2-dependent RNA inheritance: Characterization of transmitting cells

4.2.1 Dnmt2 expression supports a role in the germline

Having no clear indications of transcriptome control via Dnmt2 in the target tissues, the transmitting cells were investigated. High expression of Dnmt2 mRNA in testicular samples versus a panel of other tissues supports a functional relevance of Dnmt2 in the germline (**Fig. 9A**). A closer look at Dnmt2 expression in testis and additionally in mature cauda epididymal sperm (herein: epididymal) and early embryos (E7.5) of both wild type and Dnmt2$^{-/-}$ mice confirmed the high mRNA expression in the wild type germline (**Fig. 9B**). Schematically illustrated in **Figure 9C**, sperm mature along the cauda and caput, and RNA (Krawetz et al. 2011; Girard et al. 2006) as well as protein (Belleannee et al. 2011) expression between testicular samples and epididymal sperm vary. Thus, sperm purity was assessed and confirmed as described in the following. Analysis under the microscope indicated purity of sperm samples (**Fig. 9D**), which was then validated by Agilent Bioanalyzer profiles which displayed essentially no full-length 18S and 28S rRNA peaks (Johnson et al. 2011) (**Fig. 9E**). Further, northern blots of testicular and sperm RNA were carried out to confirm that spR-12 (Kawano et al. 2012) was only detectable in pure sperm and piR-1 (Girard et al. 2006) only in total testis RNA (**Fig. 9F**). Dnmt2 expression analysis of testis and mature sperm by Western blotting revealed Dnmt2 protein expression in testis, however essentially no Dnmt2 protein expression in mature, epididymal sperm (**Fig. 9G**). A high mRNA expression versus essentially no protein in sperm might be explained by sperm being translationally silent (Johnson et al. 2011) and by the requirement of certain mRNAs immediately upon fertilization (Grunewald et al. 2005; Ostermeier et al. 2004; Avendaño et al. 2009). Given the role of Dnmt2 in tRNA methylation in general and Dnmt2's high expression in the germline, the transmitting cells of RNA TEI were analyzed in further depth, especially with respect to tRNAs.

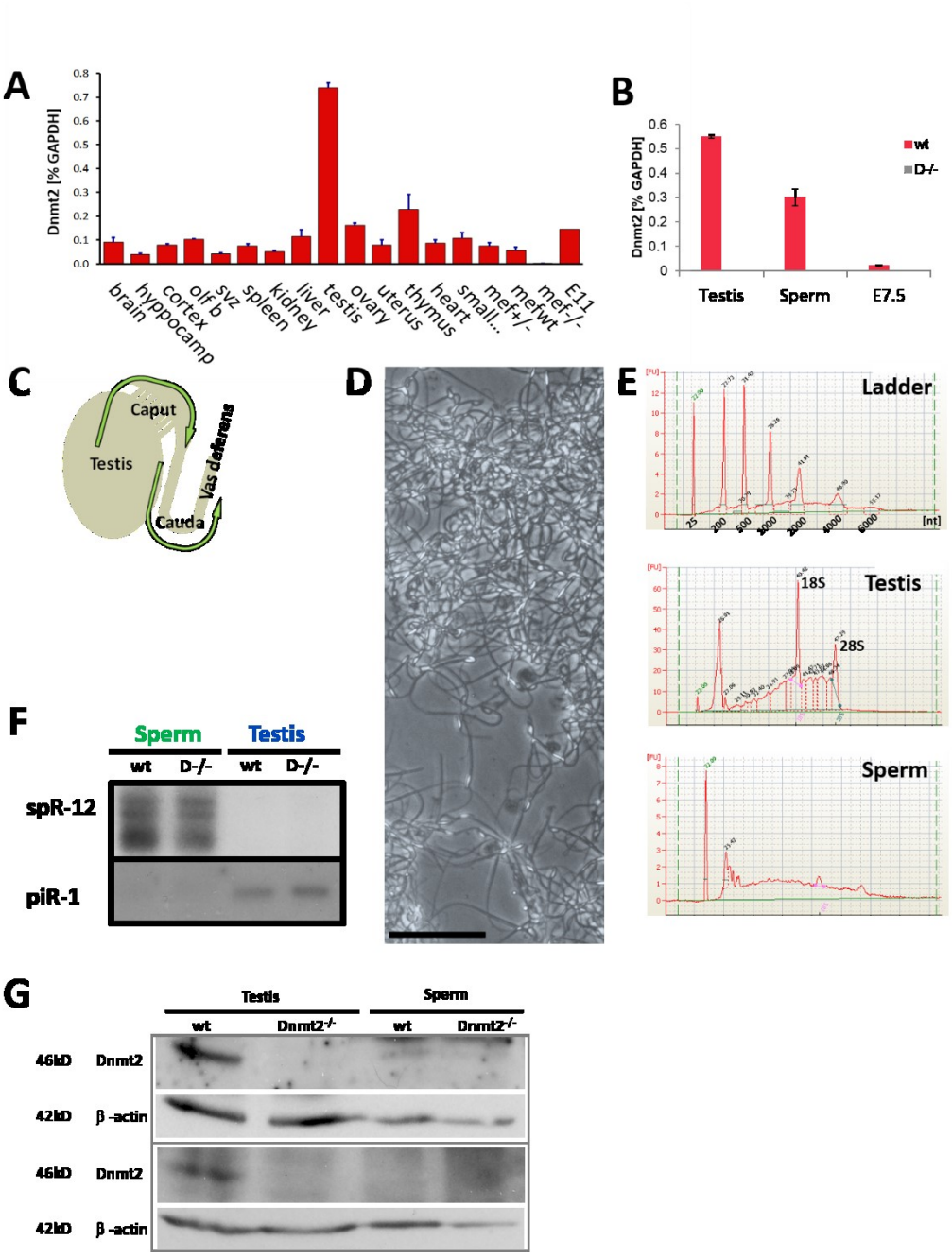

Figure 9. Dnmt2 expression supports a role in the germline. A. RNA expression profiling of Dnmt2 by qRT-PCR in a panel of wt tissues shows high expression in the male germline. **B.** qRT-PCR analysis of Dnmt2 in the transmitting (testis, mature sperm) and target (E7.5) tissues and cells of both genotypes confirms high expression in the germline. **C.** Quality control steps of mature cauda epididymal sperm isolation. Schematic of testis, caput epididymis, cauda epididymis, and vas deferens. **D.** Microscopic analysis shows visual purity (scale bar = 100µm). **E.** Bioanalyzer data show essentially no full-length rRNA peaks (Johnson et al., 2011). **F.** Northern blots show characteristic signals for each tissue: spR-12 RNA (Kawano et al., 2012) and piR-1 (Girard et al., 2006) expression is mutually exclusive in sperm versus testis. **G.** Western Blot of testis and sperm protein extracts show essentially no Dnmt2 protein expression in wt sperm. 2 independent replicates are shown. (Data for panel A provided by Francesca Tuorto).

4.2.2 Dnmt2$^{-/-}$ germline tissues show no phenotypic or functional aberrations

To detect any structural differences between testes of both genotypes, paraffin-embedded sections were hematoxylin-eosin stained and microscopically examined (**Fig. 10A**). Additionally, DNA and RNA content of these sections was analyzed by acridine orange staining (**Fig. 10B**). These assays showed that the testicular tissues had no phenotypic differences and sperm production and DNA and RNA content was comparable. To confirm the notion that sperm production took place at physiological levels, a viability assay of epididymal sperm was carried out. Dnmt2$^{-/-}$ mice produced mature and viable epididymal sperm at wild type percentages (**Fig. 10C**). As such, Dnmt2$^{-/-}$ mice are fertile, show no microscopic testicular aberrations, and produce viable sperm in physiological quantities.

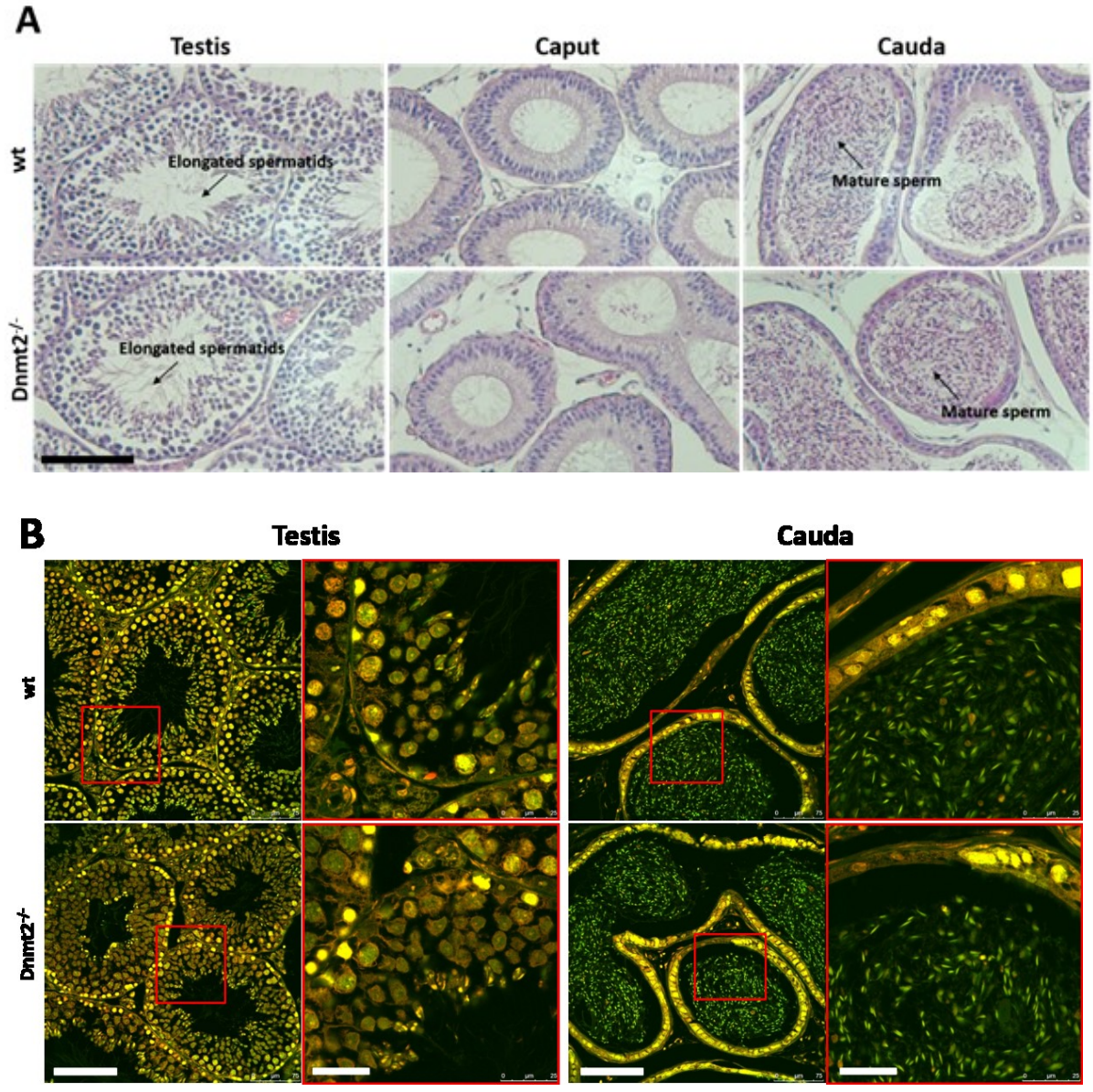

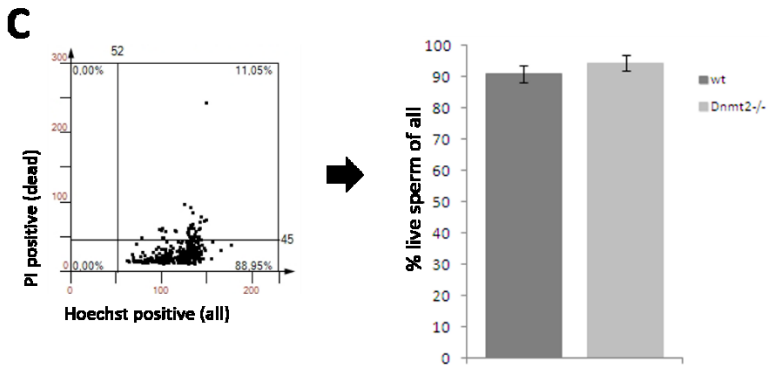

Figure 10. Dnmt2$^{-/-}$ germline cells show no phenotypic or functional aberrations. A. Haematoxylin and eosin stainings of testis and epididymal (caput and cauda) sections. No significant differences can be seen between wt and Dnmt2$^{-/-}$ samples. Sperm production is present in testis, and cauda epididymi contain mature sperm (scale bar = 100µm). **B.** Nucleic acid content of wt and Dnmt2$^{-/-}$ tissues is comparable. Acridine orange staining of testis and cauda epididymi sections (scale bar = 100µm). Small red squares are shown in higher magnification to the right of each image (scale bar = 25µm). RNA is stained in red, DNA is stained in green; colocalization of both signals appears as yellow. **C.** PI and Hoechst stainings show no significant difference between wt and Dnmt2$^{-/-}$ sperm viability. In this live/dead staining, each Hoechst-positive (x-axis) signal represents a sperm cell and each PI-positive (y-axis) signal represents a dead cell (Diercks et al., 2012). An exemplary result of one replicate is shown (wt). Each genotype was analyzed in biological triplicates from 3 different mice and additional technical replicates. The percentage of live sperm was normalized to false positive signals and is shown in a bar plot with standard deviation. (Data were generated with support from Beatrix Imkeit and Vera Gramm, in the laboratory of Johannes Schenkel, DKFZ).

4.2.3 Characterization of RNA in sperm

The most established functions of Dnmt2, i.e. tRNA methylation and its contribution to tRNA stability, led to the analysis of tRNA methylation and tRNA integrity in testis and sperm.

4.2.3a Dnmt2 mediates C38 methylation on tRNA^{AspGUC}, tRNA^{GlyGCC}, and tRNA^{ValAAC} in sperm

The known C38 methylation activity of Dnmt2, also in testis (Tuorto et al. 2012), was confirmed to be present in sperm by 454 deep sequencing (**Fig. 11A**). In parallel, as Dnmt2-mediated methylation is known to confer tRNA stability (Schaefer et al. 2010; Tuorto et al. 2012), Northern blots were performed.

4.2.3b Dnmt2 confers tRNA integrity in sperm

Northern blotting confirmed that wild type (Kawano et al. 2012; Peng et al. 2012) as well das Dnmt2$^{-/-}$ sperm contain high quantities of tRNA degradation products. The Northern blots also revealed a prominent fragmentation of the Dnmt2 target tRNA^{Gly} in Dnmt2-deficient sperm (**Fig. 11B**), which is likely caused by the lack of Dnmt2-mediated C38 methylation (Tuorto et al. 2012). 5' fragments of the Dnmt2 substrate tRNA^{Asp} did not appear to be influenced in the same manner, which is similar to published observations, where it became clear that tRNA^{Asp} 3' fragments are much more abundant than 5' fragments in Dnmt2 deficient mice (Tuorto et al. 2015). An important question was whether other RNAs were directly or indirectly affected by the Dnmt2 deficiency. This was approached by smallRNA-Seq.

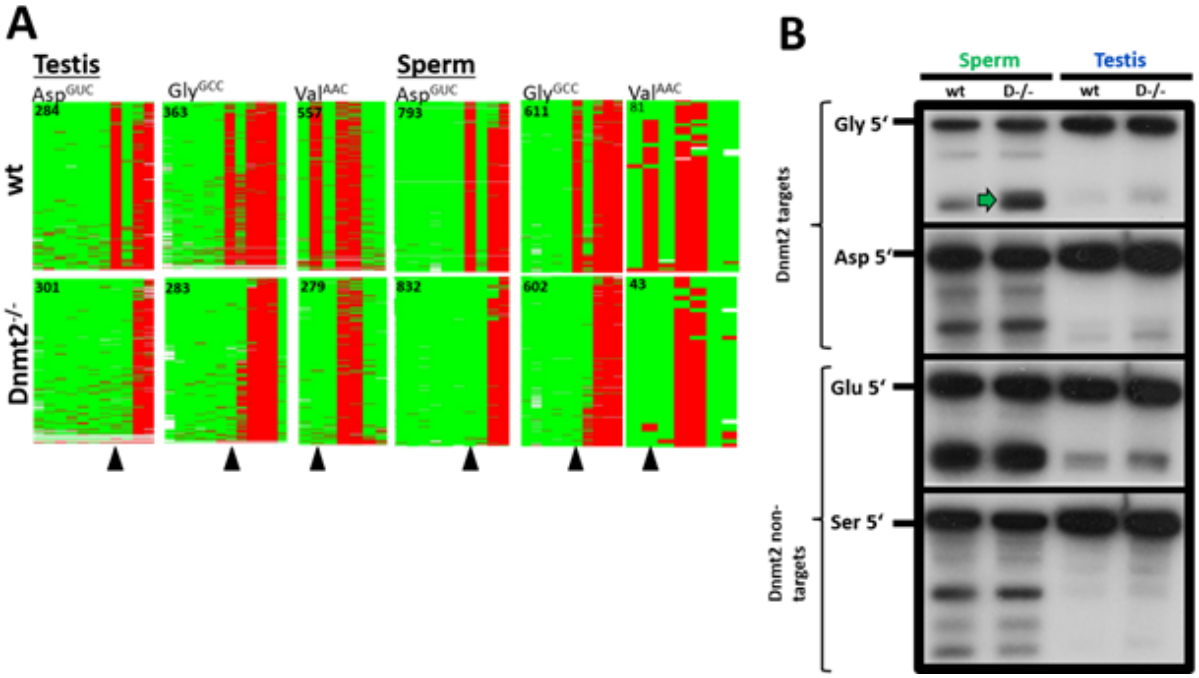

Figure 11. Dnmt2 confers tRNA methylation and integrity in sperm. A. Bisulfite sequencing maps for the three known tRNA targets of Dnmt2, of testis and sperm. Each row represents one sequence read, each column a cytosine residue. Green boxes represent unmethylated cytosine residues, red boxes indicate methylated cytosine residues, sequencing gaps are shown in white. Numbers in maps indicate the number of reads, and cytosine C38 is indicated with red arrowheads. **B.** Northern blotting of sperm and testis RNA confirms that tRNA fragments appear enriched in sperm. Additionally, when comparing wild type and Dnm2$^{-/-}$ samples, the Dnmt2 substrate tRNA^{Gly} is substantially more degraded in the mutant background than two non-substrates (tRNA^{Glu} and tRNA^{Ser}), as indicated by a green arrow. No concrete increase in 5' fragments of Dnmt2 substrate tRNA^{Asp} were detectable, as further elucidated in the text.

4.2.3c Dnmt2$^{-/-}$ sperm show only subtle smallRNA expression changes

As sperm contain high quantities of RNA break down products (Kawano et al. 2012; Peng et al. 2012) and results so far indicated a possible role of tRNAs or tRNA-derived fragments (tRFs) (Lee et al. 2009) in Dnmt2-deficient mice, smallRNA-Seq of epididymal sperm was carried out. Sequencing data were analyzed with respect to length distribution, composition (classes of RNAs), and differential expression. High levels of rRNA reads were evident and expected, as the vast majority of mature mammalian sperm RNA are products of rRNA fragmentation (Johnson et al. 2011). Due to the known fragmentation of rRNA in sperm, the efficiency of an rRNA depletion via commercially available hybridization kits was questionable, and was thus omitted, resulting in high amounts of rRNA reads. Length distribution analyses exhibit no significant differences specifically between the genotypes (**Fig. 12A**). Testicular Dnmt2$^{-/-}$ sample (1) shows a clear peak at 24nt (**Fig. 12A**), which is possibly caused by rRNA fragmentation products as can be seen by a higher rRNA content of the 21-25nt fraction for this sample (**Fig. 12B**). An in-depth analysis of the RNA composition of each sequenced sample and additionally the RNA composition of different length categories demonstrated only minor differences (**Fig. 12B**), which were analyzed in further depth. DESeq analysis revealed that only 11 piRNAs (Piwi-interacting RNA) and 6 tRFs were deregulated in Dnmt2$^{-/-}$ versus wild type sperm RNA (**Fig. 13**).

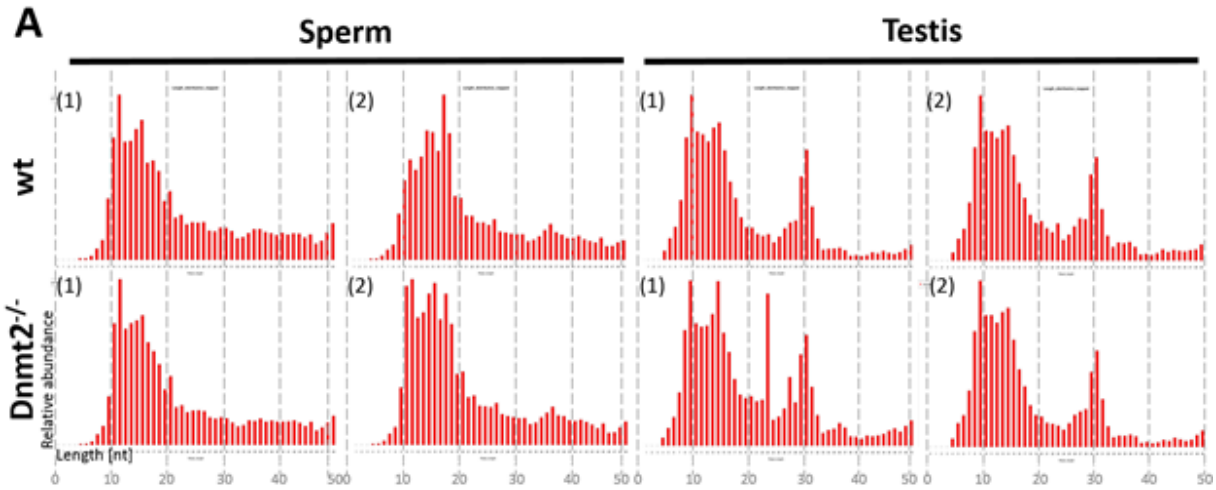

Figure 12. Dnmt2$^{-/-}$ sperm show only subtle smallRNA profile changes. A. Length distribution plots of all reads, with nucleotide lengths 1-50 (as sequenced) on the x-axis and relative abundance (normalized to total reads of the respective sample) on the y-axis. Replicates (marked (1) and (2)) show reproducibility. Observable differences between the genotypes are discussed in the text. **B.** Detailed analysis of the composition of the sequenced RNA. Duplicates of each sperm and testis are depicted. First, all (1-50nt) reads were analyzed with respect to composition. In smaller graphs below, all reads were broken down into length categories and re-analyzed.

Sperm

	RNA	Fold change	q-value
↓	Mus_musculus_chr3.trna282-GlyCCC_(96115177-96115247)_Gly_(CCC)_71_bp_Sc:_51.51	0.213488106	0.000212814
↓	FR0303691|Piwi-interacting_RNA_(piRNA)	inf	0.000304613
↓	FR0240364|Piwi-interacting_RNA_(piRNA)	inf	0.004066375
↓	Mus_musculus_chr3.trna754-GluTTC_(96191399-96191328)_Glu_(TTC)_72_bp_Sc:_72.33	0.218060399	0.005643839
↓	FR0116597|Piwi-interacting_RNA_(piRNA)	inf	0.014664879
↓	FR0072818|Piwi-interacting_RNA_(piRNA)	0.007568229	0.016455664
↓	FR0143401|Piwi-interacting_RNA_(piRNA)	0.007568229	0.016455664
↓	Mus_musculus_chr11.trna1817-GlnCTG_(68938180-68938109)_Gln_(CTG)_72_bp_Sc:_73.65	0.253818611	0.022431755
↓	FR0125708|Piwi-interacting_RNA_(piRNA)	0.008086897	0.024651193
↓	FR0295724|Piwi-interacting_RNA_(piRNA)	0.028209431	0.025003497
↓	Mus_musculus_chr13.trna64-GlnCTG_(21264220-21264291)_Gln_(CTG)_72_bp_Sc:_73.65	0.261616788	0.027349611
↓	Mus_musculus_chr13.trna982-GlnCTG_(22025901-22025830)_Gln_(CTG)_72_bp_Sc:_73.65	0.26155121	0.031274993
↓	FR0089666|Piwi-interacting_RNA_(piRNA)	inf	0.031274993
↓	FR0363328|Piwi-interacting_RNA_(piRNA)	0.134272267	0.036593192
↓	FR0393263|Piwi-interacting_RNA_(piRNA)	0.033927214	0.040257206
↓	FR0282618|Piwi-interacting_RNA_(piRNA)	0.034324031	0.043758657
↓	Mus_musculus_chr4.trna626-AlaCGC_(131681174-131681245)_Ala_(CGC)_72_bp_Sc:_59.08	0.294250691	0.047497886

Testis

	RNA	Fold change	q-value
↓	FR0050719|Piwi-interacting_RNA_(piRNA)	0.085700025	5.99E-19
↑	FR0354334|C/D_box_guide_small_nucleolar_RNA_(snoRNA)_SNORD46_/_U46	3.913449335	1.02E-15
↑	FR0009892|C/D_box_small_nucleolar_RNA_(snoRNA)	3.506090179	3.14E-11
↑	FR0055923|Piwi-interacting_RNA_(piRNA)	11.60133522	3.48E-09
↓	FR0081670|Piwi-interacting_RNA_(piRNA)	0.04602845	2.11E-07
↑	FR0354047|C/D_box_guide_small_nucleolar_RNA_(snoRNA)_SNORD46_/_U46	2.636186838	1.88E-06
↓	FR0232546|C/D_box_small_nucleolar_RNA_(snoRNA)	0.055312425	1.15E-05
↓	FR0032453|Piwi-interacting_RNA_(piRNA)	0.089932292	5.83E-05
↑	FR0239952|H/ACA_box_guide_small_nucleolar_RNA_(snoRNA)_ACA17_/_SNORA17	4.183956567	5.99E-05
↑	FR0031409|Piwi-interacting_RNA_(piRNA)	7.174148524	0.001280998
↓	FR0296528|Piwi-interacting_RNA_(piRNA)	inf	0.001625955
↑	FR0297833|small_nucleolar_RNA_(snoRNA)_U39	2.599756193	0.005950271
↑	FR0350066|C/D_box_guide_small_nucleolar_RNA_(snoRNA)_SNORD39_/_U39	2.633178603	0.006099254
↓	FR0016791|Piwi-interacting_RNA_(piRNA)	0.023347987	0.00665195
↓	FR0154304|Piwi-interacting_RNA_(piRNA)	inf	0.011281383

Figure 13. Dnmt2$^{-/-}$ sperm show only few smallRNA expression changes. Differential expression analysis by DESeq of sperm wt and Dnmt2$^{-/-}$ duplicates revealed that merely 17 RNAs were deregulated between the genotypes; 11 piRNAs and 6 tRNA fragments. In testicular samples, 15 RNAs were deregulated: 8 piRNAs and 7 snoRNAs. Hits are sorted by significance (q-value, cut-off at 0.05) and marked as up- (green arrow) or down-regulated (red arrow) in the mutant. Infinite fold change (inf) occurs when expression in one genotype was 0.

Possible involvement of the deregulated RNAs in different pathways were considered. As tRFs have been confirmed to bind and regulate siRNA pathway components (Durdevic, Mobin, et al. 2013; Cole et al. 2009; Haussecker et al. 2010) and as piRNAs are responsible for silencing of transposable elements (TEs) (Di Giacomo et al. 2013), both of these routes were considered and tested for deregulation. The RNA-induced silencing complex (RISC) includes the Argonaute (AGO) protein, which binds tRFs (Haussecker et al. 2010). A RISC reporter assay (Béthune, Artus-Revel, and Filipowicz 2012) (kindly provided by Julien Béthune, University of Heidelberg) was used to assay whether the RNA-Seq detected deregulation of tRFs, or the observed differences of tRFs from previous Northern blots (**Fig. 11B**) might influence the efficiency of this pathway (**Fig. 14A**). The differences in RISC efficiencies between wild type and Dnmt2$^{-/-}$ MEFs were measured and were not significant (**Fig. 14B**).

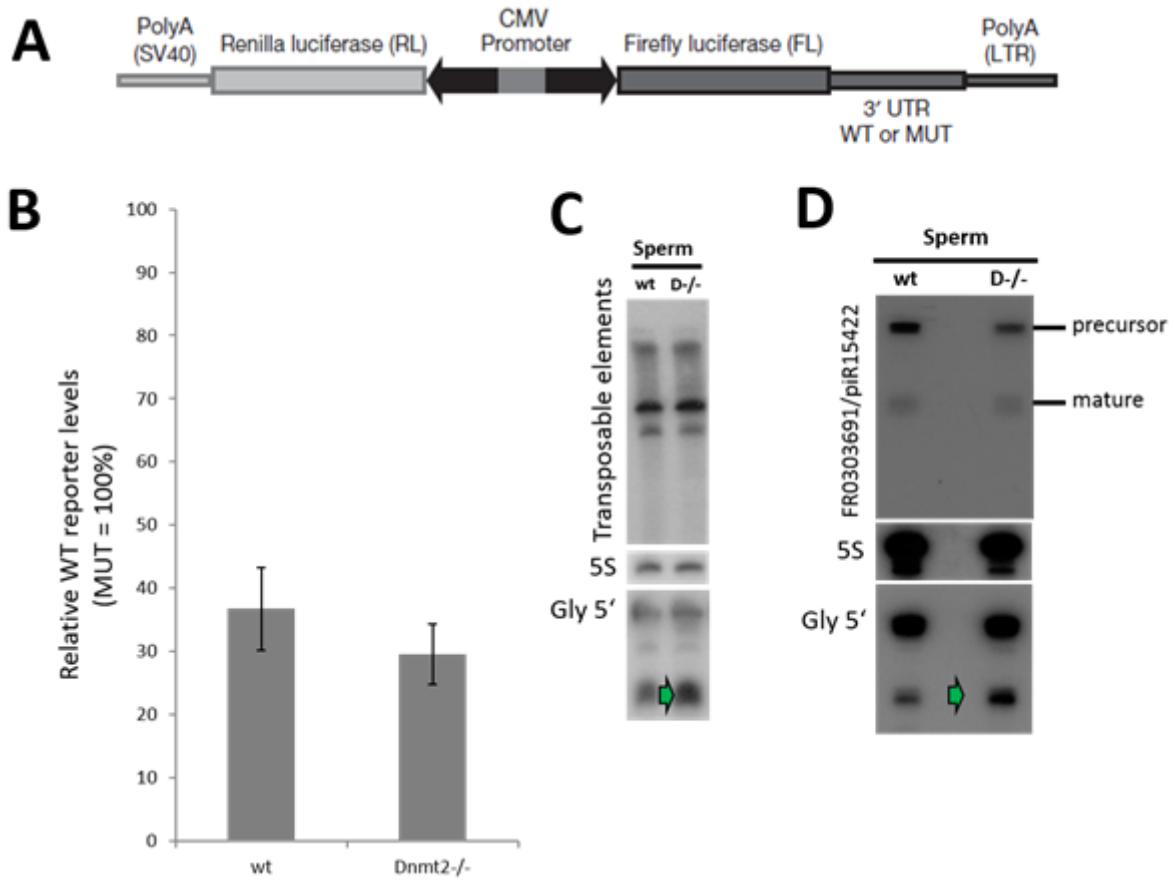

Figure 14. Candidate deregulated sperm small RNAs do not coincide with changes in small-RNA machinery or transposon control. A. RNA-induced silencing complex (RISC) reporter assay schematic (modified from Béthune et al., 2012). The construct has a control renilla luciferase (RL) without any miRNA target sequences, and a firefly luciferase (FL) fused to the 3'UTR of the hmga2 transcript with six consecutive let-7 miRNA target sites (WT). An additional, otherwise identical construct has mutated (MUT) let-7 target sites. MUT and WT constructs are separately transfected. FL and RL signals are normalized to a negative transfection control, then the FL signal is calculated as % of RL. It is then determined what % of the WT construct FL is expressed in comparison to the FL MUT (mutated) target. **B.** Results of the reporter assay on MEFs show no significant difference between the genotypes (biological duplicates, each with technical triplicates). The Dnmt2$^{-/-}$ silencing pathway functions at a comparable level to the wild type background. **C.** The deregulation of piRNAs detected in Dnmt2$^{-/-}$ sperm does not seem to have an effect on expression of transposable elements (TEs) in sperm. The TE mix consisted of probes for L1 5UTR, L1 ORF2, IAP 3LTR, and IAP GAG. 5S rRNA probe shows equal loading and a tRNA^{Gly} 5' probe shows the anticipated fragmentation difference as previously observed (green arrow). **D.** Northern blot probing for the most significantly downregulated piRNA (FR0303691/piR15422) from small RNA-Seq results. 5S rRNA probe shows a slight difference in loading and a tRNA^{Gly} 5' probe shows the anticipated fragmentation difference as previously observed (green arrow).

To test whether the deregulation of piRNAs could lead to effects on repetitive element expression, a Northern blot analysis was carried out on sperm (**Fig. 14C**). The different probes applied were used for detection of the retrotransposon LINE1 5' untranslated region (L1 5UTR), LINE1 open reading frame 2 (L1 ORF2), intracisternal A particle 3' long terminal repeat (IAP 3LTR), and the IAP GAG (Di Giacomo et al. 2013). As controls, a 5S rRNA and a $tRNA^{Gly}$ probes were applied, which showed equal loading (5S) and the previously observed difference in $tRNA^{Gly}$ fragmentation in $Dnmt2^{-/-}$ sperm. The results of these experiments confirmed that no major effects could be detected between the tested wild type and $Dnmt2^{-/-}$ sperm small RNA pathways. **Figure 14D** shows that indeed, the most deregulated sperm RNA-Seq hit, piRNA (FR0303691/piR15422), does not show a substantially differential expression between wild type and $Dnmt2^{-/-}$ sperm. Together, these experiments led to the conclusion that the few differences in small RNA-Seq of sperm may have been caused by physiological variation, without biological relevance. Additionally, the differentially regulated small RNAs of RNA-Seq displayed no overlap with differentially regulated transcripts from the RNA-Seq data of ESCs or E7.5. As the only major difference between wild type and $Dnmt2^{-/-}$ tissues seemed to be restricted to C38 methylation and its role in tRNA stability, this prompted a deeper analysis of pathways involved in the regulation of this highly specific activity.

4.3 Examination of biological pathways that control Dnmt2-mediated tRNA methylation

The experimental approaches so far demonstrated that mouse Dnmt2 is highly expressed in the germline and functions as a three-tRNA-specific methyltransferase that contributes to tRNA integrity in sperm. These functions have no phenotypic effects on the examined cells or mice upon knockout of Dnmt2, however are likely to be key regulatory functions of RNA-mediated inheritance. To be able to find indications of the biological mechanism of Dnmt2-dependent RNA-mediated inheritance, it was sought to find regulators of C38 methylation that may act in the same pathways as Dnmt2.

4.3.1 Screening of tissues and cell culture conditions reveals nutrient control of C38 methylation

To uncover the conditions that might alter C38 methylation, a screening experiment of both physiological as well as non-physiological conditions was carried out. Different tissues,

differentiation states, stresses, and nutrients, in cell culture as well as in live mice were assayed by bisulfite sequencing of $tRNA^{AspGUC}$ (and other Dnmt2 target tRNAs) (**Fig. 15A**).

Recent research demonstrated that $tRNA^{AspGUC}$ C38 methylation can be decreased by depriving yeast cultures of the micronutrient queuine (Q) (Müller et al. 2015). This nutrient was thus analyzed in depth, along with other conditions. The majority of tested conditions evoked no C38 methylation changes, however a few nutrient-deprived conditions resulted in a clear $tRNA^{AspGUC}$ C38 methylation decrease.

Mouse tissues under physiological conditions were examined with respect to methylation levels. The sequenced tissues generally showed very high C38 methylation (between 92% and 100%) (**Fig. 15A**). This was also the case for tissues that are involved in the two known phenotypes of $Dnmt2^{-/-}$ mice: bone marrow (92%) in translation and differentiation (Tuorto et al. 2015) and testis (98%), sperm (97%), and early embryos (96%) in inheritance (Kiani et al. 2013). The only exception to this was the testis P5 samples (testis of 5 day-old mice), in which C38 methylation appeared slightly decreased (85%). This is elucidated in detail in the discussion. Under non-physiological conditions, i.e. in axenic (germ-free) mice, methylation levels were also comparable to control tissues (testis 98% vs. 98%; sperm 97% vs. 97%; embryos 96% vs. 98%).

Analyzing cell lines under standard laboratory conditions, methylation levels appeared slightly lower than those of mouse tissues, and under some non-physiological conditions, methylation levels were decreased substantially. Q is present in most animal and plant material (Katze, Basile, and McCloskey 1982). However, treatment of serum with charcoal is known to deplete the serum of hormones (Drouin, Lagacé, and Labrie 1976), fatty acids (Chen 1967), and Q (Katze 1978). When this depleted serum was added to cell culture media instead of standard fetal calf serum, C38 methylation decreased (see “HeLa Ctrl” at 96% vs. “HeLa charcoal” at 56%) (**Fig. 15A**). Horse serum is known for naturally low levels of the micronutrient Q (Langgut and Kersten 1990), and Lonza UltraCulture (herein referred to as Lonza) medium has only very few and very pure constituents from animal source and can be applied without FCS. Both DMEM supplemented with horse serum (see “HeLa Horse serum” at 65%) and Lonza medium on its own (see “HeLa Lonza” at 52% or “MEFs Lonza” at 74%) elicited C38 methylation decreases when compared to controls (see “HeLa Ctrl” at 96% and “MEFs Ctrl” at 85%) (**Fig. 15A**). Culturing MEFs under hypoxic conditions in standard medium seemed to have no clear effect on C38 methylation (see “MEFs Hypoxia” at 86% vs. “MEFs

Ctrl" at 85%), however the combination of Lonza media (which alone caused a decrease to 74%) together with a hypoxic environment appeared to have a synergistic effect on C38 methylation (see "MEFs Lonza + hypoxia" at 64%). MEFs that were cultured with galactose instead of glucose, enhancing oxidative mitochondrial metabolism (Aguer et al. 2011), or MEFs induced to differentiate could be speculated to have gained C38 methylation (see "MEFs Ctrl" at 85% to "MEFs -glu +gal" at 97%, "MEFs Adipogenic" at 93%, and "MEFs Osteogenic" at 94%).

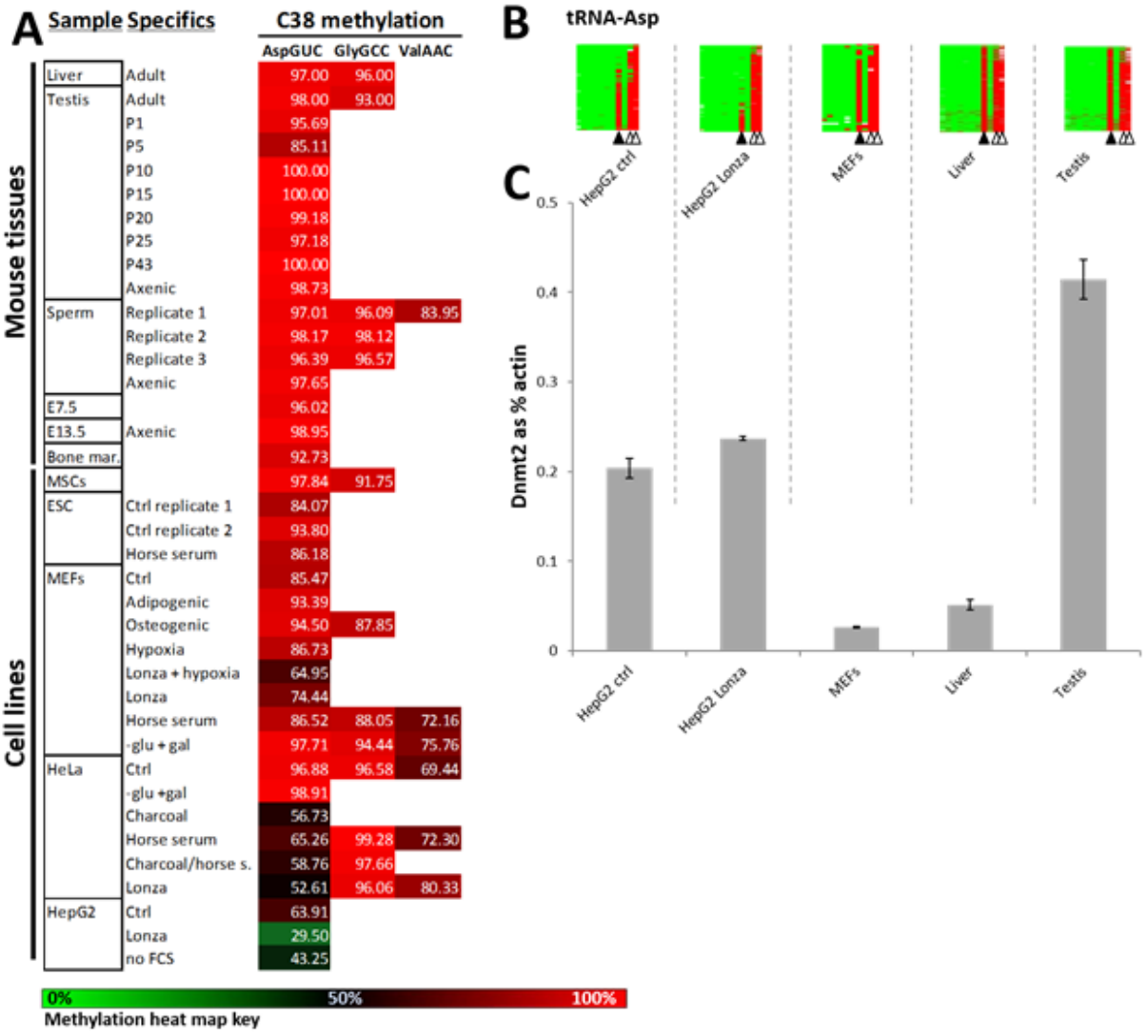

Figure 15. Screening of different conditions reveals nutrient control over C38 methylation. A. C38 methylation was tested in a variety of conditions by targeted bisulfite sequencing, in all cases on $tRNA^{AspGUC}$, and additionally in some on $tRNA^{GlyGCC}$ and $tRNA^{ValAAC}$. For only one mouse tissue sample, a decrease in C38 methylation from the generally fully methylated status could be observed for $tRNA^{AspGUC}$ (P5 testis). P1 stands for 5 day old mice, P5 for 5 day old mice, and so on. For a few cell culture conditions within a cell line, C38 methylation level fluctuation was observed. C38 methylation

levels of $tRNA^{GlyGCC}$ and $tRNA^{ValAAC}$ were generally not affected. (horse s. – horse serum). **B.** A selection of heat maps are shown, presenting a decrease in C38 methylation (black arrowheads) in HepG2 Lonza vs. HepG2 ctrl, while C48/49 methylation (white arrowheads) remained unaffected (Panels A and B include limited contributions by Francesca Tuorto and Tanja Musch). **C.** The decreases of C38 methylation shown in **B** is not proportional to Dnmt2 expression, as shown by qRT-PCR of correspronding samples immediately below. Levels of C38 methylation in Lonza medium are low while Dnmt2 levels remain high. Additionally, low levels of Dnmt2 in MEF cultures suffice to fully methylate C38.

To understand whether observable changes in C38 methylation were caused by a change in Dnmt2 expression, qRT-PCR was performed and revealed that the nutrient levels that had an effect on C38 methylation had no correlating effect on Dnmt2 expression (**Fig. 15B+C**). This is in line with the fact that C38 methylation was only affected on $tRNA^{AspGUC}$, however not on the other Dnmt2 targets, $tRNA^{GlyGCC}$ or $tRNA^{ValAAC}$ (**Fig. 15A**).

4.3.2 Micronutrient Q controls Dnmt2-mediated $tRNA^{AspGUC}$ methylation

Under physiological conditions, the nucleobase Q replaces guanine (G) in the wobble position of GUN anticodons ($tRNA^{AspGUC}$, $tRNA^{HisGUG}$, $tRNA^{TyrGUA}$, and $tRNA^{AsnGUU}$). Thus, cultures in which a decrease of C38 methylation was observed were tested for the presence of queuosinilated tRNAs (Q-tRNAs) by acryloyl aminophenylboronic acid (APB) Northern blotting. Q-tRNAs carry an additional ribose moiety when compared to non-Q-tRNAs (G-tRNAs), which slows down their migratory properties on gels containing polyacrylamide covalently bound to APB (Igloi and Kossel 1985). This allows to separate and quantify them by gel electrophoresis and subsequent blotting. For this purpose, $tRNA^{HisGUG}$ probes were used, as Q-$tRNA^{HisGUG}$ can be separated from G-$tRNA^{HisGUG}$. Unfortunately, Q-$tRNA^{AspGUC}$ could not be separated from G-$tRNA^{AspGUC}$ on APB gels, presumably due to an additional mannosylation of Q which is known to be present on Q-$tRNA^{AspGUC}$ (Kasai et al. 1976), and a resulting change in migratory properties (Zaborske et al. 2014). All cultures that were tested and exhibited a decrease in C38 methylation in comparison to a control medium, did in fact lack Q (**Fig. 16A**). As specific developmental stages of *Drosophila melanogaster* are known to have low Q levels (Zaborske et al. 2014), these samples were used to confirm that a decrease in C38 methylation is also evident here (**Fig. 16A**). To evince that Q is necessary for physiological C38 methylation levels,

synthetic Q was obtained for rescue experiments (kindly provided by Hans-Dieter Gerber, University of Marburg). The synthetic Q was readily accepted by the cells and incorporated into tRNA (**Fig. 16A**). Upon addition of Q to previously Q-deprived cultures, C38 methylation could be induced to full methylation levels (**Fig. 16A**). Queuosinilation thus acts as a regulator of C38 methylation on $tRNA^{AspGUC}$ in mammalian cells.

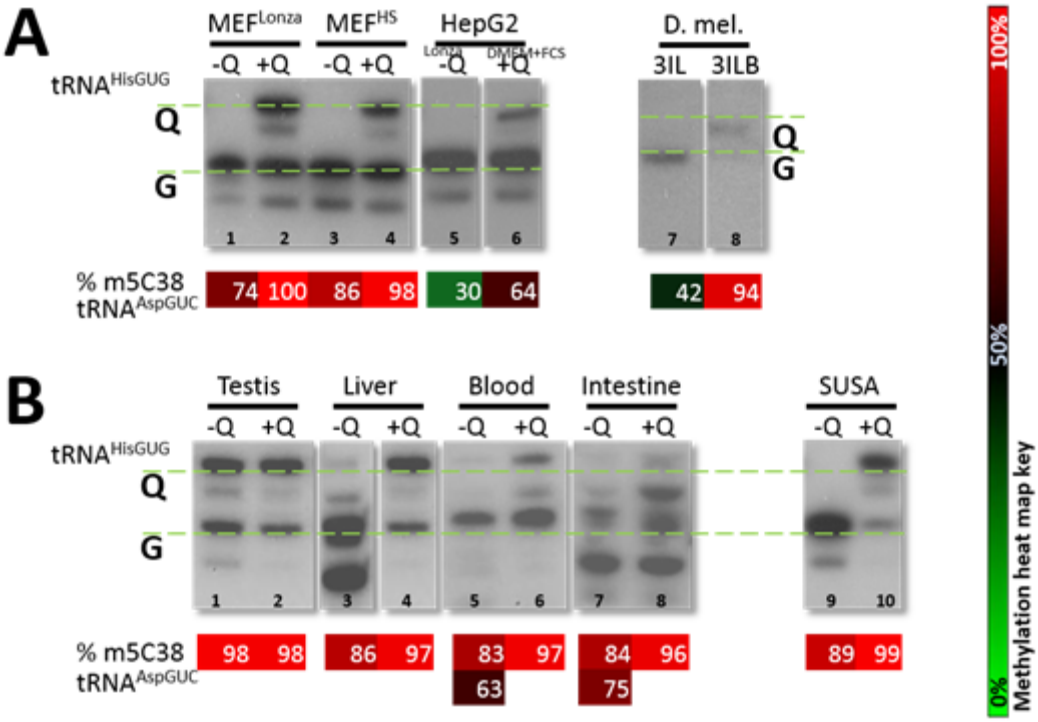

Figure 16. Micronutrient Q controls Dnmt2-mediated $tRNA^{AspGUC}$ methylation. Acryloyl aminophenylboronic acid (APB) gels show queuosinilation levels of $tRNA^{HisGUG}$ in different samples. Each horizontal black bar marks 2 lanes to be compared (both always on the same gel; some images edited for sake of order). Corresponding $tRNA^{AspGUC}$ methylation levels by 454 bisulfite sequencing are given as % methylated underneath each lane (% m5C38). **A.** Different cell cultures show relatively low C38 methylation in –Q media. As a parallel control, *Drosophila melanogaster* samples of 3rd instar larvae (3IL) and 3IL brain (3ILB) are shown (lanes 7 and 8). The addition of synthetic Q (lanes 2 and 4) or growth in +Q media (DMEM+FCS, lane 6), reliably resulted in an increase of C38 methylation levels when compared to –Q samples. (HS – horse serum). **B.** Different –Q and +Q mouse tissues are shown. Lanes 1-4 compare –Q axenic NMRI mice to normal (+Q) BL/6 controls. Lanes 5-8 compare –Q NMRI to rescued +Q NMRI mice. Blood and intestinal –Q samples (lanes 5 and 7) were 454-sequenced as independent duplicates from different mice (after only 5 weeks of a –Q diet) and are presented in a second row. Lanes 9 and 10 show a testicular germ cell tumor line cultured with or without Q. (HepG2 data was partially generated by Tanja Musch. Axenic mice were held by Larissa Ziegler, in the facilities of Kurt Reifenberg, DKFZ).

4.3.3 Q deficiency as a mimick of Dnmt2 mutation

To test for similarities between Q deficiency and Dnmt2 deficiency in mice or whether a lack of Q mimicks a lack of Dnmt2, a Q-free (–Q) environment was established *in vivo*. As mammals cannot synthesize their own Q, their gut flora or nutrition provides them with Q (Reyniers et al. 1981; Farkas 1980). Thus, a germ-free mouse model (axenic NMRI mice) receiving a Q-free diet was required. A small axenic mouse colony was held with –Q feed for 9 weeks. –Q diets resulted in different tissues showing different levels of queuosnilated tRNA, with a coinciding change in C38 methylation on $tRNA^{AspGUC}$ (**Fig. 16B**). Tissues composed of cells with a high production or turnover rate, i.e. blood (Ogawa 1993) and small intestine (Cheng and Leblond 1974; Ogawa 1993) had very low levels of Q-tRNA after 9 weeks, whereas testis, composed of cells with very low turnover rates (Teerds et al. 1989), retained high levels of Q-tRNA (**Fig. 16B**). In these slow-turnover tissues, Q is salvaged, i.e. recycled and thus is continuously incorporated into tRNA (Fergus et al. 2015). In order to efficiently remove Q from all tissues and avoid salvage, mice may have to be held on a Q-free diet for substantially longer periods of time. Obtaining a second generation of mice in a –Q diet was currently not successful. The presence of vaginal plugs indicated successful mating, and an increase in female body weight in one case gave the impression of pregnancy, however no offspring were found. The diet may have to be optimized to create a nutritional environment that will increase the rate of pregnancy and offspring. The liquid diet seemed to stick to the fur upon excretion, which led to an increase in grooming around the anus, and mice did not seem as active as mice on a control diet. However, no cause for nutritional deficiencies was evident when considering the composition of the diet. Regardless of not having any litters or long-term –Q colonies, even for this shorter period of –Q feeding there is a clear relationship between Q-content of tissues and C38 methylation levels (**Fig. 16B**). Less Q on tRNAs results in reduced levels of C38 methylation on $tRNA^{AspGUC}$. In parallel to the axenic mice, and to complement the *in vivo* data, an available testicular germ cell tumor cell line (SUSA) was cultured in –Q medium. The results demonstrated that –Q can in fact lead to reduction of C38 methylation in testicular tissues, and argues that the high Q levels and C38 methylation in axenic mouse testis may well be due to slow tissue turnover (**Fig. 16B**). Prolonged –Q mouse diets may thus result in substantially lower C38 methylation levels and may present a second model to parallel Dnmt2 mutants.

The presented data shows that physiological $tRNA^{AspGUC}$ C38 methylation depends on the nutrient Q in mice.

5. Discussion

The biological functions of Dnmt2 are gradually being determined, with the most recent discoveries of its role in polypeptide synthesis and contribution to proper haematopoiesis (Tuorto et al. 2015), and RNA-mediated inheritance (Kiani et al., 2013). The data presented in this thesis contributes findings on Dnmt2's function with respect to its (1) high target specificity and its (2) activity in response to environmental factors. (3) Additional findings may facilitate further research on its role in RNA-mediated inheritance.

5.1 Dnmt2-dependent RNA inheritance: the target tissues

5.1.1 Dnmt2 deficiency has no observable effect on embryo morphology and mild or no effects on the transcriptome of embryonic cells

Dnmt2$^{-/-}$ mice are viable and fertile (Goll et al. 2006), and in line with this, no major phenotypic aberrations could be detected on the examined cells and tissues. To move from the macro to the molecular levels, RNA-Seq was performed. Instead of using mRNA-enrichment protocols, rRNA depletion was applied in order to also capture possible changes in ncRNA. As the detected differences between wild type and Dnmt2$^{-/-}$ samples could mostly not be validated, these are likely due to natural variation between samples rather than due to the mutation itself (**Fig. 6**). Transcripts with a high fold change and significant q-values generally had low normalized read counts (**Fig. 5**), which means that small absolute differences in expression can lead to large relative differences in expression and thus be detected as differentially expressed. The fact that most of the tested differences could not be reproduced by qRT-PCR added to the notion of minor or no effects of a Dnmt2 deletion on the embryo and ESC transcriptomes. These results are in line with previous studies which showed only minute changes in the transcriptome of Dnmt2$^{-/-}$ MEFs, liver samples, and bone marrow samples (Tuorto et al. 2012; Tuorto et al. 2015).

5.1.2 Dnmt2 is a highly specific tRNA methyltransferase with three target cytosines

The WTBS approach did not only confirm that Dnmt2 methylates C38 of $tRNA^{AspGUC}$, $tRNA^{GlyGCC}$, and $tRNA^{ValAAC}$, but revealed that Dnmt2 is most likely specific to only these three target cytosines. The largest fraction (99.1%) of all detected methylated cytosines belonged to the validated tRNA targets. The remaining marginal fraction (0.9%) belonged to a much larger number of non-validated targets (**Fig. 8A+B**). 128 candidate methylation sites were found in only 42 RNAs, averaging to 3 methylation sites per transcript, compared to only 1 site per RNA within the known substrates. This indication that these candidates may be part of background noise was further underlined by targeted amplicon sequencing, which failed to confirm a promising candidate. There is a residual chance that there are additional targets, however it is likely that these are false positives, as discussed in the following. The origin of false positives may stem from biological, biochemical, as well as mapping factors. Many false positives may well be eliminated by sequencing additional replicates in order to compensate for random batch effects. miRNAs also appeared to be potentially methylated transcripts, with multiple unconverted cytosines (**Supplemental Table S1**). As strong secondary structure is known to decrease bisulfite conversion efficiencies (Schaefer et al. 2009), it is conceivable that miRNAs may bind complementary RNAs and/or proteins of the miRNA pathway and thus be partially protected from bisulfite conversion. Thorough protein removal from samples, for example by proteinase K digest following RNA isolation may be a factor to consider in future approaches (Warnecke et al. 2002). Improvements are in progress for mapping with higher confidence. For example, reads in which a high fraction (e.g. 80%) of cytosines remained unconverted can be filtered, as strong secondary structure or bound proteins may have protected these transcripts. The mapping of bisulfite converted reads can be a challenge, as the complexity decreases from 4 to only 3 bases. In combination with the short length of fragmented or naturally short transcripts, this can be a cause for incorrect mapping. Due to the loss of complexity, homopolymeric regions such as in the Vax2os candidate become likely and cause reads to map incorrectly.

It was shown that Dnmt2 most likely has no methylation targets outside of $tRNA^{AspGUC}$, $tRNA^{GlyGCC}$, and $tRNA^{ValAAC}$. With this substrate specificity, and knowing that Dnmt2 is required for

RNA mediated inheritance (Kiani et al., 2013), RNAs in transmitting cells were characterized, with a special focus on tRNAs.

5.2 Dnmt2-dependent RNA inheritance: Characterization of transmitting cells

5.2.1 The molecular function of Dnmt2 in the male germline seems to be restricted to tRNA methylation and integrity

The high levels of Dnmt2 mRNA in testis as well as sperm and comparably lower expression in other tissues argues for a specific role of Dnmt2 in the germline (**Fig. 9A+B**). The three targets, $tRNA^{AspGUC}$, $tRNA^{GlyGCC}$, and $tRNA^{ValAAC}$ are indeed methylated in testis as well as sperm (**Fig. 11A**). In contrast to the high levels of Dnmt2 mRNA, essentially no Dnmt2 protein was detected in mature sperm (**Fig. 9G**). This may indicate a minor role of Dnmt2 in the sperm cell itself but a task for Dnmt2 immediately after fertilization within the zygote, possibly to assure proper tRNA integrity. A number of mRNAs evade fragmentation in sperm, and this pool of mRNAs has been suggested to be needed immediately upon fertilization (Grunewald et al. 2005; Ostermeier et al. 2004; Avendaño et al. 2009). This notion is supported by the presence of maternal Dnmt2 mRNA in zebrafish before the start of the zygotic transcription (Rai et al. 2007). Dnmt2 is not essential for embryogenesis, however it may be needed at this point for unknown mechanisms that allow RNA-mediated inheritance in mice. As it has been shown that Dnmt2 protein is detectable at considerable levels in immature sperm isolated from the testis and not the epididymis (Kiani et al., 2013), Dnmt2 is possibly loaded into sperm and then degraded along with other proteins as part of maturation along the epididymis (Belleannee et al. 2011; Krawetz 2005). The high expression of Dnmt2 protein levels in testis could be speculated to be involved in assuring sufficient Dnmt2 to be loaded into sperm for tRNA methylation within sperm before reaching full maturity in the epididymis, where Dnmt2 protein levels are low. It is not yet clear whether these expression patterns of Dnmt2 may be necessary for RNA-mediated inheritance or other biological processes.

Dnmt2 and its role in tRNA methylation does not seem to play a role in testis functionality, i.e. in sperm production and sperm viability (**Fig. 10C**). The bulk RNA and DNA content of

testicular and sperm Dnmt2$^{-/-}$ cells appear normal and are unlikely to play a role in RNA-mediated inheritance (**Fig. 10B**). The only observable difference between wild type and Dnmt2$^{-/-}$ samples was the lack of substrate methylation and stronger fragmentation of sperm tRNA^{Gly} in the mutant (**Fig. 11A+B**). Thus, the biological function of Dnmt2 in the germline is most likely assurance of tRNA integrity via C38 methylation, which is in line with publications on Dnmt2 in other tissues (Schaefer et al., 2010; Tuorto et al., 2012; Tuorto et al., 2015).

5.2.2 Dnmt2$^{-/-}$ sperm show increased tRNA^{Gly} fragmentation, whereas changes in expression levels of other small RNAs are limited

RNAs of sperm were deep-sequenced, since sperm RNAs have been shown to be the carrier of heritable information in a Dnmt2-dependent fashion (Kiani et al., 2013; Rassoulzadegan et al., 2006) and Dnmt2 was shown to methylate and stabilize tRNA in sperm (**Fig. 11A+B**). The highly abundant tRFs in proportion to full-length tRNAs, especially so in a Dnmt2$^{-/-}$ background (**Fig. 11B**) were hypothesized to be responsible for a purpose other than the classical role of tRNAs in translation. tRFs have been shown to play roles in a number of biological processes, for example a 5'-tRNA^{Val}-tRF of 26nt is known to have the capacity to reduce protein synthesis by binding to the ribosome and interfering with peptidyl transferase activity (Gebetsberger et al. 2012). Additionally, it has been shown that tRFs bind to DICER (Durdevic, Mobin, et al. 2013; Cole et al. 2009) and AGO proteins (Haussecker et al. 2010; Kumar and Mudunuri 2014; Karaiskos et al. 2015) and regulate RNA silencing. As Dnmt2 has been shown to play roles in both siRNA-mediated virus control (Durdevic, Hanna, et al. 2013) and in retrotransposon silencing (Phalke et al. 2009), small RNA pathways seemed to be a promising pathway to pursue. Also, small RNA pathway components play key roles right after fertilization, i.e. in the maternal-to-zygotic transition (Lykke-andersen et al. 2008; Svoboda and Flemr 2010; Suh and Blelloch 2011). Interestingly, a recent publication showed that tRFs, including derivatives of the Dnmt2 substrates tRNA^{Asp} and tRNA^{Gly}, are capable of displacing the RNA-binding protein YBX1 from 3' UTRs of several mRNAs, thereby decreasing the transcripts stabilities (Goodarzi et al. 2015). Thus, the small RNAs of sperm were sequenced to detect possible deregulation of tRFs and other regulatory RNAs.

Unexpectedly, small RNA-Seq of sperm showed only marginal changes. When viewing different classes of RNAs and what fraction of all sequenced RNAs they populate, some minor changes and fluctuations can be observed (**Fig. 12A+B**). However, when analyzing the data specifically for each transcript individually, only very few transcripts appeared as deregulated in Dnmt2$^{-/-}$ samples (**Fig. 13**). In sperm, these were exclusively tRNAs and piRNAs. These RNAs were considered and pathways in which these short transcripts may play a role were analyzed for possible effects. piRNAs posed a promising path, as several studies have detected tRNA-derived piRNAs (Keam et al. 2014; Hirano et al. 2014; García-López et al. 2014; Kwon et al. 2014). Additionally, Dnmt2 is responsible for nonrandom sister chromatid segregation, which may be connected to piRNA metabolism as well (Yadlapalli and Yamashita 2013). It has also been revealed that tRFs bind and regulate small RNA machinery that are involved in siRNA and piRNA pathways (Durdevic, Mobin, et al. 2013). Finally, a few small nucleolar RNAs (snoRNAs) appeared deregulated in Dnmt2$^{-/-}$ testis (however not in sperm) (**Fig. 13**), and some snoRNAs have been shown to be capable of target repression in a miRNA-like fashion (Thomson et al. 2014).

However, the RISC reporter assay showed that miRNA mediated RNA silencing processes were not affected in Dnmt2$^{-/-}$ MEFs. Moreover, Northern blot analyses displayed that the most significant RNA-Seq piRNA hit was not strongly deregulated and the general piRNA-mediated transposable element suppression was not substantially altered between the genotypes (**Fig. 14B-D**). These experiments indicated that the differences in small RNA-Seq between the genotypes may originate from simple physiological variation and not have a biological effect.

The presented data suggest that the increased abundance of tRFs (**Fig. 11B**) does not influence the analyzed small RNA pathways or the transcriptome substantially. Interestingly, a recent publication has shown that tRNA-derived small RNAs bind to AGO, however indeed do not mediate target repression and are thus speculated to carry out other unknown tasks (Thomson et al. 2014). The proteome rather than the transcriptome is a potential tRF-target to consider for several reasons. A special class of 5' tRFs (tiRNAs; tRNA-derived stress-induced RNAs) have been shown to be capable of reprogramming protein synthesis (Sobala and Hutvagner 2013), for example by displacing transcription factors from RNAs (Ivanov et al. 2011), and additionally cause assembly of stress granules, which are a sign of improper translation initiation (Emara et al. 2010;

Yamasaki et al. 2009). Further, we have recently shown that a lack of Dnmt2-mediated tRNA methylation can lead to codon mistranslation, as C38 methylation is suggested to be necessary for discrimination of near-cognate codons during polypeptide synthesis (Tuorto et al. 2015). Importantly, it has also been demonstrated that tRNA pools vary in their composition during different biological states, for example in proliferation versus differentiation (Gingold et al. 2014). Thus, loss of integrity and function of specific tRNAs, as can be seen in sperm samples for $tRNA^{Gly}$ (**Fig. 11B**), could potentially act in one of these translation-altering ways in early embryos.

In conclusion, Northern blotting showed that Dnmt2 stabilizes tRNAs in mouse sperm, the biological significance that this may have on RNA-mediated inheritance however remains to be established.

5.2.2b Potential sources for inconsistencies in sperm small RNA-Seq data

To understand the acquired data and inconsistencies with Northern blots better, sources for artifacts and differences between datasets were analyzed. In 2012, Peng et al. published that 67% of spermatozoal RNAs are tRNA-derived (Peng et al. 2012), however a number of other datasets did not show this extreme enrichment (Kawano et al. 2012; Gapp et al. 2014; García-López et al. 2014; Gan et al. 2011), including the dataset presented in this thesis. The fact that there are differences in sequencing results of mature sperm from different publications, and also that the fragmentation difference between wild type and $Dnmt2^{-/-}$ on Northern blots was not reproduced by small RNA-Seq, may stem from different sources. Some of the post-transcriptional RNA modifications can prevent proper cDNA synthesis by causing the reverse transcriptase to stall, leading to artifacts (Maden et al. 1995; Motorin et al. 2007). Additionally, the biochemical ligation of adaptors may be a source for differences in the datasets. As most small regulatory RNAs have a 5’ phosphate and a 3’ hydroxyl group, adaptor ligation steps in sequencing kits have been optimized for this purpose. However, since during RNA turnover reactions or RNase-mediated degradation, 3’ phosphoryl and 5’ hydroxyl ends can be present on RNAs (Hafner et al. 2008), polynucleotide kinase (PNK) was additionally used in this thesis to create appropriate 5’ phosphate and 3’ hydroxyl ends. This PNK step was taken to assure correct adapter ligation onto

all present RNAs and RNA fragments, and was not carried out by others (Gapp et al. 2014; Kawano et al. 2012; Peng et al. 2012; García-López et al. 2014). Other minor methodological differences can be found between the published datasets, however it is not clear whether these can explain all the observable differences in mature sperm small RNA content.

A Northern blot is more direct in this sense, as the probe directly binds to the target, independent of the chemical nature of the transcript ends. The numerous steps in a library preparation, including reverse transcription, the necessity for precise biochemical modifications on RNA ends, and PCR amplification, may be sources for artifacts.

In summary, Northern blots were regarded a direct approach with few error sources, and clearly showed an enrichment of $tRNA^{Gly}$ fragmentation in $Dnmt2^{-/-}$ sperm.

5.3 Examination of biological pathways that control Dnmt2-mediated tRNA methylation

To this point, the analyses concentrated on targets of Dnmt2, i.e. downstream factors of Dnmt2. These analyses confirmed Dnmt2's three-substrate specificity and its function in tRNA integrity. However, the second major aspect to be investigated were the upstream factors that control Dnmt2. The question arose whether there are any conditions under which Dnmt2 activity can be hampered. Finding such conditions could give new perspectives on how and why RNA-mediated inheritance (Kiani et al., 2013) and Dnmt2-mediated accurate polypeptide synthesis (Tuorto et al. 2015) occurs. The screening included physiological conditions such as differentiation and development, as well as stress conditions such as hypoxia and nutrient deprivation.

5.3.1 Micronutrient Q controls Dnmt2-mediated $tRNA^{AspGUC}$ methylation

In a broad overview, it appeared that the methylation levels of C38 seem to vary slightly between mouse tissues versus mouse cell cultures, and the different media that were tested have different magnitudes of effect, depending on which cell line they were applied to.

C38 methylation of $tRNA^{AspGUC}$ in all sequenced mouse tissues was between 92% and 100%, with the exception of testis P5, where a slight decrease seems to be evident (to 85.11%) (**Fig. 15A**). It is not clear whether this is caused by technical variation. However in principle it

could be considered for further investigation, as Q levels in *Drosophila* also change during development (Zaborske et al. 2014; Jacobson, Farkas, and Katze 1981; Siard, Jacobson, and Farkas 1991) and a similar phenomenon could in theory be responsible for a decrease of C38 methylation in mouse testis.

When mouse cell lines were grown in their standard "Ctrl" media (ESC replicates 1 and 2 and MEFs in DMEM+FCS), C38 methylation levels range from approximately 84% to 93% (**Fig. 15A**). All tested conditions showed that the strongest and most consistent influence on Dnmt2-mediated $tRNA^{AspGUC}$ C38 methylation was elicited by growing cells in medium deprived of Q. C38 methylation levels in human cell cultures appeared to be more sensitive to depletion of Q than in mouse cell cultures, as can be seen by the strong decrease of methylation from 96.88% in HeLa Ctrl cells (DMEM+FCS) to 56.73% in DMEM plus charcoal treated FCS, or even 52.61% in Lonza medium (**Fig. 15A**). It is currently unclear why this difference between mouse and human cultures may be the case. In mouse ESCs and MEFs, Lonza medium led to a drop from 85.47% C38 methylation in DMEM plus FCS to 74.44%. Culturing MEFs not only in Lonza, but creating a hypoxic environment in addition, appears to enhance the –Q effect on C38 methylation (MEF Ctrl at 85.47% vs. MEF Lonza 74.44% vs. MEF Lonza+hypoxia 64.95%) (**Fig. 15A**). Other stress factors (e.g. heat shock of *Drosophila* cells) have been shown to influence tRNA fragmentation (Schaefer et al., 2010), however a decrease in C38 methylation has not been published following stress. It is conceivable that it takes multiple environmental cues or long exposure to these to elicit a strong C38 methylation decrease, such as can be observed upon Q depletion under hypoxic conditions (**Fig. 15A**). This hypothesis is underlined by the observation that hypoxic cell culture of HeLa cells in medium supplemented with horse serum (low in Q) for just 48 hours will still allow a high level of Q-modification on tRNAs, however longer depletion (as in this thesis, 8 days) under hypoxic conditions is suspected to decreased activity of the queuine-insertase enzyme (Fergus et al. 2015), thus leading to reduced Q-tRNA levels and reduced C38 methylation. Thus, duration and combination of environmental insults may be important to observe effects.

Interestingly, inducing MEFs to undergo adipogenic or osteogenic differentiation appeared to lead to an increase in $tRNA^{AspGUC}$ C38 methylation (**Fig. 15A**). This is in line with a recent and thorough review of Q, which does not prove but suggests that Q-modification of

tRNAs may partially be a result of differentiation, according to research on mouse as well as human cell lines (Fergus et al. 2015).

The fact that C38 methylation levels on $tRNA^{GlyGCC}$ and $tRNA^{ValAAC}$ were not affected by the nutritional changes, and neither were C48 and C49 on $tRNA^{AspGUC}$, shows that the effects were highly site- and substrate-specific and likely neither dependent on Dnmt2 activity itself nor on methyl-donor availability. The fact that Dnmt2 expression levels determined by qRT-PCR did not correlate with $tRNA^{AspGUC}$ C38 methylation levels underpinned the notion that a decrease of this methylation did not depend on Dnmt2 quantities (**Fig. 15B+C**). The lack of nutrients thus did not have a direct effect on Dnmt2 activity itself, however likely on $tRNA^{AspGUC}$ and its suitability as a substrate for Dnmt2, possibly due to steric reasons.

To validate the notion that the factor behind the C38 methylation dynamics is Q, APB Northern blots were employed. The acquired data confirmed that a reduction in Q coincides with lower C38 methylation levels than if Q was added (**Fig. 16A**). Supplying cells with Q, be it through addition of Q-containing FCS to media or through addition of pure Q, showed increased levels of C38 methylation when compared to –Q media (**Fig. 16A**). The data on *Drosophila* 3rd instar larvae, which are known to have low levels of Q (Zaborske et al. 2014), and demonstration that these samples have only 42% of their $tRNA^{AspGUC}$ C38 methylated, supports the idea that Q plays a major role in C38 methylation, also in the fruit fly. Additionally, without discussing their results in detail, Ott et al. had previously published autoradiograms of two-dimensional thin-layer chromatograms which showed that the amoebae *Dictyostelium discoideum* normally shows high $tRNA^{Asp}$ methylation levels, however an axenic strain grown in –Q media shows substantially less m5C (Ott and Kersten 1985), which was later confirmed by bisulfite sequencing (Müller et al. 2015). Thus, Q appears to have a direct influence on the methylation level of the Dnmt2 substrate $tRNA^{AspGUC}$ in several organisms.

Cytosine-C5 methylation on tRNAs (Chan et al. 2012) and especially so $tRNA^{Asp}$ C38 methylation (Tuorto et al. 2015; Shanmugam et al. 2015) has been shown to play an important role in fine-tuning of the proteome. Fine-tuning of the proteome rather than the transcriptome would be in line with the observation of only minor transcriptome effects. This may also explain why no major difference in 5' fragmentation of $tRNA^{Asp}$ between wild type and Dnmt2$^{-/-}$ sperm

can be observed on Northern blots (**Fig. 11B**). 5' tRFs from $tRNA^{Asp}$ have been shown to be rather low in other $Dnmt2^{-/-}$ tissues, and $tRNA^{Asp}$ C38 methylation is important for precise translation (Tuorto et al. 2015) and amino acid charging (Shanmugam et al. 2015). Thus, the lack of C38 methylation may be sufficient to have effects on the proteome, without further 5' fragmentation of $tRNA^{Asp}$. Interestingly, natural variation in queuosinilation levels of tRNAs has also been shown to play a role in proteome control through stage-specific codon selection in *Drosophila* (Zaborske et al. 2014).

The results in this thesis show that the dependency of Dnmt2-mediated C38 methylation on Q is conserved from protists and fungi (Müller et al. 2015) to flies and mammals.

5.3.2 Q deficiency as a potential mimick of Dnmt2 mutation *in vivo*

The mouse model of Q-deficiency gave insights into effects of diet on tRNA methylation *in vivo*. The salvage of Q and turnover rates of tissue seem to play an important role in the experimental setup. In tissues with a high production or turnover rate, Q levels appeared to be decreased before those in testicular tissue, which has a low turnover (**Fig. 16B**). However, it could be observed that even testis had slightly more non-queuosinilated tRNA when Q was depleted. Additionally, it was shown that in principle, cells of testicular origin (SUSA cell line) can be Q-depleted and also show a decrease in $tRNA^{AspGUC}$ C38 methylation (**Fig. 16B**). To eliminate all Q from mice, additional steps may be necessary. Bedding such as wood chips could potentially be chewed and ingested by mice. It is not known whether this plant product could provide the mice with Q. On a technical note, on APB Northern blots it appears that no detection of Q-tRNAs can still allow C38 methylation (**Fig. 16A, Lanes 3 and 5**). This may stem from the nature of the applied method. As described previously (**Chapter 4.3.2**), +Q and –Q $tRNA^{Asp}$ could not be resolved on APB gels (Zaborske et al. 2014), presumably due to mannosyl-Q on this tRNA (Kasai et al. 1976). Thus $tRNA^{His}$ probes were used as a means to determine Q-content in tRNAs. However, $tRNA^{Asp}$ is the first tRNA to be Q-saturated when Q is available (Reyniers et al. 1981), and may therefore have higher Q-levels than what can actually be observed on the shown APB gels for $tRNA^{His}$. Consequently, queuosinilation of $tRNA^{Asp}$ before $tRNA^{His}$ may lead to relatively high C38

methylation, even when Q-tRNA^{His} is very low. Eliminating factors that may provide mice with Q, such as wood bedding, and maintaining mice on a Q-free diet for prolonged periods of time could decrease C38 methylation further.

The presented data shows that C38 methylation is dependent on the micronutrient Q in mice not only in cell culture, but also *in vivo*.

5.4 Summary and conclusions

The presented work suggests by whole-transcriptome bisulfite sequencing that Dnmt2 is a three-tRNA-specific methyltransferase (tRNA^{GlyGCC}, tRNA^{AspGUC}, tRNA^{ValAAC}). C38 methylation was conserved in all analyzed tissues and cells, including a variety of mouse and human samples, and including the tissues that have been shown to be involved in Dnmt2$^{-/-}$ phenotypes, such as sperm and early embryos in the Kit* paramutant phenotype (Kiani et al., 2013). It was observed that the methylation activity of Dnmt2 contributes to tRNA integrity in the male germline and may thereby potentially contribute to RNA-mediated inheritance, through a currently unknown mechanism. The three-tRNA-specificity also explains the observation that Dnmt2 deletion shows no major effects on transcriptome expression levels in ESCs, E7.5 embryos, and in previous studies in MEFs, liver samples, and bone marrow samples (Tuorto et al. 2012; Tuorto et al. 2015). Interestingly, the methylation activity of Dnmt2 on tRNA^{AspGUC} is partially dependent on the micronutrient Q, not only in protists and fungi (Müller et al. 2015), but also in fruit flies, mice, and human cells.

Taken together, Dnmt2's highly selective tRNA-methylation specifically regulates proper tRNA function and homeostasis in the mouse germline and Dnmt2's partial dependence on nutrition is conserved across multiple species.

5.5 Perspectives and hypotheses

The mechanisms through which C38 methylation may contribute to RNA-mediated inheritance remain enigmatic. However, the presented data in conjunction with published data allows to speculate on possible mechanisms and on the direction and potential of future research.

A long-term –Q mouse model may be able to mimic the important effects of a Dnmt2 mutation on $tRNA^{Asp}$, and thus give insight into how nutritional factors could influence the inheritance pathways governed by Dnmt2. Both $tRNA^{Asp}$ methylation (Shanmugam et al. 2015; Tuorto et al. 2015) as well as $tRNA^{Asp}$ queuosinilation (Zaborske et al. 2014) have implications in translational fidelity, which makes a role for these factors in the early embryonic proteome plausible. An early Q-publication showed by chromatography that, similarly to what can be observed when Dnmt2 was absent in mouse sperm, the mere lack of Q can in fact destabilize $tRNA^{Asp}$ in the protist *Dictyostelium discoideum* (Ott and Kersten 1985). They also suggest that the levels of Q- versus G-tRNAs plays a role in gene regulation, especially of genes encoding proteins of redox chains. It has also been demonstrated that oxidative stress in yeast can lead to an increase in 5-methylcytosine levels on tRNA ($tRNA^{Leu}$), which in turn leads to translational biases of genes with respective anticodons (Chan et al. 2012), and oxidative stress in *Drosophila* can lead to increased tRNA ($tRNA^{Gly}$) fragmentation (Schaefer et al. 2010). With regard to codon bias in context of tRNA methylation, the lack of C38 methylation on $tRNA^{AspGUC}$ leads to a reduction of synthesis of poly-aspartate containing proteins (Shanmugam et al. 2015) and additionally to a reduction of fidelity for discrimination between tRNA(Asp) and the near-cognate tRNA(Glu), which results in incorrect protein folding (**Fig. 17A**) (Tuorto et al. 2015). A similar mechanism is speculative, however conceivable, for Q-deficiency, as this affects C38 methylation of $tRNA^{Asp}$ as well (**Fig. 17B**). Especially aspartate- and glutamate- rich proteins could thus be selectively affected by such a mechanism. Deletion of Dnmt2 has been shown to have bias effects on specific sets of genes involved in transcriptional regulation and gene expression (Shanmugam et al. 2015), and differences in tRNA pool composition have previously been shown to be directly linked to cellular programs such as differentiation versus proliferation (Gingold et al. 2014). It is thus conceivable that regulation of tRNA integrity through Q and/or Dnmt2 may elicit modifications in translational programs in the offspring. As both tRNA queuosinilation and the tRNA methyltransferase Dnmt2 are highly conserved (Schaefer and Lyko 2010; Fergus et al. 2015) and have indeed both been suggested to play roles in translational fine-tuning, this route may be worth pursuing.

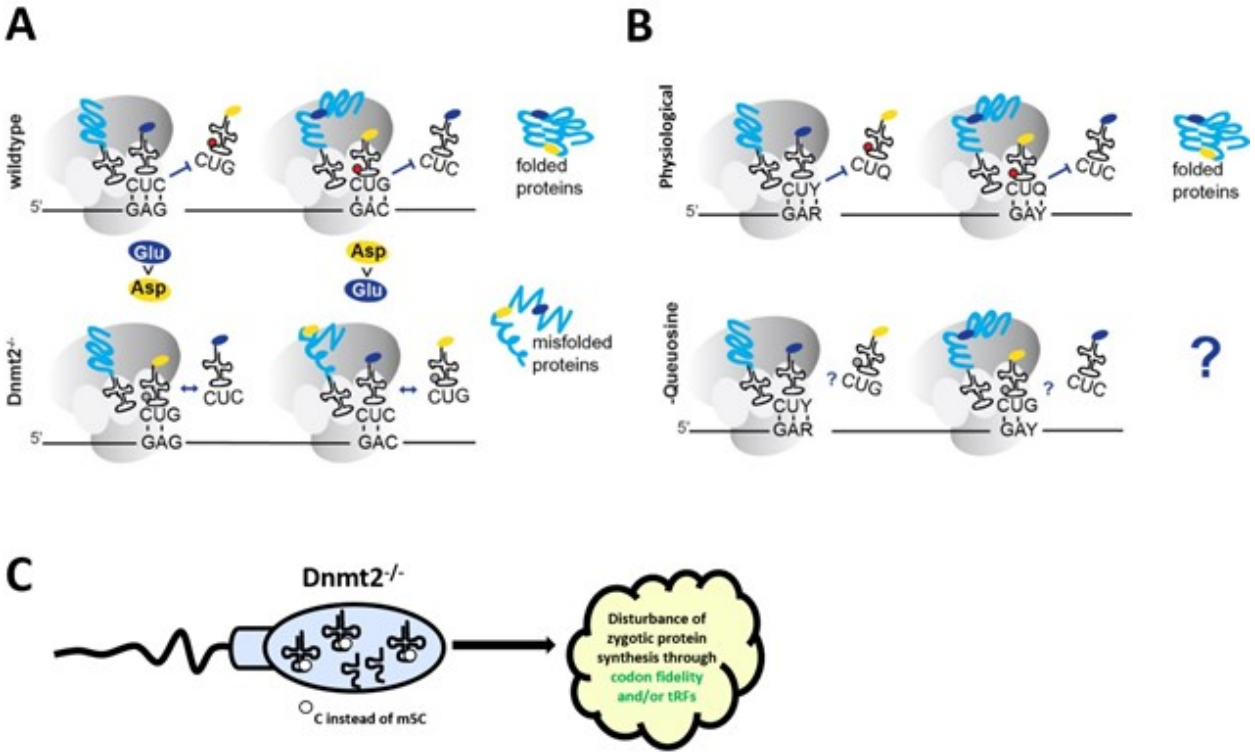

Figure 17. Potential model of how sperm tRNA integrity may influence the embryonic proteome. A. Proposed mechanism for codon fidelity through Dnmt2. In the wild type (top), physiological methylation (red dot) of $tRNA^{AspGUC}$ allows correct discrimination between aspartate (yellow) and glutamate (purple) tRNAs and results in normal translation and protein folding. In the $Dnmt2^{-/-}$ background (bottom), the lack of C38 methylation (gray dot) on $tRNA^{AspGUC}$ leads to reduction of fidelity for discrimination between tRNA(Asp) and the near-cognate tRNA(Glu) codons. Misfolded proteins are the result. (Panel A modified from Tuorto et al., 2015). **B.** Speculative model for codon fidelity through Q. Under physiological conditions (top), G is replaced by Q in GUN anticodons (here: $tRNA^{AspGUC}$ to $tRNA^{AspQUC}$) and allows the discrimination of GAR(Glu) and GAY(Asp). Under Q-deficiency (bottom), C38 methylation of $tRNA^{AspGUC}$ decreases and leads to a decrease in codon fidelity and protein homeostasis. (Panel B provided by Francesca Tuorto). **C.** Schematic model of delivery of unmethylated tRNAs and tRFs from $Dnmt2^{-/-}$ sperm into the zygote. The lack of integrity of unmethylated tRNAs is suggested to cause disturbances in protein synthesis in the zygote. Alternatively and possibly through the mother, tRFs may cause deregulation of proper protein synthesis.

Interestingly, a recent study analyzed inheritance of the *Kit* paramutation through oocytes (Yuan et al. 2015). Surprisingly, they show that deleting *Drosha* or *Mov10l1*, which are necessary for miRNA and piRNA biogenesis, respectively, causes an increase in transmission of the *Kit* paramutation. They conclude that oocytic miRNAs or piRNAs could be a suppressing factor for inheritance of the paramutation. Intriguingly, qRT-PCR of tRFs present in oocytes showed that

some fragments are present at significantly lower levels in zygotes than in oocytes, and it was thus speculated that this might be due to fertilization-triggered usage and consumption of tRFs during early embryogenesis (Peng et al., 2012). It is not known whether a small RNA mediated suppression of *Kit* paramutation might be oocyte specific and whether it may involve tRNA-derived RNAs as well.

As summarized in **Figure 17C**, a potential mechanism on mammalian Dnmt2-dependent RNA-mediated inheritance might function either via (a) Dnmt2's role in tRNA fragmentation (Tuorto et al., 2012) and via small RNA mechanisms, possibly also through the female germline (Yuan et al. 2015; Peng et al. 2012) and/or (b) through Dnmt2's role in accurate protein synthesis via tRNA methylation (Tuorto et al. 2015; Shanmugam et al. 2015).

A long-term Q-free mouse model may be a promising system to further deepen our knowledge on RNA inheritance and Dnmt2. Variations in Q levels have been suggested to also be controlled by differences in gut microbiota between individual flies of one species (Zaborske et al. 2014). If Q-deficiency does have an effect on RNA TEI, this would be a sophisticated system to allow the environment to regulate whether a temporary and possibly adaptive trait could or could not be transmitted for a few generations, depending on whether the conditions are favorable for this or not.

Clarifying the mechanisms behind RNA inheritance will help to understand non-Mendelian transmission of pathological states over several generations. RNA mediated inheritance is an attractive system to explain a variety of unresolved complex disorders and could potentially be used as a diagnostic marker.

Future work may include zygote proteomics approaches in order to determine the regulatory differences between wild type and Dnmt2$^{-/-}$ and also –Q zygotes. It is not known whether the mechanism that Dnmt2 employs to allow RNA-mediated inheritance may only be active in mice where a paramutation is present. Thus, research targeted specifically to deciphering mechanisms of paramutation may require additional analyses of the paramutant itself in a Dnmt2$^{-/-}$ background. As a tool to understand whether environmental factors such as Q may influence RNA-mediated inheritance in a way that Dnmt2 does, may be to establish a Q-free axenic *Kit* mutant mouse model.

6. Materials and Methods

6.1 Mouse husbandry, breeding, and embryos

Mouse lines were held by the DKFZ animal facility and work was carried out under ethical and scientific guidelines according to the Federation of European Laboratory Animal Science Association (FELASA). Organs were isolated immediately post-mortem. Used strains were C57BL/6 wild type and *Dnmt2*$^{-/-}$ (B6;129-Trdmt1$^{tm1Bes/J}$). Mice were bred on a 10-h light, 14-h dark cycle with free access to drinking water and standard food. Where necessary, mice were sacrificed by cervical dislocation.

Embryos were obtained from pregnant mice post-mortem at the stated time (E7.5 or E8.5). Embryos were isolated from the uterus. Then, extraembryonic tissue, including the ectoplacental cone, was removed.

The axenic NMRI mice were held in isolators in a sterile environment in the germ-free facilities of the DKFZ. NMRI control mice were fed on an autoclavable diet (3307 PML15) (Provimi Kliba SA, CH). The –Q diet was based on a previously published chemically-defined diet (Table 1 of Marks & Farkas, 1997). The diet was changed in the following way: the dropwise addition of "Solution B" was not carried out. Instead, all components of "Solution B" were added to the diet in powder form and fresh diet was dissolved in an appropriate amount of sterile water on a daily basis. Tyr-Ethyl Ester was replaced with L-Tyr. The diet was prepared in a fashion that addition of 40mL to 12.5 g resulted in the desired nutrient concentrations. The diet was delivered by Altromin, Germany.

The addition of Q to feed to rescue C38 methylation was done by sterile filtration and UV irradiation of a 100 µM stock of queuine-hydrochloride in sterile water (powder was kindly provided by Hans-Dieter Gerber, University of Marburg). The stock was stored at -20 °C and a final concentration of 20 ng/mL was fed to the mice, mixed into their diet. According to two publications, this concentration appeared to be a realistic normal dietary intake (Katze, Basile, and McCloskey 1982; Fergus et al. 2015). After feeding mice with the custom –Q diet and rescuing C38 methylation with Q, the colony was tested and had remained germ free throughout the experiment.

6.2 Mouse genotyping

DNA was isolated from mouse tail tips as follows. 200 µL of tail buffer (150 mM NaCl, 4 mM EDTA, 1% SDS, 20 mM Tris pH7.5, fresh 20 mg/mL proteinase K) was added to a piece of tail in a 1.5 mL microcentrifuge tube and incubated over night at 55 °C. Tubes were then vortexed and spun down. 100 µL saturated NaCl was applied to each sample, mixed, and spun for 4 min at 13000 rpm (top speed). The aqueous phase was added to 600 µL 100% EtOH in a fresh tube. Tubes were spun for at least 4 min at 13000 rpm. Supernatant was removed and the pellet was air-dried and resuspended in approximately 200 µL ddH_2O.

Each sample was then subjected to PCR with *Dnmt2* and *NSun2* genotyping primers in separate reaction vessels. The PCR conditions were identical for each primer set; denaturation at 95 °C for 3 min, followed by 30 cycles of; [denaturation 95 °C for 30 sec, primer annealing at 57 °C for 30 sec, extension at 72 °C for 45 sec], completed with a final elongation at 72 °C for 5 min.

PCR products were separated on 2% agarose (Sigma) gels (in TBE/Tris borate EDTA; 40 mM Tris base, 1 mM EDTA, 20 mM acetic acid) with the Fermentas 100+500 bp ladder loaded on either side, powered by a BioRad Power PAC 3000 or similar device. Gels were poured with ethidium bromide (Roth) and DNA bands were then visualized on a Herolab transilluminator and 440K camera connected to a computer.

6.3 Sperm harvest

Epidydimides and vasa deferentia, generally of at least three adult mice, were isolated, adipose tissue and blood vessels were removed, and they were squeezed to allow sperm to swim out (García-López et al. 2014) into 37 °C warm Hank's Balanced Salt Solution (HBSS) for 10 min. Sperm were collected by pipetting into a 1.5 mL microcentrifuge tube and spun at 800 g for 5 min to eliminate larger cells and cell debris. Pellets were resuspended in water for 2 min and then spun for 5 min at 800 g (personal communication with Jafar Kiani, University of Nice Sophia Antipolis). Pellets were then resuspended in somatic cell lysis buffer (0.1% SDS, 0.5% Triton X in RNase-free water) (Peng et al. 2012) for 2 min, spun at 1600 g for 5 min, washed in water and spun for 2000

g for 5 min. Pellets were resuspended in approximately 200 µL of TRIzol (Invitrogen) and vortexed. Purities were validated with multiple approaches (**Fig. 9C-F**).

6.4 Cell culture – embryonic stem cells (ESCs)

ESCs were cultured in medium with the following composition: 425 mL knock-out DMEM (Gibco), 75 mL heat inactivated fetal calf serum (Hyclone), 5 mL non-essential amino acids (100x stock, Gibco), 5 mL penicillin/streptomycin (100x stock, Gibco), 5 mL glutamine (200 mM, Gibco), 4 µL β-mercaptoethanol, 25 µL LIF (working concentration of 500 U/mL) (ESG1106, Merck Millipore). ESCs were grown on a primary MEF feeder layer. First, 10 cm dishes were coated with a 0.2% gelatin solution (2% stock G1393, Sigma) for 1 hour at 37 °C. Supernatant was removed. $2x10^6$ MEFs were seeded per dish and allowed to attach for 1 hour. ESC lines were: J1 ESCs, originally derived from mouse strain 129S4/SvJae, and Dnmt2$^{-/-}$ cells derived from J1 ESCs by inactivating the Dnmt2 gene by targeted deletion of the catalytic motif (Okano, Xie, and Li 1998). After 3 days of culture, including a medium change, the feeder cells were removed by serial passaging as follows: MEFs and ESCs were harvested by washing twice in PBS and addition of trypsin-EDTA (0.25% trypsin, Gibco). Cells were washed once by centrifugation, resuspended in their appropriate medium, and this cell mixture was allowed to attach on gelatin-coated dishes for 40-60 min at 37 °C. All cells that had not attached were re-plated into gelatin-coated dishes for an additional 40-60 min. The supernatant (non-attached cells) were then spun down and pellets were snap-frozen in liquid nitrogen. This allowed harvest of pure ESCs without any MEF contaminants, as MEFs attach significantly faster. The purity of the harvest was very high, which was ultimately confirmed by WTBS of Dnmt2$^{-/-}$ ESCs. If any wild type MEFs would have contaminated the Dnmt2$^{-/-}$ samples, the eradication of C38 methylation on tRNAs would not have occurred (**Fig. 7A**).

6.5 Cell culture – other cell lines

Unless otherwise stated, the normal (control) medium that was used in cell culture was; Dulbecco's modified Eagle's medium (DMEM) supplemented with 10% heat-inactivated FBS, 2

mM L-glutamine and a commercial cocktail of antibiotics (penicillin/streptomycin at 0.1 mg/mL) (P/S) (Invitrogen). MEFs and HeLa were grown in the control medium. HepG2 were grown in control medium supplemented with 1 mM sodium pyruvate (S/P).

6.6 Cell culture – screening conditions

For adipogenic differentiation, MEFs were induced with medium containing 0.5 mM isobutylxanthine (Sigma), 50 µM indomethacin (Sigma), 1 µM dexamethasone (Sigma), 1 µg/ml insulin (Sigma), 10% FCS, and 2 mM glutamine. Osteogenic differentiation of MEFs was induced by 100 nM dexamethasone, 50 µg/mL acorbis acid, and 10 mM β–glycerolphosphate (all Sigma).

For all –Q conditions, StemPro Accutase (Gibco) was used for cell dissociation instead of trypsin, as trypsin is of animal source and may contain significant levels of Q. Horse serum was acquired from Sigma and was supplemented to media as 10% of the total volume. Ultraculture serum-free medium (Lonza) was supplemented with 2 mM L-glutamine and P/S. "no FCS" media (**Fig. 15A**) was DMEM with P/S and S/P. "-glu +gal" medium was DMEM without glucose, however with P/S, FCS, and 2.25 g of D(+)-galactose (cell culture grade, Sigma G5388) per 500mL medium.

For charcoal treatment of serum, dextran coated charcoal was used (Sigma). A protocol was chosen where 500 mg of charcoal were added to 50 mL of serum (10% w/v) (Katze 1978; Padilla, Howe, and Boldt 1988). This was incubated at 55 °C for 30 min, spun down at 12000 g at 4 °C for 20 min, and sterile filtered. The successful removal was evident on APB gels (**Fig. 16A**).

For Q addition to cultures, a reasonable concentration normally present in cell culture media appeared to be 20nM (Fergus et al. 2015; Katze, Basile, and McCloskey 1982). The same stock as described above for the axenic NMRI mice was used.

Hypoxic cell culture was done in a hypoxic chamber at 37 °C, 5% CO_2, and 1% atmospheric oxygen.

Culturing durations: ESCs in horse serum – 18 days; MEFs under hypoxic conditions – 8 days; MEFs in Lonza under hypoxic conditions – 9 days; MEFs in Lonza – 38 days; MEFs with horse serum – 14 days; MEFs in –glu+gal – 17 days; HeLa in –glu+gal – 21 days; HeLa with charcoal

treated serum – 11 days; HeLa with charcoal treated horse serum – 11 days; HeLa in Lonza – 36 days; HepG2 in Lonza – 37 days; HepG2 without FCS – 13 days.

6.7 Cell culture – freezing and thawing

Cells were frozen at -80 °C (decreasing 1 °C/minute). The freezing solution was 10% DMSO (dimethylsulphoxide, Sigma) and 90% media (supplemented with a percentage of serum appropriate for the respective cell line). Unless otherwise stated, cells were incubated at 37 °C and 5% CO_2 in a Thermo Scientific HERA cell 150 incubator.

6.8 RISC reporter assay

The RISC (RNA-induced silencing complex) reporter assay was carried out as previously published (Béthune, Artus-Revel, and Filipowicz 2012), with some modifications. As described for **Figure 14A+B**, the construct has a control renilla luciferase (RL) without any miRNA target sequences, and a firefly luciferase (FL) fused to the 3'UTR of the hmga2 transcript with six consecutive let-7 miRNA target sites. An additional, otherwise identical construct has mutated (MUT) let-7 target sites. MUT and WT constructs are separately transfected. FL and RL signals are normalized to a negative transfection control, then the FL signal is calculated as % of RL. It is then determined what % of the WT construct FL is expressed in comparison to the MUT FL target. The construct was kindly provided by Julien Béthune (University of Heidelberg), and was produced to sufficient quantities using One Shot® TOP10 Chemically Competent *E. coli* (ThermoFisher) with the included protocol. Briefly, 0.5 µg of the ampicillin resistant plasmids (pFL-hmga2wtRL and pFL-hmga2mutRL) was added to the competent cells, placed on ice for 5 min, then at 42 °C for 2 min, then on ice for 5 min, followed by a 40 min incubation at 37 °C with 950 µL of LB medium. 100 µL of this was used to inoculate 200 mL of LB including 200 µL of a 100x ampicillin stock, and incubated over night at 37 °C. The plasmids were extracted using the Qiagen Plasmid Maxi Kit, following the included protocol. For transfecting MEFs, the Lipofectamine® LTX with Plus™ Reagent was used according to company instructions. 8 x 10^3 MEFs were seeded per well in a 96-well format. For each genotype (wild type MEFs or Dnmt2$^{-/-}$ MEFs), triplicates were seeded for

the negative controls (no plasmid), for the WT-plasmid transfection, and for the MUT-plasmid transfection. This was carried out in biological duplicates. Plasmids were added at 100 ng per well. Cells were grown for 24 hours before they were transfected. Another 24 hours later, luciferase activities were determined using the Dual Luciferase Reporter Assay System (Promega) on a SPECTROstar Omega plate reader by BMG Labtech.

6.9 RNA isolation and quality control

Tissue was prepared for RNA isolation by placing a small piece in approximately 1 mL of TRIzol (Invitrogen) in a 2 mL microcentrifuge tube. The tissue was homogenized with an electric homogenizer. Cell pellets were homogenized by vortexing and using pestels. RNA extraction was performed according to the Invitrogen TRIzol RNA isolation protocol and included a phase separation, where RNA is in the aqueous phase and can be taken off and precipitated via isopropyl alcohol. The RNA pellet was washed in 75% EtOH and later dissolved in water. The nucleic acid concentrations and purity for further analysis were analyzed on the NanoDrop ND-1000 Spectrophotometer. RNA integrity was measured on a Bioanalyzer (Agilent) or TapeStation (Agilent). Samples were stored at -80 °C.

6.10 RNA-Seq – lab

Concentration, purity, and integrity of RNA was measured as described for the RNA isolation. The Ambion Turbo DNase was applied to each sample as follows: 1 µL DNase, 2 µL 10x buffer, 0.5 µL RNaseOUT, 16.5 µL of RNA (maximally 2 µg/µL). The total volume of 20 µL was incubated at 37 °C for 30 min. A phenol-chloroform extraction was carried out to get rid of the protein. The reaction of 20 µL was added to 180 µL water and 200 µL acid phenol (Ambion), then vortexed and spun at top speed for 10 min. The upper aqueous phase contained the RNA and was transferred to a fresh tube, to which chloroform and water were added in equal amounts and tubes were again vortexed and spun. The aqueous phase was transferred to another tube, to which 10 µL 3 M pH 5.2 NaAc (sodium acetate) and three volumes EtOH were added. RNA was precipitated at -80 °C over night and harvested by spinning at top speed for 30 min. RNA was

dissolved in 10 µL water and rRNA depletion was carried out according to the Ribo Minus Eukaryote System V2 (Ambion) protocol. Resulting depleted RNA was then submitted to the Genomics and Proteomics Core Facility at the DKFZ for quality control and library preparation using the TruSeq RNA Sample Preparation Kit (Illumina). Finally, RNA was sequenced in a 100 bp paired end approach on an Illumina HiSeq 2000 platform.

6.11 RNA-Seq – analysis

The sequenced reads were trimmed at the ends by removing bases with a quality score <30. Reads shorter than 30 nt were discarded. The trimmed reads were mapped to the NCBI mm9 genome using Tophat v2.0.11 (Trapnell, Pachter, and Salzberg 2009). The mapped data was further analyzed using DESeq v1.12.1 to find differentially expressed transcripts (Anders and Huber 2010) using the standard procedures for library normalization and variance estimation and Cuffdiff v2.0.2 (Trapnell et al. 2013). Calculated *P* values were subjected to multiple testing correction and transcripts with a q value (corrected *P*-value) below 0.05 were considered differentially expressed.

6.12 Small RNA-Seq – lab

Total RNA was isolated as described in section **6.9 RNA isolation and quality control**. Small RNA library preparation was done with the NEBNext Small RNA Library Preparation kit and according to the manufacturer's description, with minor changes. Before library preparation, an RNA end repair was carried out to dephosphorylate 3' and phosphorylate 5' ends following natural fragmentation processes. 3' dephosphorylation was done by mixing 24.5 µL of RNA with 0.5 µL of RNaseOUT, 3 µL of 10x buffer, and 1 µL of T4 polynucleotide kinase (TaKaRa). This was incubated at 37 °C for 20 min. 5' phosphorylation ensued by the addition of 2 µL of 10 mM dATP. Another 37 °C incubation step followed for 20 min before this was placed on ice. A phenol/chloroform extraction followed: RNA samples were filled up to 200 µL with water and 20 µL 3M NaAc (pH 5.2) were added. This was mixed and 1 volume (220 µL) of phenol/chloroform/isoamylalcohol was added, vortexed, and spun at room temperature (RT)

and top speed for 5 min. The supernatant was transferred to a fresh tube and vortexed in 200 µL $CHCl_3$, spun as before, and the supernatant transferred into 1 volume (approximately 200 µL) of isopropanol and 20 µg of Glycoblue. Samples were placed at -80 °C for 1 hour, spun down at 4 °C and top speed for 30 min, washed with cold 75% EtOH, spun for 5 min at 4 °C, and the resulting pellet was resuspended in 13 µL RNase-free water. From here, the NEB Next Small RNA Library Preparation protocol was followed. Following adaptor ligation and cDNA synthesis, cDNA was amplified with 15 cycles of PCR, libraries were size selected for an insert size of 1-60 nt (without adapters), and purified using the QIAQuick PCR Purification kit (Qiagen). Small RNA libraries were validated using Qubit 2.0 Fluorometer (Life Technologies-Invitrogen) and Agilent 2100 Bioanalyzer or 2200 Tapestation (Agilent Technologies). Appropriate and compatible barcodes were selected and samples were pooled in equimolar ratios on a single lane on an Illumina HiSeq 2000 machine at the Genomics and Proteomics Core Facility of the DKFZ. A 50 bp single-end sequencing approach was applied.

6.13 Small RNA-Seq – analysis

Sequencing reads were quality trimmed on both ends, where the aggregate quality score was below 30, using the FASTQ Quality Trimmer tool integrated in Galaxy. All tools used in this analysis were pre-integrated or integrated manually into Galaxy. Reads were then adapter-trimmed using cutadapt (Martin 2011) version 1.2.1. Reads were mapped to a compilation of transcript databases, using Bowtie. The compilation contained the UCSC table browser refSeq sequences, arb-silva rRNA sequences, genomic tRNA database sequences (P. P. Chan and Lowe 2009), and ensemble ncRNA sequences.

6.14 454 bisulfite sequencing – lab and analysis

Total RNA was extracted and DNase treated as described for sections **6.9 RNA isolation and quality control** and **6.10 RNA-Seq.** The DNase reaction was stopped and immediately applied to the EZ RNA Methylation Kit (Zymo Research). The kit manual was followed, with a maximum of 3 µg input and the end product dissolved in 10 µL of water.

2 µL of this bisulfite converted RNA was used for the cDNA synthesis, which was carried out with the SuperScript III Reverse Transcriptase (all reagents from Invitrogen here), RNaseOUT Recombinant Ribonuclease Inhibitor, 5x First Strand Buffer, and 0.1 M DTT. The reaction was as follows: 65 °C for 5 min of; 2 µL sample, 1 µL of the Reverse 454 Primer, 0.5 µL 10 mM dNTPs (deoxyribonucleotides), and 3 µL water. The samples were cooled on ice and the following mix was added: 2 µL First Strand Buffer, 0.5 µL DTT, 0.5 µL RNaseOUT, and 0.5 µL SuperScript. The conditions for the reverse transcription were: 10 min RT, 15 min 50 °C, 15 min 70 °C, 4 °C indefinitely. The PCR was carried out immediately after this. 10 µL of cDNA were added to 32.5 µL of water, 5 µL PCR ReddyMix, 1 µL of the Forward 454 Primer, 1 µL dNTPs, and 0.5 µL (5 U/µL) of ThermoprimePlus polymerase. The PCR was: 3 min 96 °C, 33 x [30 sec 96 °C, 45 sec 45 °C, and 45 sec 68 °C], and a final 2 min 72 °C step.

Amplicons were separated on and cut from 2% agarose gels and DNA was eluted using the PeqGold Gel Extraction Kit S-line (PeqLab). For 454 sequencing, concentrations were determined with the Quant-iT PicoGreen reagent and according to the Roche 454 Junior protocol. The Fluostar OPTIMA (BMG Labtech) plate reader was used for measurements. The amplicons were then included in the library preparation preparation and sequenced in an equimolar sample pool on the Roche 454 Junior platform. The acquired sequencing reads were analyzed with the help of an internal software package (provided by Cassandra Falckenhayn). The programs made graphical representation in heat maps possible, as seen in **Figure 11A**.

6.15 Whole transcriptome bisulfite sequencing – lab

The in the following elucidated protocol was provided by Mark Hartmann and Matthias Schäfer and is briefly outlined in **Figure M1**. RNA was isolated from ESCs as described previously. Total RNA was fractionated by a modified version of the online available *Mello Lab Small RNA Cloning Protocol* (Gu, Conte, Tuschl). The fractionation results in a long RNA fraction (>200 nt) and a small RNA fraction (<200 nt). At RT, in RNase-free siliconized tubes, 400 µL of MirVana lysis/binding buffer was mixed with 48µL of MirVana Homogenate buffer by inverting several times. 30 µg of total RNA in a total volume of 80µL were added, mixed by inversion, and incubated at RT for

exactly 5 min. 1/3rd volume of 100% EtOH were added (176 µL) and mixed by inversion. This was incubated at RT for exactly 20 min. 0.8 µg Glycoblue were then added and spun at exactly 21°C and 2500 x g for 8 min to pellet the long RNAs. Pellet may be fluffy at this step. The supernatant was carefully transferred to a fresh tube and contained the small fraction. The pellet (long fraction) was washed with 1 mL of cold 75% EtOH and spun at 4 °C and maximum speed for at least 20 min. Supernatant was taken off carefully and discarded. The pellet was air dried completely and resuspended in 48 µL of RNase-free water. The previously recovered supernatant containing the small fraction in a fresh tube was filled completely with isopropanol alcohol (approximately 800 µL). RNA was precipitated at -80 °C for at least 10 min. 20 µg of Glycoblue were added and the tube spun at 4 °C at top speed for 5 min. The pellet was washed with cold 70% EtOH and spun again. Supernatant was carefully discarded, pellet was air dried and resuspended in 48 µL RNase-free water. Concentration, purity, and integrity were measured as described for the RNA isolation.

rRNA depletion was then carried out according to the Ribo Minus Eukaryote System V2 (Ambion) protocol. The long fraction gave sufficient material to split this into two Ribo Minus reactions and later pool them. Briefly, the Ribo Minus probe was hybridized and rRNA was captured and removed. The depleted RNA was precipitated in EtOH and NaAc as described in the manual (the Magnetic Bead Clean Up Module was not used). The total long fraction was dissolved in 18 µL and the small in 18 µL final volume.

The long fraction was further processed with the NEBNext – Magnesium RNA Fragmentation Module. This was carried out as described in the manual. A 3 min fragmentation at 94 °C had previously been established to be most suitable for a peak at approximately 300 nt (and thus appropriate length for the final 100 bp paired end sequencing) for the used ESC RNA. The fragmented RNA was precipitated in EtOH/NaAC with 20 µg of Glycoblue and finally dissolved in 17 µL water.

The Ambion Turbo DNase was applied to each sample as follows: 1 µL DNase, 2 µL 10x buffer, 0.5 µL RNaseOUT, 16.5 µL of RNA (maximally 2 µg/µL). The total volume of 20 µL was incubated at 37 °C for 30 min.

This volume was immediately applied to the EZ RNA Methylation Kit (Zymo Research). The kit manual was followed and the end product dissolved in 24.5 µL of water. As a final step before library preparation, an RNA end repair was carried out to dephosphorylate 3' and phosphorylate 5' ends following chemical fragmentation and other natural fragmentation processes. 3' dephosphorylation was done by mixing 24.5 µL of bisulfite converted RNA with 0.5 µL of RNaseOUT, 3 µL of 10x buffer, and 1 µL of T4 polynucleotide kinase (TaKaRa). This was incubated at 37 °C for 20 min. 5' phosphorylation ensued by the addition of 2 µL of 10 mM dATP. Another 37 °C incubation step followed for 20 min before this was placed on ice. A phenol/chloroform extraction followed: RNA samples were filled up to 200 µL with water and 20 µL 3M NaAc (pH 5.2) were added. This was mixed and 1 volume (220 µL) of phenol/chloroform/isoamylalcohol was added, vortexed, and spun at RT and top speed for 5 min. The supernatant was transferred to a fresh tube and vortexed in 200 µL $CHCl_3$, spun as before, and the supernatant transferred into 1 volume (approximately 200 µL) of isopropanol and 20 µg of GlycoBlue (ThermoFisher). Samples were placed at -80 °C for 1 hour, spun down at 4 °C and top speed for 30 min, washed with cold 75% EtOH, spun for 5 min at 4 °C, and the resulting pellet was resuspended in 13 µL RNase-free water.

The library preparation was done according to the NEBNext Small RNA Library Preparation protocol. Following adaptor ligation and cDNA synthesis, cDNA was amplified with 12 cycles of PCR and purified using the QIAQuick PCR Purification kit (Qiagen). Appropriate and compatible barcodes were selected and samples were pooled in equimolar ratios on a single lane on an Illumina HiSeq 2000 machine at the Genomics and Proteomics Core Facility of the DKFZ. A 100 bp paired-end sequencing approach was applied.

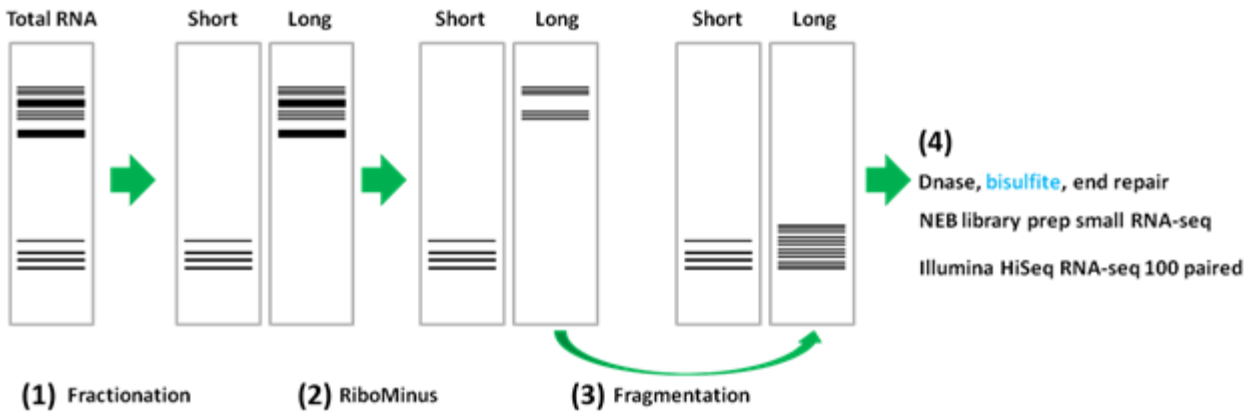

Figure M1. Schematic of whole transcriptome bisulfite sequencing workflow. 30µg total RNA of each sample are treated as follows: Short and long RNAs are (1) separated by ethanol fractionation and (2) each depleted for rRNA by RiboMinus. The long fraction is then (3) fragmented in order to allow thorough sequencing. Samples are (4) Dnase treated, bisulfite converted, end repaired, and finally used as input for the small RNA-Seq library preparation and HiSeq sequencing. (Unpublished internal protocol by Mark Hartmann and Matthias Schaefer).

6.16 Whole transcriptome bisulfite sequencing – analysis

The sequencing data was essentially treated as previously published (Müller et al. 2015), with additional steps. A quality trimming was carried out to a minimum aggregate score of 30, using the Galaxy-integrated fastq quality trimmer. Resulting data was adaptor-trimmed using cutadapt version 1.8.1 (Martin 2011). Before mapping, a CCA tail (Phizicky and Hopper 2010; Findeiss et al. 2011) was added to tRNA sequences in the reference. The acquired sequences were aligned to all known genomic tRNA sequences (P. P. Chan and Lowe 2009), and all reads that mapped to tRNAs were removed from the dataset and separately analyzed. The remaining reads were mapped transcriptome wide (compilation contained the UCSC table browser refSeq sequences, arb-silva rRNA sequences, and ensemble ncRNA sequences). The mapping procedure employed a customized script (Sebastian Bender) of bsmap version 2.74 (Xi and Li 2009), allowing for a 5% mismatch rate per read and reporting all repeat hits. As bsmap was originally made for DNA sequence alignments, reads are also automatically reverse complemented and the mapper attempts to map these. However, as we sequenced RNA, these reverse complement reads were disregarded. Reads shorter than 20 nt were also discarded. Internal Python scripts were applied to calculate bisulfite conversion for each cytosine position and R scripts subsequently generated

heatmap plots. The candidate list for new methylation hits was carried out by filtering. RNAs with methylated cytosines were removed from the candidate list if this methylation mark was not lost in the Dnmt2$^{-/-}$ sample. A methylation mark was considered a candidate if the methylation ratio was >0.5 in the wild type and <0.1 in the Dnmt2 mutant. A final filter set a cut-off at a minimum coverage of >100x per candidate and genotype.

6.17 cDNA synthesis and qRT-PCR

The QuantiTect Kit by Qiagen was used according to protocol. Briefly, 100 ng to 1 µg RNA were used per sample. gDNA WipeOut was used and incubated for 2 min at 42 °C. The RT primer mix was used for the reverse transcription at 42 °C for 28 min. Enzyme inactivation at 95 °C for 3 min was followed by cooling and qRT-PCR. A Roche LightCycler was employed with the provided SYBR Green. The PCR conditions were 1 cycle of 95 °C for 15 min, 50 cycles of [95 °C 15 sec; 60 °C 40 sec reading], and a final melting curve from 65 °C to 95 °C, read every 1 °C.

6.18 Northern blot – urea-PAGE (polyacrylamide gel electrophoresis)

20% gels were prepared with Roth solutions (Rotiphorese Sequencing Gel Concentrate, Sequencing Gel Diluent, Sequencing Gel Buffer Concentrate), and 200 µL 10% APS and 10 µL TEMED (Roth) were added immediately before pouring. Gels were pre-run for 1 h in 0.5x TBE (Tris borate EDTA; 40 mM Tris base, 1 mM EDTA, 20 mM acetic acid) at 100 V. RNA samples were denatured at 80 °C for 5 min, placed on ice, mixed with RNA loading Dye (Fermentas), and gel pockets were washed out prior to loading. 3-15 µg of RNA were loaded and run in parallel to 8 µL 10bp O'Range Ruler (Fermentas). The gel was run at 100 V for 1 hour, at 260 V for 1 more hour. Gels were stained in SYBR Gold (Invitrogen) for 20 min (SYBR Gold diluted in TBE 1:10000). The transfer of separated RNA from the polyacrylamide gel to the positively charged Nytran SuperCharge membranes (Schleicher and Schuell) was carried out on a PeqLab electroblotter. The transfer was run at approximately 5 V and 250 mA for 35 min. The blotted nucleic acids were chemically crosslinked by applying 180 µL of cross-linking solution (0.5 g 1-ethyl-3-(3-dimethylaminopropyl) carbodiimide, 130 µL methyl-imidazole, 50 µL 1 M HCl) and then UV-

crosslinked to the membrane by auto-crosslinking (120 mJ) on the UV Stratalinker 1800 (Stratagene).

6.19 Northern blot – hybridization

Membranes were baked for 1 hour at 80 °C and pre-hybridized in hybridization buffer [12.5 mL of 20x SSC (3 M NaCl, 0.3 M sodium citrate), 1 mL 1 M Na_2HPO_4 pH 7.2, 17.5 mL 20% SDS, 1 mL 100x Denhardt's solution, 17 mL water] for 1 hour at 42.5 °C in a rotator. In parallel, probes were readioactively end-labelled for 1 hour at 37 °C. Labelling was performed in 9 µL water, 2 µL 10x T4 Polynucleotide Kinase Buffer, 3 µL 2 µM oligonucleotide probe, 5 µL γ-P^{32}-ATP (10 µCi/µL), and 1 µL T4 Polynucleotide Kinase (TaKaRa). Radioactivity was acquired from Hartmann Analytics and laws and regulations were abided. The labelled probe was then applied to the membrane in hybridization buffer and was incubated at 42.5 °C over night on a rotator. Membranes were washed twice for 15 min at 42.5 °C with 3x SSC, 5% SDS and for 15 min at RT with 1x SSC, 1% SDS. Membranes were then exposed on film. Membranes were stripped by washing the membrane in water and incubating at 80 °C 2x 60 min in stripping buffer [25 mL of 50% formamide, 2.5 mL 50 mL Tris/HCl pH 7.5, 2.5 g of SDS pellets]. Finally, membranes were rinsed 2x 5 min in 2x SSC and stored at -20 °C until further use or re-hybridized immediately.

6.20 Northern blot – Acryloyl aminophenylboronic acid (APB) gels

APB gels were prepared and run with a few modifications (kindly provided by Zdenek Paris, Institue of Parasitology Czech Republic) of a recently published paper (Zaborske et al. 2014), which was based on the original method (Igloi and Kossel 1985). Boronate gels were prepared as follows: for 3 gels, 14 g urea were added to 10.57 mL 30% acrylamide solution (Roth) and filled to a total volume of 33 mL with 1x TAE, after which 166.65 mg of APB was added. To completely dissolve, the mixture was shaken and warmed to 37 °C. 180 µL 10% APS and 30 µL TEMED (Roth) was added and immediately poured. In a total volume of 50 µL, 2.5 - 15 µg of RNA were deacetylated in 100 mM Tris-HCl pH9 for 30 min at 37 °C. EtOH precipitation followed: 50 µL of the sample were added to 150 µL 100% EtOH and 20 µL NaAc and 1 µL glycoblue. RNA was

precipitated for 1 hour at -80 °C and spun down at top speed for 30 min at 4 °C. Pellets were washed in 75 % EtOH and resuspended in 20 µL water plus 20 µL of 2x RNA loading dye. For quality control purposes, a periodate oxidation control was run on each gel. The oxidation of the ribose moiety of Q produces a single band that migrates faster than Q-tRNA or G-tRNA. The controls were deacetylated as described above, however the pellets resuspended in 50 mM NaAc pH5.2 and 2.5 mM $NaIO_4$ (in a total volume of 50 µL) for 2 hours at 37 °C in the dark. Freshly prepared glucose was then added to a 2 mM concentration and incubated for 30 min at 37 °C in the dark. The treated control RNA was purified on Microspin G-50 Columns (GE Healthcare) and EtOH precipitated, washed, and resuspended as described above. Samples were then denatured for 10 min at 70 °C, loaded, and run at 4 °C in 1 x TAE until the bromphenol blue marker had run out. This was generally achieved by 90 V for 30 min and 140 V for 3 hours. Gels were blotted as described for Northern blots.

6.21 Western blot and protein isolation

SDS-PAGE was prepared by pouring a 12% separation gel and a 5% stacking gel. The 12% gel was composed of 3.29 mL water, 4 mL 30% acrylamide (Rotiporese), 2.5 mL 1.5 M TrisCl pH 8.8, 100 µL 10% SDS, 100 µL 10% APS, 6 µL TEMED. The 5% gel was adjusted accordingly. Sperm proteins were isolated using a urea extraction method. The sperm pellet was subjected to the urea buffer 1:1 (pellet volume:buffer volume) in the BioRuptor for 1 cycle, set to High. The urea buffer consisted of 8 M urea, 4 % SDS, 0.08% bromphenol blue, 125 mM Tris pH6.8, 10 mM EDTA, 50 mM DTT. The sample was applied to gels as was, along with 8 µL of Prestain Ladder on the side. Multiple buffers were tested on both sperm and testis samples. The urea buffer was most efficient in protein isolation for sperm. For testis protein isolation, a direct-load Ripa buffer gave higher protein yields with desired quality. The buffer consisted of: 0.10% SDS, 0.5% NP40, 150 mM KCl, 0.5% Sodiumdeoxycholate, 1 mM DTT, 1x Protease Inhibitor, in PBS. Protein samples were loaded into the gel and run at 90 V in the 5% gel layer and at 120 V in the 12% gel layer. Gels were then equilibrated in blotting buffer, as was the nitrocellulose membrane. Blotting buffer was: 200 mL methanol, 100 mL 10x borate buffer pH 8.8, 4 mL 0.5 M EDTA, 1 mL 1 M DTT,

filled to 1 L with water. The wet transfer was carried out as follows: 5 min 100 mA, 5 min 200 mA, 5 min 300 mA, 45 min 400 mA, and ponceau-staining. Membranes were blocked by shaking for 1 hour at RT or at 4 °C over night in a red western solution (5%FBS, 2,5% BSA, 0,1% Tween, PBS, 0,05% N2N3, red pigment, in water), before antibodies were applied in the below stated solution and concentration. The addition of Western Lightning Plus ECL solution (PerkinElmer) allowed signal detection upon exposure to film. The applied antibodies were; β-actin (Abcam mouse ab8226, 1:3000) in 5% PBS-milk, and rabbit anti-Dnmt2 antibody (Santa-Cruz, 1:500) in red western solution. Stripping of membranes was carried out as follows: PBS rinse, 20 min at 80 °C in stripping buffer (0.1 M glycin pH3), PBS rinse.

6.22 Histology

Tissue was fixed and stored according to standard protocols (Wilkinson 1998). Briefly, testis were removed and washed in PBS before being transferred into vials containing ice-cold freshly prepared PFA (4% paraformaldehyde dissolved in PBS at 60 °C and then cooled). Samples were incubated over night and PFA was then washed twice in saline solution (8.3 g of NaCL in 1 L of RNase-free water), each for 1 hour at 4 °C. They were then washed in 1:1 saline solution:ethanol for 1 hour at 4 °C. Two washes with 70% EtOH for 1 hour each followed, before being stored at 4 °C and subsequently being embedded in paraffin and cut into 5-7 µm sections on a water microtome. Embedding was carried out by a 1 hour incubation in 50% paraffin, 50% xylene, followed by 3 incubations of 1 hour each in 100% paraffin and allowed to solidify over night at 4 °C. For hematoxylin-eosin stainings, the following steps were applied to slides in a staining jar underneath a fume hood. 15 min xylene, 15 min xylene, 5 min 100% EtOH, 5 min 100% EtOH, 2 min 70% EtOH, 2 min 50% EtOH, 2 min 30% EtOH, 3 x 2 min water, 30-60 sec hematoxylin (60 sec maximum), water rinse, bluring reagent (alkaline solution/weak ammonia solution, 0.08% in H2O) until stain is blue (~30 sec), water rinse. Followed by 5 min Eosin (0.5% x88311), water wash, 30% EtOH wash, 70% EtOH wash, 100% EtOH wash, 2x xylene wash, then 1-2 drops of mounting medium were added and a cover slip placed over the sections. Slides were dried for 24 hours at RT.

Acridine orange staining was carried out based on a published method (Bertalanffy 1960), with some adjustments (as suggested online by John Kiernan, University of Western Ontario). Paraffin sections on glass slides were pre-wetted and then stained in acridine orange (0.05 g in 500 mL distilled water and 5 mL acetic acid) for 30 min. Slides were rinsed in 0.5% acetic acid (in 100% EtOH), and rinsed two more times in 100% EtOH, before being rinsed in xylene twice. Mounting resin and glass cover slips were applied.

6.23 Sperm viability

Sperm viability was assayed in collaboration with Vera Gramm, Beatrix Imkeit, and Johannes Schenkel (DKFZ, Germany). The applied protocol is given in the following and partially repeated word for word as the procedure abided to these steps (Diercks et al. 2012). In brief, 2 epidydmides and vasa deferentia were placed in 625 µL of 37 °C warm cryoprotective media (CPM) [18% (w/v) raffinose (Sigma-Aldrich, USA), 3% (w/v) skim milk (BD Diagnostics, USA), and 477 µM monothioglycerol (Sigma-Aldrich, USA) in distilled water], and spermatozoa were allowed to disperse from the tissue for 10 min. 20 µL of spermatozoa in CPA were stained with two dyes for 5 min at 37 °C: 1 µL of a 1:1 mix of Hoechst 33342 stain (for all spermatozoa) (0.001 mg/mL in distilled water; Invitrogen, USA) and propidium iodide (PI) (M3181.0010, 0.0001 mg/mL in distilled water; Genaxxon, Germany) (to identify cells with compromised membranes). Fluorescence microscopy was carried out with an inverted microscope with appropriate filters (wavelength of the emitted light; Hoechst 33342: 461 nm, PI: 617 nm) by using a fluorescence microscope (Axio Observer Z1; Carl Zeiss AG, Germany). The slide containing 10 µL of the spermatozoa suspension was covered with a pre-warmed coverslip and placed onto an inverted microscope (TissueFAXSi, Tissue Gnostics, Austria). For the membrane integrity assay, 25 fields of view were acquired (with a 40x objective lens) with TissueFAXSi software controlling the camera (PCO270xs, PCO, Germany), filters, and stage movement (Märzhäuser, Germany). Typical exposure times were 110 ± 30 msec (DAPI filter) and 270 ± 20 msec (Texas Red filter). The process including all adjustments took no longer than 5 to 7 min. Fluorescence microscopy images were processed with TissueQuest software (TissueGnostics, Austria). All spermatozoa were identified

by Hoechst 33342 stain. Cell density was expressed in scattergrams where each dot represented one cell. Hoechst 33342 mean staining intensity (y axis) of every cell was plotted vs. the identified cell size (x axis) (Hoechst 33342 stained area). Cut-off values for distinguishing PI-positive from PI-negative cells were set according to the negative controls.

6.24 Oligonucleotide sequences

Purpose	Name	Sequence (5'-3')	Source
RNA-Seq validation			
E7.5 RNA-Seq qRT-PCR	Gm17821-fwd	GAAAGGTTGGACCATGTAGAGAC	Reinhard Liebers
E7.5 RNA-Seq qRT-PCR	Gm17821-rev	GCTTAGTTCATAATGTTGTTCCACC	Reinhard Liebers
E7.5 RNA-Seq qRT-PCR	Psap-fwd	GCAGAGATGTGAAGACGGCG	Reinhard Liebers
E7.5 RNA-Seq qRT-PCR	Psap-rev	CTCACAGGTCTTCTCCAGGTAATG	Reinhard Liebers
E7.5 RNA-Seq qRT-PCR	Rrm2-fwd	CTTCGTTGTCTTTCCCATCG	Reinhard Liebers
E7.5 RNA-Seq qRT-PCR	Rrm2-rev	CCTTGGGATCTTTAATGTAAGTGTC	Reinhard Liebers
E7.5 RNA-Seq qRT-PCR	Ass1-Fwd	ATCTACGAGACCCCAGCA	Reinhard Liebers
E7.5 RNA-Seq qRT-PCR	Ass1-Rev	CACCAGCTCTTCATTGTAGAGT	Reinhard Liebers
E7.5 RNA-Seq qRT-PCR	Nampt-fwd	CCAGGAGGCCAAAGAAGTGTAC	Reinhard Liebers
E7.5 RNA-Seq qRT-PCR	Nampt-rev	GGGTCTGTGTTTTCCACTGTGA	Reinhard Liebers
E7.5 RNA-Seq qRT-PCR	Sgk1-fwd	CCAGGGGCACATCGTCC	Reinhard Liebers
E7.5 RNA-Seq qRT-PCR	Sgk1-rev	GTTTCAACTGGAGAGGCTTGTTC	Reinhard Liebers
E7.5 RNA-Seq qRT-PCR	Csf1r-Fwd	CCTTGACAGCAATACCTACG	Reinhard Liebers
E7.5 RNA-Seq qRT-PCR	Csf1r-Rev	ACGTTGAATCCCACTTCG	Reinhard Liebers
E7.5 RNA-Seq qRT-PCR	Hivep3-Fwd	GAGATGGTCTCTGGGTCAG	Reinhard Liebers
E7.5 RNA-Seq qRT-PCR	Hivep3-Rev	CCAGCTGATGGACTTCG	Reinhard Liebers
ESC RNA-Seq qRT-PCR	Rps3a1-Fwd	TGAAGTGAGCCTTGCTGATCTAC	Reinhard Liebers
ESC RNA-Seq qRT-PCR	Rps3a1-Rev	CAAATACCCATCGGTCGTCTTG	Reinhard Liebers
ESC RNA-Seq qRT-PCR	Psma6-Fwd	AGCAGATCCCAGGTACAGA	Reinhard Liebers
ESC RNA-Seq qRT-PCR	Psma6-Rev	CTGCAGGATCACACTTGTACA	Reinhard Liebers
ESC RNA-Seq qRT-PCR	Itgb1-Fwd	ATGTCACCAATCGCAGCAAAG	Reinhard Liebers
ESC RNA-Seq qRT-PCR	Itgb1-Rev	CATTCTCCAGATCATCTTTCATAGAG	Reinhard Liebers
ESC RNA-Seq qRT-PCR	Mbtps1-Fwd	GGCTGCTCACACTTGAAGATC	Reinhard Liebers
ESC RNA-Seq qRT-PCR	Mbtps1-Rev	GAATGGCTCTCAGCAATCG	Reinhard Liebers
ESC RNA-Seq qRT-PCR	Fgfr1-Fwd	CCTGGAGCATCATAATGGATTCTG	Reinhard Liebers
ESC RNA-Seq qRT-PCR	Fgfr1-Rev	CCACTGAATGTGAGGCTGCG	Reinhard Liebers
ESC RNA-Seq qRT-PCR	Atp13a-Fwd	TGTCATCACTAGCCTGAAGGAG	Reinhard Liebers
ESC RNA-Seq qRT-PCR	Atp13a-Rev	GAGAGGAGTGCCGACTTCTGT	Reinhard Liebers
ESC RNA-Seq qRT-PCR	Mau2-Fwd	GCAGCAAGCCTGTTGTCAGAG	Reinhard Liebers
ESC RNA-Seq qRT-PCR	Mau2-Rev	CCACTCGGGCATACTCAGC	Reinhard Liebers
ESC RNA-Seq qRT-PCR	Tenm3-Fwd	GCCATCCCACAAGCAGCA	Reinhard Liebers
ESC RNA-Seq qRT-PCR	Tenm3-Rev	GCGTCGTCCCTGTCCCTG	Reinhard Liebers
ESC RNA-Seq qRT-PCR	Klhl13-Fwd	GAAACTGTGCCTTGGAAGT	Reinhard Liebers
ESC RNA-Seq qRT-PCR	Klhl13-Rev	TGAACATAGCTTTGAAGTAGTCAC	Reinhard Liebers
ESC RNA-Seq qRT-PCR	Zfp827-Fwd	TGAGTGTGATGTGTGCCA	Reinhard Liebers
ESC RNA-Seq qRT-PCR	Zfp827-Rev	ACTGCTCACACTTGTAGTGGTT	Reinhard Liebers
ESC RNA-Seq qRT-PCR	Hspb1-Fwd	GGCTGAAGGCTGGTGCG	Reinhard Liebers
ESC RNA-Seq qRT-PCR	Hspb1-Rev	GATGTAGCCATGTTCGTCCTG	Reinhard Liebers
Northern probes			
Northern - piRNA	FR0303691-PIR15422	CAAACCTGGTATGGATGCAGACAGC	Reinhard Liebers
Northern - sperm purity	spR-12	GCCCATGACCCGCCCACCCTG	Kawano et al., 2012
Northern - sperm purity	piR-1	AAAGCTATCTGAGCACCTGTGTTCATGTCA	Girard et al., 2006
Northern - Gly 5'	Gly-ms738	TCTACCACTGAACCACCGAT	Matthias Schäfer
Northern - Asp 5'	Asp-ms791	ACCACTATACTAACGAGGA	Matthias Schäfer
Northern - Glu 5'	Glu5'	TTCCCTGACCGGGAATCGAACCC	Francesca Tuorto
Northern - Ser 5'	Ser5'	CACTCGGCCCACCTCGTC	Francesca Tuorto
Northern - 5S rRNA control	5SrRNA	GGGTGGTATGGCCGTAGAC	Francesca Tuorto
Northern - transposable elements	L15UTR-R	GGAGTGCTGCGTTCTGATGA	Di Giacomo et al., 2013
Northern - transposable elements	L1ORF2-R	GCTGCTCTTGTATTTGGAGCATAGA	Di Giacomo et al., 2013
Northern - transposable elements	IAP3LTR-F	GCACATGCGCAGATTATTTGTT	Di Giacomo et al., 2013
Northern - transposable elements	IAPGag-R	GCCAATCAGCAGGCGTTAGT	Di Giacomo et al., 2013
Northern APB - HisGUG	HIS-fly(1)-mm(1)-h	CTAACCACTATACGATCACGGC	Reinhard liebers
Dnmt2			
Dnmt2 qRT-PCR	mDnmt28ex	TTGGCTGACTTTCTTCAACTACTGC	Francesca Tuorto
Dnmt2 qRT-PCR	oIMR5958	AGCCTGTGGCTTCAGTATCA	Francesca Tuorto
Genotyping Dnmt2	Dnmt2Gen3-Ex6	CCAGAGGGCTGCTGATACAAAC	Francesca Tuorto
Genotyping Dnmt2	Dnmt2Gen2-In10	TGGCAATCTTGTCTGGTCA	Francesca Tuorto
Genotyping Dnmt2	oIMR5957-In11	AAAGCAGGAAAATGCCTGAA	Francesca Tuorto
WTBS validation			
WTBS candidate	Gm26391-NR_046140.1-Fwd	GTtTGATtTtGGAAGtTAAGtAGGG	Reinhard Liebers
WTBS candidate	Gm26391-NR_046140.1-Rev	CCTACAaCACCCaaTATTCCCA	Reinhard Liebers
454 sequencing			
454 bisulfite sequencing preparation	AspGUC-fwd	TGTTAGTATAGTGGTgAGTAT	Francesca Tuorto
454 bisulfite sequencing preparation	AspGUC-rev	CTCCCCATCAAAAAATTA	Francesca Tuorto
454 bisulfite sequencing preparation	GlyGCC-fwd	GGTGGTTTAGTGGTAGAATT	Francesca Tuorto
454 bisulfite sequencing preparation	GlyGCC-rev	TACATTAACCAAAAATC	Francesca Tuorto
454 bisulfite sequencing preparation	ValAAC-fwd	GTTTTTGTAGTGTAGTGGTtAT	Francesca Tuorto
454 bisulfite sequencing preparation	ValAAC-rev	TATTTCCACCCAATTTCAAACC	Francesca Tuorto
454 adapter	454 adapter fwd (adaptor A, Lib-A)	CGTATCGCCTCCCTCGCGCCATCAG	Roche
454 adapter	454 adapter rev (adaptor B, Lib-A)	CTATGCGCCTTGCCAGCCCGCTCAG	Roche
Small RNA-Seq			
Small RNA Seq adaptor	NEBNext 3' SR Adaptor for Illumina	AGATCGGAAGAGCACACGTCT	NEB

7. Supplements

Candidate ID	Candidate symbol	C-position	wt meth. ratio	wt coverage	Dnmt2$^{-/-}$ meth. ratio	Dnmt2$^{-/-}$ coverage
ENSMUST00000083462	Mir99b	7	0.555223881	335	0	143
ENSMUST00000083462	Mir99b	9	0.706930693	505	0.013793103	145
ENSMUST00000083462	Mir99b	10	0.702970297	505	0.04137931	145
ENSMUST00000083462	Mir99b	11	0.702970297	505	0.013793103	145
ENSMUST00000083462	Mir99b	18	0.706930693	505	0	145
ENSMUST00000083462	Mir99b	19	0.699009901	505	0.013793103	145
ENSMUST00000083462	Mir99b	22	0.704142012	507	0.013793103	145
ENSMUST00000083462	Mir99b	23	0.700197239	507	0	145
ENSMUST00000083462	Mir99b	27	0.63599182	489	0.020689655	145
ENSMUST00000155159	Vax2os	2225	0.656174334	413	0.004926108	203
ENSMUST00000155159	Vax2os	2229	0.685082873	362	0.005524862	181
ENSMUST00000155159	Vax2os	2233	0.694533762	311	0	198
ENSMUST00000155159	Vax2os	2237	0.663082437	279	0	216
ENSMUST00000155159	Vax2os	2241	0.62601626	246	0	234
ENSMUST00000155159	Vax2os	2245	0.700934579	214	0	252
ENSMUST00000155159	Vax2os	2249	0.648351648	182	0	271
ENSMUST00000155159	Vax2os	2253	0.58	150	0	289
ENSMUST00000177555	Rn5s	118	0.571072319	401	0.09375	224
ENSMUST00000177575	n-R5s108	118	0.571072319	401	0.09375	224
ENSMUST00000177589	n-R5s121	118	0.571072319	401	0.09375	224
ENSMUST00000177889	n-R5s146	118	0.571072319	401	0.09375	224
ENSMUST00000177995	Gm22109	118	0.571072319	401	0.09375	224
ENSMUST00000178027	Gm22291	118	0.571072319	401	0.09375	224
ENSMUST00000178066	n-R5s141	118	0.571072319	401	0.09375	224
ENSMUST00000178069	Gm23284	118	0.571072319	401	0.09375	224
ENSMUST00000178106	n-R5s100	118	0.571072319	401	0.09375	224
ENSMUST00000178203	n-R5s111	118	0.571072319	401	0.09375	224
ENSMUST00000178499	n-R5s105	118	0.571072319	401	0.09375	224
ENSMUST00000178520	n-R5s149	118	0.571072319	401	0.09375	224
ENSMUST00000178755	n-R5s103	118	0.571072319	401	0.09375	224
ENSMUST00000178804	n-R5s123	118	0.571072319	401	0.09375	224
ENSMUST00000178820	n-R5s142	118	0.571072319	401	0.09375	224
ENSMUST00000178859	n-R5s144	118	0.571072319	401	0.09375	224
ENSMUST00000178975	n-R5s139	118	0.571072319	401	0.09375	224
ENSMUST00000178983	n-R5s134	118	0.571072319	401	0.09375	224
ENSMUST00000179080	n-R5s136	118	0.571072319	401	0.09375	224
ENSMUST00000179081	Gm25018	118	0.571072319	401	0.09375	224
ENSMUST00000179107	n-R5s104	118	0.571072319	401	0.09375	224
ENSMUST00000179143	n-R5s113	118	0.571072319	401	0.09375	224
ENSMUST00000179275	n-R5s133	118	0.571072319	401	0.09375	224
ENSMUST00000179431	n-R5s117	118	0.571072319	401	0.09375	224
ENSMUST00000179432	Gm25212	118	0.571072319	401	0.09375	224
ENSMUST00000179476	n-R5s138	118	0.571072319	401	0.09375	224
ENSMUST00000179500	n-R5s122	118	0.571072319	401	0.09375	224
ENSMUST00000179542	n-R5s143	118	0.571072319	401	0.09375	224
ENSMUST00000179704	n-R5s107	118	0.571072319	401	0.09375	224
ENSMUST00000179843	Gm26391	118	0.571072319	401	0.09375	224
ENSMUST00000179995	n-R5s110	118	0.571072319	401	0.09375	224
ENSMUST00000180096	n-R5s128	118	0.571072319	401	0.09375	224
ENSMUST00000180334	n-R5s124	118	0.571072319	401	0.09375	224
NM_028053.2	Tmem38b	1572	0.601902174	736	0.018617021	752
NM_028053.2	Tmem38b	1605	0.502883506	2601	0.074390244	1640
NM_028053.2	Tmem38b	1612	0.665950591	1862	0.063583815	865
NR_029536.1	Mir99b	7	0.555223881	335	0	143
NR_029536.1	Mir99b	9	0.706930693	505	0.013793103	145
NR_029536.1	Mir99b	10	0.702970297	505	0.04137931	145
NR_029536.1	Mir99b	11	0.702970297	505	0.013793103	145
NR_029536.1	Mir99b	18	0.706930693	505	0	145
NR_029536.1	Mir99b	19	0.699009901	505	0.013793103	145
NR_029536.1	Mir99b	22	0.704142012	507	0.013793103	145
NR_029536.1	Mir99b	23	0.700197239	507	0	145
NR_029536.1	Mir99b	27	0.63599182	489	0.020689655	145
NR_046127.1	Gm25018	57	0.544897959	980	0.010118044	1186
NR_046127.1	Gm25018	63	0.56693712	986	0.024201355	1033
NR_046127.1	Gm25018	67	0.579918033	976	0.02672148	973
NR_046127.1	Gm25018	68	0.589322382	974	0.031914894	940
NR_046127.1	Gm25018	78	0.705882353	1462	0.026128266	1263
NR_046127.1	Gm25018	91	0.557637997	3895	0.04188666	2841

NR_046127.1	Gm25018	92	0.540081177	3942	0.025017373	2878
NR_046127.1	Gm25018	94	0.538480697	4015	0.017012589	2939
NR_046127.1	Gm25018	95	0.533581165	4035	0.020594193	2962
NR_046127.1	Gm25018	111	0.527195668	4247	0.061510791	2780
NR_046127.1	Gm25018	118	0.599489796	3528	0.049204771	2012
NR_046140.1	Gm26391	57	0.544897959	980	0.010118044	1186
NR_046140.1	Gm26391	63	0.56693712	986	0.024201355	1033
NR_046140.1	Gm26391	67	0.579918033	976	0.02672148	973
NR_046140.1	Gm26391	68	0.589322382	974	0.031914894	940
NR_046140.1	Gm26391	78	0.705882353	1462	0.026128266	1263
NR_046140.1	Gm26391	91	0.557637997	3895	0.04188666	2841
NR_046140.1	Gm26391	92	0.540081177	3942	0.025017373	2878
NR_046140.1	Gm26391	94	0.538480697	4015	0.017012589	2939
NR_046140.1	Gm26391	95	0.533581165	4035	0.020594193	2962
NR_046140.1	Gm26391	111	0.527195668	4247	0.061510791	2780
NR_046140.1	Gm26391	118	0.599489796	3528	0.049204771	2012
NR_046147.1	Gm22109	57	0.544897959	980	0.010118044	1186
NR_046147.1	Gm22109	63	0.56693712	986	0.024201355	1033
NR_046147.1	Gm22109	67	0.579918033	976	0.02672148	973
NR_046147.1	Gm22109	68	0.589322382	974	0.031914894	940
NR_046147.1	Gm22109	78	0.705882353	1462	0.026128266	1263
NR_046147.1	Gm22109	91	0.557637997	3895	0.04188666	2841
NR_046147.1	Gm22109	92	0.540081177	3942	0.025017373	2878
NR_046147.1	Gm22109	94	0.538480697	4015	0.017012589	2939
NR_046147.1	Gm22109	95	0.533581165	4035	0.020594193	2962
NR_046147.1	Gm22109	111	0.527195668	4247	0.061510791	2780
NR_046147.1	Gm22109	118	0.599489796	3528	0.049204771	2012
NR_046152.1	Gm25212	57	0.544897959	980	0.010118044	1186
NR_046152.1	Gm25212	63	0.56693712	986	0.024201355	1033
NR_046152.1	Gm25212	67	0.579918033	976	0.02672148	973
NR_046152.1	Gm25212	68	0.589322382	974	0.031914894	940
NR_046152.1	Gm25212	78	0.705882353	1462	0.026128266	1263
NR_046152.1	Gm25212	91	0.557637997	3895	0.04188666	2841
NR_046152.1	Gm25212	92	0.540081177	3942	0.025017373	2878
NR_046152.1	Gm25212	94	0.538480697	4015	0.017012589	2939
NR_046152.1	Gm25212	95	0.533581165	4035	0.020594193	2962
NR_046152.1	Gm25212	111	0.527195668	4247	0.061510791	2780
NR_046152.1	Gm25212	118	0.599489796	3528	0.049204771	2012
NR_046154.1	Gm22291	57	0.544897959	980	0.010118044	1186
NR_046154.1	Gm22291	63	0.56693712	986	0.024201355	1033
NR_046154.1	Gm22291	67	0.579918033	976	0.02672148	973
NR_046154.1	Gm22291	68	0.589322382	974	0.031914894	940
NR_046154.1	Gm22291	78	0.705882353	1462	0.026128266	1263
NR_046154.1	Gm22291	91	0.557637997	3895	0.04188666	2841
NR_046154.1	Gm22291	92	0.540081177	3942	0.025017373	2878
NR_046154.1	Gm22291	94	0.538480697	4015	0.017012589	2939
NR_046154.1	Gm22291	95	0.533581165	4035	0.020594193	2962
NR_046154.1	Gm22291	111	0.527195668	4247	0.061510791	2780
NR_046154.1	Gm22291	118	0.599489796	3528	0.049204771	2012
NR_046155.1	Gm23284	57	0.544897959	980	0.010118044	1186
NR_046155.1	Gm23284	63	0.56693712	986	0.024201355	1033
NR_046155.1	Gm23284	67	0.579918033	976	0.02672148	973
NR_046155.1	Gm23284	68	0.589322382	974	0.031914894	940
NR_046155.1	Gm23284	78	0.705882353	1462	0.026128266	1263
NR_046155.1	Gm23284	91	0.557637997	3895	0.04188666	2841
NR_046155.1	Gm23284	92	0.540081177	3942	0.025017373	2878
NR_046155.1	Gm23284	94	0.538480697	4015	0.017012589	2939
NR_046155.1	Gm23284	95	0.533581165	4035	0.020594193	2962
NR_046155.1	Gm23284	111	0.527195668	4247	0.061510791	2780
NR_046155.1	Gm23284	118	0.599489796	3528	0.049204771	2012

Supplementary Table S1. Candidate Dnmt2 methylation sites as determined bioinformatically. Candidates are displayed by their IDs (column 1) and symbols (column 2). Additional columns give the candidate methylated cytosine position, the methylation ratio of this C in the wt, the coverage of this C in the wt, followed by these two parameters for Dnmt2$^{-/-}$. For this shortlist, the candidate C had to have a methylation ratio of >0.5 in the wt and <0.1 in the mutant, while in both genotypes the C had to be covered >100x. With these parameters set, 128 cytosine candidates on 42 RNAs appear.

8. List of Publications

Kiani, Jafar, Valérie Grandjean, **Reinhard Liebers**, Francesca Tuorto, Hossein Ghanbarian, Frank Lyko, François Cuzin, and Minoo Rassoulzadegan. 2013. "RNA-Mediated Epigenetic Heredity Requires the Cytosine Methyltransferase Dnmt2." PLoS Genetics 9 (5): e1003498. doi:10.1371/journal.pgen.1003498.

Liebers, Reinhard, Minoo Rassoulzadegan, and Frank Lyko. 2014. "Epigenetic Regulation by Heritable RNA." PLoS Genetics 10 (4): e1004296. doi:10.1371/journal.pgen.1004296.

Tuorto, Francesca, Friederike Herbst, Nader Alerasool, Sebastian Bender, Oliver Popp, Giuseppina Federico, Sonja Reitter, **Reinhard Liebers**, Georg Stoecklin, Hermann-Josef Gröne, Gunnar Dittmar, Hanno Glimm & Frank Lyko. 2015. "The tRNA Methyltransferase Dnmt2 Is Required for Accurate Polypeptide Synthesis during Haematopoiesis," The EMBO Journal. 1–13.

Tuorto, Francesca, **Reinhard Liebers**, Tanja Musch, Matthias Schaefer, Sarah Hofmann, Stefanie Kellner, Michaela Frye, Mark Helm, Georg Stoecklin, and Frank Lyko. 2012. "RNA Cytosine Methylation by Dnmt2 and NSun2 Promotes tRNA Stability and Protein Synthesis." Nature Structural & Molecular Biology, (August). Nature Publishing Group: 1–7. doi:10.1038/nsmb.2357.

9. References

Abbasi-Moheb, Lia, Sara Mertel, Melanie Gonsior, Leyla Nouri-Vahid, Kimia Kahrizi, Sebahattin Cirak, Dagmar Wieczorek, et al. 2012. “Mutations in NSUN2 Cause Autosomal-Recessive Intellectual Disability.” *American Journal of Human Genetics* 90 (5). The American Society of Human Genetics: 847–55. doi:10.1016/j.ajhg.2012.03.021.

Abd El Naby, W S, T H Hagos, M M Hossain, D Salilew-Wondim, a Y Gad, F Rings, M U Cinar, et al. 2013. “Expression Analysis of Regulatory microRNAs in Bovine Cumulus Oocyte Complex and Preimplantation Embryos.” *Zygote (Cambridge, England)* 21 (1): 31–51. doi:10.1017/S0967199411000566.

Aguer, Céline, Daniela Gambarotta, Ryan J. Mailloux, Cynthia Moffat, Robert Dent, Ruth McPherson, and Mary-Ellen Harper. 2011. “Galactose Enhances Oxidative Metabolism and Reveals Mitochondrial Dysfunction in Human Primary Muscle Cells.” *PLoS ONE* 6 (12): e28536. doi:10.1371/journal.pone.0028536.

Alarcón, Claudio R, Hyeseung Lee, Hani Goodarzi, Nils Halberg, and Sohail F Tavazoie. 2015. “N6-Methyladenosine Marks Primary microRNAs for Processing.” *Nature* 519 (7544): 482–85. doi:10.1038/nature14281.

Alarcón, Claudio R., Hani Goodarzi, Hyeseung Lee, Xuhang Liu, Saeed Tavazoie, and Sohail F. Tavazoie. 2015. “HNRNPA2B1 Is a Mediator of m6A-Dependent Nuclear RNA Processing Events.” *Cell*, 1299–1308. doi:10.1016/j.cell.2015.08.011.

Anders, Simon, and Wolfgang Huber. 2010. “Differential Expression Analysis for Sequence Count Data.” *Genome Biology* 11 (10). BioMed Central Ltd: R106. doi:10.1186/gb-2010-11-10-r106.

Auxilien, Sylvie, and Tobacco Etch Virus. 2012. “The Human tRNA M 5 C Methyltransferase Misu Is,” no. November: 1–8.

Avendaño, Conrado, Anahí Franchi, Estella Jones, and Sergio Oehninger. 2009. “Pregnancy-Specific B-1-Glycoprotein 1 and Human Leukocyte Antigen-E mRNA in Human Sperm: Differential Expression in Fertile and Infertile Men and Evidence of a Possible Functional Role during Early Development.” *Human Reproduction* 24 (2): 270–77. doi:10.1093/humrep/den381.

Belleannee, Clémence, Maya Belghazi, Valérie Labas, Ana-Paula Teixeira-Gomes, Jean Luc Gatti, Jean-Louis Dacheux, and Françoise Dacheux. 2011. “Purification and Identification of Sperm Surface Proteins and Changes during Epididymal Maturation.” *Proteomics* 11 (10): 1952–64. doi:10.1002/pmic.201000662.

Bertalanffy, Felix D. 1960. “ANNALS OF THE NEW YORK ACADEMY OF SCIENCES A NEW METHOD FOR CYTOLOGICAL DIAGNOSIS.” *Annals of the New York Academy of Sciences* 84: 225–38.

Béthune, Julien, Caroline G Artus-Revel, and Witold Filipowicz. 2012. “Kinetic Analysis Reveals Successive Steps Leading to miRNA-Mediated Silencing in Mammalian Cells.” *EMBO Reports* 13 (8): 716–23. doi:10.1038/embor.2012.82.

Blanco, Sandra, Agata Kurowski, Jennifer Nichols, Fiona M Watt, Salvador Aznar Benitah, and Michaela Frye. 2011. “The RNA-Methyltransferase Misu (NSun2) Poises Epidermal Stem Cells to Differentiate.” *PLoS Genetics* 7 (12): e1002403. doi:10.1371/journal.pgen.1002403.

Brzezicha, Bartosz, Marcin Schmidt, Izabela Makalowska, Artur Jarmolowski, Joanna Pienkowska, and Zofia Szweykowska-Kulinska. 2006. “Identification of Human tRNA:m5C Methyltransferase Catalysing Intron-Dependent m5C Formation in the First Position of the Anticodon of the Pre-tRNA Leu (CAA).” *Nucleic Acids Research* 34 (20): 6034–43. doi:10.1093/nar/gkl765.

Bygren, L O, Gunnar Kaati, and Sören Edvinsson. 2001. “Longevity Determined by Paternal Ancestors’ Nutrition during Their Slow Growth Period” 7: 53–59.

Carone, Benjamin R, Lucas Fauquier, Naomi Habib, Jeremy M Shea, Caroline E Hart, Ruowang Li, Christoph Bock, et al. 2010. “Paternally Induced Transgenerational Environmental Reprogramming of Metabolic Gene Expression in Mammals.” *Cell* 143 (7). Elsevier Inc.: 1084–96. doi:10.1016/j.cell.2010.12.008.

Chan, Clement T Y, Yan Ling Joy Pang, Wenjun Deng, I Ramesh Babu, Madhu Dyavaiah, Thomas J Begley, and Peter C Dedon. 2012. “Reprogramming of tRNA Modifications Controls the Oxidative Stress Response by Codon-Biased Translation of Proteins.” *Nature Communications* 3 (may): 937. doi:10.1038/ncomms1938.

Chan, Patricia P, and Todd M Lowe. 2009. “GtRNAdb: A Database of Transfer RNA Genes Detected in Genomic Sequence.” *Nucleic Acids Research* 37 (Database issue): D93–97. doi:10.1093/nar/gkn787.

Chen, Raymond F. 1967. “MACROMOLECULES : Removal of Fatty Acids from Serum Albumin by Charcoal Treatment Removal of Fatty Acids by Charcoal Treatment from Serum Albumin.” *Journal of Biological Chemistry* 242 (25): 173–81.

Chen, Tong, Ya-Juan Hao, Ying Zhang, Miao-Miao Li, Meng Wang, Weifang Han, Yongsheng Wu, et al. 2015. “m6A RNA Methylation Is Regulated by MicroRNAs and Promotes Reprogramming to Pluripotency.” *Cell Stem Cell* 16 (3). Elsevier Inc.: 289–301. doi:10.1016/j.stem.2015.01.016.

Cheng, H, and C P Leblond. 1974. “Origin, Differentiation and Renewal of the Four Main Epithelial Cell Types in the Mouse Small Intestine. V. Unitarian Theory of the Origin of the Four Epithelial Cell Types.” *The American Journal of Anatomy* 141 (4): 537–61. doi:10.1002/aja.1001410407.

Cole, Christian, Andrew Sobala, Cheng Lu, Shawn R Thatcher, Andrew Bowman, John W S Brown, Pamela J Green, Geoffrey J Barton, and Gyorgy Hutvagner. 2009a. “Filtering of Deep Sequencing Data Reveals the Existence of Abundant Dicer-Dependent Small RNAs Derived from tRNAs.” *RNA (New York, N.Y.)* 15 (12): 2147–60. doi:10.1261/rna.1738409.

Di Giacomo, Monica, Stefano Comazzetto, Harpreet Saini, Serena De Fazio, Claudia Carrieri, Marcos Morgan, Lina Vasiliauskaite, Vladimir Benes, Anton J Enright, and Dónal O’Carroll. 2013. “Multiple Epigenetic Mechanisms and the piRNA Pathway Enforce LINE1 Silencing during Adult Spermatogenesis.” *Molecular Cell* 50 (4): 601–8. doi:10.1016/j.molcel.2013.04.026.

Diercks, Ann-Kathrin, Heinrich F. Bürgers, Anna Schwab, and Johannes Schenkel. 2012. “Improved Assessment of Frozen/thawed Mouse Spermatozoa Using Fluorescence Microscopy.” *Journal of Veterinary Science* 13 (3): 315. doi:10.4142/jvs.2012.13.3.315.

Dominissini, Dan, Sharon Moshitch-Moshkovitz, Schraga Schwartz, Mali Salmon-Divon, Lior Ungar, Sivan Osenberg, Karen Cesarkas, et al. 2012. “Topology of the Human and Mouse m6A RNA Methylomes Revealed by m6A-Seq.” *Nature* 485 (7397). Nature Publishing Group: 201–6. doi:10.1038/nature11112.

Dominissini, Dan, Sharon Moshitch-moshkovitz, Schraga Schwartz, Lior Ungar, Sivan Osenberg, Karen Cesarkas, Jasmine Jacob-hirsch, et al. 2012. “Topology of the Human and Mouse M 6 A RNA Methylomes Revealed by M 6 A-Seq.” *Nature*. Nature Publishing Group. doi:10.1038/nature11112.

Dong, a, J a Yoder, X Zhang, L Zhou, T H Bestor, and X Cheng. 2001. “Structure of Human DNMT2, an Enigmatic DNA Methyltransferase Homolog That Displays Denaturant-Resistant Binding to DNA.” *Nucleic Acids Research* 29 (2): 439–48. http://www.pubmedcentral.nih.gov/articlerender.fcgi?artid=29660&tool=pmcentrez&rendertype=abstract.

Drouin, J, L Lagacé, and F Labrie. 1976. “Estradiol-Induced Increase of the LH Responsive to LH Releasing Hormone (LHRH) in Rat Anterior Pituitary Cells in Culture.” *Endocrinology* 99 (6): 1477–81. doi:10.1210/endo-99-6-1477.

Durdevic, Zeljko, Katharina Hanna, Beth Gold, Tim Pollex, Sara Cherry, Frank Lyko, and Matthias Schaefer. 2013a. “Efficient RNA Virus Control in Drosophila Requires the RNA Methyltransferase Dnmt2.” *EMBO Reports* 14 (3). Nature Publishing Group: 269–75. doi:10.1038/embor.2013.3.

Durdevic, Zeljko, Mehrpouya Balaghy Mobin, Katharina Hanna, Frank Lyko, and Matthias Schaefer. 2013a. “Report The RNA Methyltransferase Dnmt2 Is Required for Efficient Dicer-2-Dependent siRNA Pathway Activity in Drosophila.” *CellReports* 4 (5). The Authors: 931–37. doi:10.1016/j.celrep.2013.07.046.

Ebert, Margaret S, and Phillip a Sharp. 2012. “Roles for microRNAs in Conferring Robustness to Biological Processes.” *Cell* 149 (3). Elsevier Inc.: 515–24. doi:10.1016/j.cell.2012.04.005.

Edelheit, Sarit, Schraga Schwartz, Maxwell R Mumbach, Omri Wurtzel, and Rotem Sorek. 2013. “Transcriptome-Wide Mapping of 5-Methylcytidine RNA Modifications in Bacteria, Archaea, and Yeast Reveals m5C within Archaeal mRNAs.” *PLoS Genetics* 9 (6): e1003602. doi:10.1371/journal.pgen.1003602.

Emara, Mohamed M., Pavel Ivanov, Tyler Hickman, Nemisha Dawra, Sarah Tisdale, Nancy Kedersha, Guo Fu Hu, and Paul Anderson. 2010. “Angiogenin-Induced tRNA-Derived Stress-Induced RNAs Promote Stress-Induced Stress Granule Assembly.” *Journal of Biological Chemistry* 285 (14): 10959–68. doi:10.1074/jbc.M109.077560.

Evsikov, Alexei V, Joel H Graber, J Michael Brockman, Ales Hampl, Andrea E Holbrook, Priyam Singh, John J Eppig, Davor Solter, and Barbara B Knowles. 2006. “Cracking the Egg: Molecular Dynamics and Evolutionary Aspects of the Transition from the Fully Grown Oocyte to Embryo.” *Genes & Development* 20 (19): 2713–27. doi:10.1101/gad.1471006.

Farkas, W. R. 1980. “Effect of Diet on the Queuosine Family of tRNAs of Germ-Free Mice.” *Journal of Biological Chemistry* 255 (14): 6832–35.

Feng, Suhua, Shawn J Cokus, Xiaoyu Zhang, Pao-Yang Chen, Magnolia Bostick, Mary G Goll, Jonathan Hetzel, et al. 2010. “Conservation and Divergence of Methylation Patterning in Plants and Animals.” *Proceedings of the National Academy of Sciences of the United States of America* 107 (19): 8689–94. doi:10.1073/pnas.1002720107.

Fergus, Claire, Dominic Barnes, Mashael Alqasem, and Vincent Kelly. 2015. *The Queuine Micronutrient: Charting a Course from Microbe to Man*. *Nutrients*. Vol. 7. doi:10.3390/nu7042897.

Ferguson-Smith, Anne C, and Mary-Elizabeth Patti. 2011. “You Are What Your Dad Ate.” *Cell Metabolism* 13 (2). Elsevier Inc.: 115–17. doi:10.1016/j.cmet.2011.01.011.

Findeiss, Sven, David Langenberger, Peter F Stadler, and Steve Hoffmann. 2011. “Traces of Post-Transcriptional RNA Modifications in Deep Sequencing Data.” *Biological Chemistry* 392 (4): 305–13. doi:10.1515/BC.2011.043.

Franke, Barbara, Sita H H M Vermeulen, Regine P M Steegers-Theunissen, Marieke J Coenen, Mascha M V a P Schijvenaars, Hans Scheffer, Martin den Heijer, and Henk J Blom. 2009.

"An Association Study of 45 Folate-Related Genes in Spina Bifida: Involvement of Cubilin (CUBN) and tRNA Aspartic Acid Methyltransferase 1 (TRDMT1)." *Birth Defects Research. Part A, Clinical and Molecular Teratology* 85 (3): 216–26. doi:10.1002/bdra.20556.

Fullston, Tod, E Maria C Ohlsson Teague, Nicole O Palmer, Miles J Deblasio, Megan Mitchell, Mark Corbett, Cristin G Print, Julie a Owens, and Michelle Lane. 2013. "Paternal Obesity Initiates Metabolic Disturbances in Two Generations of Mice with Incomplete Penetrance to the F2 Generation and Alters the Transcriptional Profile of Testis and Sperm microRNA Content." *FASEB Journal : Official Publication of the Federation of American Societies for Experimental Biology* 27 (10): 4226–43. doi:10.1096/fj.12-224048.

Gan, Haiyun, Xiwen Lin, Zhuqiang Zhang, Wei Zhang, Shangying Liao, Lixian Wang, and Chunsheng Han. 2011. "piRNA Profiling during Specific Stages of Mouse Spermatogenesis." *RNA (New York, N.Y.)* 17 (7): 1191–1203. doi:10.1261/rna.2648411.

Gapp, Katharina, Ali Jawaid, Peter Sarkies, Johannes Bohacek, Pawel Pelczar, Julien Prados, Laurent Farinelli, Eric Miska, and Isabelle M Mansuy. 2014. "Implication of Sperm RNAs in Transgenerational Inheritance of the Effects of Early Trauma in Mice." *Nature Publishing Group* 17 (5). Nature Publishing Group: 667–69. doi:10.1038/nn.3695.

García-López, Jesús, Juan De Dios Hourcade, Lola Alonso, David B Cárdenas, and Jesús del Mazo. 2014. "Global Characterization and Target Identification of piRNAs and Endo-siRNAs in Mouse Gametes and Zygotes." *Biochimica et Biophysica Acta* 1839 (6). Elsevier B.V.: 463–75. doi:10.1016/j.bbagrm.2014.04.006.

Gebetsberger, Jennifer, Marek Zywicki, Andrea Künzi, and Norbert Polacek. 2012. "tRNA-Derived Fragments Target the Ribosome and Function as Regulatory Non-Coding RNA in Haloferax Volcanii." *Archaea (Vancouver, B.C.)* 2012 (January): 260909. doi:10.1155/2012/260909.

Geula, S, S Moshitch-Moshkovitz, D Dominissini, A AlFatah Mansour, N Kol, and M Salmon-Divon. 2015. "m6A mRNA Methylation Facilitates Resolution of Naïve Pluripotency toward Differentiation." *Science* 347 (6225): 1002–6.

Gingold, Hila, Disa Tehler, Nanna R Christoffersen, Morten M Nielsen, Fazila Asmar, Susanne M Kooistra, Nicolaj S Christophersen, et al. 2014. "A Dual Program for Translation Regulation in Cellular Proliferation and Differentiation." *Cell* 158 (6). Elsevier Inc.: 1281–92. doi:10.1016/j.cell.2014.08.011.

Girard, Angélique, Ravi Sachidanandam, Gregory J Hannon, and Michelle a Carmell. 2006. "A Germline-Specific Class of Small RNAs Binds Mammalian Piwi Proteins." *Nature* 442 (7099): 199–202. doi:10.1038/nature04917.

Goll, Mary Grace, and Timothy H Bestor. 2005. “Eukaryotic Cytosine Methyltransferases.” *Annual Review of Biochemistry* 74 (January): 481–514. doi:10.1146/annurev.biochem.74.010904.153721.

Goll, Mary Grace, Finn Kirpekar, Keith a Maggert, Jeffrey a Yoder, Chih-Lin Hsieh, Xiaoyu Zhang, Kent G Golic, Steven E Jacobsen, and Timothy H Bestor. 2006a. “Methylation of tRNAAsp by the DNA Methyltransferase Homolog Dnmt2.” *Science (New York, N.Y.)* 311 (5759): 395–98. doi:10.1126/science.1120976.

Goodarzi, Hani, Xuhang Liu, Hoang C.B. Nguyen, Steven Zhang, Lisa Fish, and Sohail F. Tavazoie. 2015. “Endogenous tRNA-Derived Fragments Suppress Breast Cancer Progression via YBX1 Displacement.” *Cell* 161 (4). Elsevier Inc.: 790–802. doi:10.1016/j.cell.2015.02.053.

Grossniklaus, Ueli, William G Kelly, Bill Kelly, Anne C Ferguson-Smith, Marcus Pembrey, and Susan Lindquist. 2013. “Transgenerational Epigenetic Inheritance: How Important Is It?” *Nature Reviews. Genetics* 14 (3). Nature Publishing Group: 228–35. doi:10.1038/nrg3435.

Grunewald, S, U Paasch, H-J Glander, and U Anderegg. 2005. “Mature Human Spermatozoa Do Not Transcribe Novel RNA.” *Andrologia* 37 (2-3): 69–71. doi:10.1111/j.1439-0272.2005.00656.x.

Guo, Hongshan, Ping Zhu, Liying Yan, Rong Li, Boqiang Hu, Ying Lian, Jie Yan, et al. 2014. “The DNA Methylation Landscape of Human.” *Nature* 511 (7511). Nature Publishing Group: 606–10. doi:10.1038/nature13544.

Hafner, Markus, Pablo Landgraf, Janos Ludwig, Amanda Rice, Tolulope Ojo, Carolina Lin, Daniel Holoch, Cindy Lim, and Thomas Tuschl. 2008. “Identification of microRNAs and Other Small Regulatory RNAs Using cDNA Library Sequencing.” *Methods (San Diego, Calif.)* 44 (1): 3–12. doi:10.1016/j.ymeth.2007.09.009.

Hardy, John, D Ph, and Andrew Singleton. 2009. “Genomewide Association Studies and Human Disease,” 1759–68.

Haussecker, Dirk, Yong Huang, Ashley Lau, Poornima Parameswaran, Andrew Z Fire, and Mark a Kay. 2010. “Human tRNA-Derived Small RNAs in the Global Regulation of RNA Silencing.” *RNA (New York, N.Y.)* 16 (4): 673–95. doi:10.1261/rna.2000810.

Heijmans, Bastiaan T, Elmar W Tobi, Aryeh D Stein, Hein Putter, Gerard J Blauw, Ezra S Susser, P Eline Slagboom, and L H Lumey. 2008. “Persistent Epigenetic Differences Associated with Prenatal Exposure to Famine in Humans.” *Proceedings of the National Academy of Sciences of the United States of America* 105 (44): 17046–49. doi:10.1073/pnas.0806560105.

Hirano, Takamasa, Yuka W Iwasaki, Zachary Yu-Ching Lin, Masanori Imamura, Naomi M Seki, Erika Sasaki, Kuniaki Saito, Hideyuki Okano, Mikiko C Siomi, and Haruhiko Siomi. 2014.

"Small RNA Profiling and Characterization of piRNA Clusters in the Adult Testes of the Common Marmoset, a Model Primate." *RNA (New York, N.Y.)* 20 (8): 1223–37. doi:10.1261/rna.045310.114.

Hommelsheim, Carl Maximilian, Lamprinos Frantzeskakis, Mengmeng Huang, and Bekir Ülker. 2014. "PCR Amplification of Repetitive DNA: A Limitation to Genome Editing Technologies and Many Other Applications." *Scientific Reports* 4: 5052. doi:10.1038/srep05052.

Hotchkiss, D. 1948. "The Quantitative Separation of Purines, Pyrimidines, and Nucleosides by Paper Chromatography." *Journal of Biological Chemistry*.

Hussain, Shobbir, Sandra Blanco Benavente, Elisabete Nascimento, Ilaria Dragoni, Agata Kurowski, Astrid Gillich, Peter Humphreys, and Michaela Frye. 2009. "The Nucleolar RNA Methyltransferase Misu (NSun2) Is Required for Mitotic Spindle Stability." *The Journal of Cell Biology* 186 (1): 27–40. doi:10.1083/jcb.200810180.

Hussain, Shobbir, Abdulrahim A Sajini, Sandra Blanco, Sabine Dietmann, Patrick Lombard, Yoichiro Sugimoto, Maike Paramor, et al. 2013a. "Report of Vault Noncoding RNA Determines Its Processing into Regulatory Small RNAs." The Authors, 255–61. doi:10.1016/j.celrep.2013.06.029.

Hussain, Shobbir, Abdulrahim a Sajini, Sandra Blanco, Sabine Dietmann, Patrick Lombard, Yoichiro Sugimoto, Maike Paramor, et al. 2013b. "NSun2-Mediated Cytosine-5 Methylation of Vault Noncoding RNA Determines Its Processing into Regulatory Small RNAs." *Cell Reports* 4 (2). The Authors: 255–61. doi:10.1016/j.celrep.2013.06.029.

Hussain, Shobbir, Francesca Tuorto, Suraj Menon, Sandra Blanco, Claire Cox, Joana V Flores, Stephen Watt, Nobuaki R Kudo, Frank Lyko, and Michaela Frye. 2013. "The Mouse Cytosine-5 RNA Methyltransferase NSun2 Is a Component of the Chromatoid Body and Required for Testis Differentiation." *Molecular and Cellular Biology* 33 (8): 1561–70. doi:10.1128/MCB.01523-12.

Igloi, Gabor L, and Hans Kossel. 1985. "Affinity Electrophoresis for Monitoring Terminal Phosphorylation and the Presence of Queuosine in RNA. Application of Polyacrylamide Containing a Covalently Bound Boronic Acid." *Nucleic Acids Research* 13 (19): ii. doi:10.1093/nar/gkq840.

Ivanov, Pavel, Mohamed M Emara, Judit Villen, Steven P Gygi, and Paul Anderson. 2011a. "Angiogenin-Induced tRNA Fragments Inhibit Translation Initiation." *Molecular Cell* 43 (4). Elsevier Inc.: 613–23. doi:10.1016/j.molcel.2011.06.022.

Jacobson, K. Bruce, W. R. Farkas, and J. R. Katze. 1981. "Presence of Queuine in Drosophila Melanogaster: Correlation of Free Pool with Queuosine Content of tRNA and Effect of

Mutations in Pteridine Metabolism." *Nucleic Acids Research* 9 (10): 2351–66. doi:10.1093/nar/9.10.2351.

Johnson, G D, E Sendler, C Lalancette, R Hauser, M P Diamond, and S a Krawetz. 2011a. "Cleavage of rRNA Ensures Translational Cessation in Sperm at Fertilization." *Molecular Human Reproduction* 17 (12): 721–26. doi:10.1093/molehr/gar054.

Jurkowski, Tomasz P, Madeleine Meusburger, Sameer Phalke, Mark Helm, Wolfgang Nellen, Gunter Reuter, and Albert Jeltsch. 2008. "Human DNMT2 Methylates tRNA(Asp) Molecules Using a DNA Methyltransferase-like Catalytic Mechanism." *RNA (New York, N.Y.)* 14 (8): 1663–70. doi:10.1261/rna.970408.

Jurkowski, Tomasz P, Raghuvaran Shanmugam, Mark Helm, and Albert Jeltsch. 2012. "Mapping the tRNA Binding Site on the Surface of Human DNMT2 Methyltransferase." *Biochemistry* 51 (22): 4438–44. doi:10.1021/bi3002659.

Kaati, G, L O Bygren, and S Edvinsson. 2002. "Cardiovascular and Diabetes Mortality Determined by Nutrition during Parents' and Grandparents' Slow Growth Period." *European Journal of Human Genetics : EJHG* 10 (11): 682–88. doi:10.1038/sj.ejhg.5200859.

Kaati, Gunnar, Lars Olov Bygren, Marcus Pembrey, and Michael Sjöström. 2007. "Transgenerational Response to Nutrition, Early Life Circumstances and Longevity." *European Journal of Human Genetics : EJHG* 15 (7): 784–90. doi:10.1038/sj.ejhg.5201832.

Karaiskos, Spyros, Ammar S Naqvi, Karl E Swanson, and Andrey Grigoriev. 2015. "Age-Driven Modulation of tRNA-Derived Fragments in Drosophila and Their Potential Targets." Biology Direct, 1–13. doi:10.1186/s13062-015-0081-6.

Kasai, H., K. Nakanishi, R. D. Macfarlane, D. F. Torgerson, Z. Ohashi, J. A. McCloskey, H. J. Gross, and S. Nishimura. 1976. "The Structure of Q Nucleoside Isolated from Rabbit Liver tRNA." *Journal of the American Chemical Society* 98 (16): 5044–46.

Katze, J R. 1978. "Q-Factor: A Serum Component Required for the Appearance of Nucleoside Q in tRNA in Tissue Culture." *Biochemical and Biophysical Research Communications* 84 (2): 527–35.

Katze, J R, B Basile, and J a McCloskey. 1982. "Queuine, a Modified Base Incorporated Posttranscriptionally into Eukaryotic Transfer RNA: Wide Distribution in Nature." *Science (New York, N.Y.)* 216 (4541): 55–56. doi:10.1126/science.7063869.

Kawano, Mitsuoki, Hideya Kawaji, Valérie Grandjean, Jafar Kiani, and Minoo Rassoulzadegan. 2012a. "Novel Small Noncoding RNAs in Mouse Spermatozoa, Zygotes and Early Embryos." *PloS One* 7 (9): e44542. doi:10.1371/journal.pone.0044542.

Keam, Simon P, Paul E Young, Alexandra L McCorkindale, Thurston H Y Dang, Jennifer L Clancy, David T Humphreys, Thomas Preiss, et al. 2014. “The Human Piwi Protein Hiwi2 Associates with tRNA-Derived piRNAs in Somatic Cells.” *Nucleic Acids Research* 42 (14): 8984–95. doi:10.1093/nar/gku620.

Khoddami, Vahid, and Bradley R Cairns. 2013. “Identification of Direct Targets and Modified Bases of RNA Cytosine Methyltransferases.” *Nature Biotechnology* 31 (5): 458–64. doi:10.1038/nbt.2566.

Kiani, Jafar, Valérie Grandjean, Reinhard Liebers, Francesca Tuorto, Hossein Ghanbarian, Frank Lyko, François Cuzin, and Minoo Rassoulzadegan. 2013a. “RNA-Mediated Epigenetic Heredity Requires the Cytosine Methyltransferase Dnmt2.” *PLoS Genetics* 9 (5): e1003498. doi:10.1371/journal.pgen.1003498.

Komara, Makanko, Aisha M Al-shamsi, Salma Ben-salem, and Bassam R Ali. 2015. “A Novel Single-Nucleotide Deletion (c . 1020delA) in NSUN2 Causes Intellectual Disability in an Emirati Child.” doi:10.1007/s12031-015-0592-8.

Krawetz, Stephen a. 2005a. “Paternal Contribution: New Insights and Future Challenges.” *Nature Reviews. Genetics* 6 (8): 633–42. doi:10.1038/nrg1654.

Krawetz, Stephen a, Adele Kruger, Claudia Lalancette, Rebecca Tagett, Ester Anton, Sorin Draghici, and Michael P Diamond. 2011. “A Survey of Small RNAs in Human Sperm.” *Human Reproduction (Oxford, England)* 26 (12): 3401–12. doi:10.1093/humrep/der329.

Kulis, Marta, and Manel Esteller. 2010. “DNA Methylation and Cancer.” *Advances in Genetics* 70 (10): 27–56. doi:10.1016/B978-0-12-380866-0.60002-2.

Kumar, Pankaj, and Suresh B Mudunuri. 2014. “Meta-Analysis of tRNA Derived RNA Fragments Reveals That They Are Evolutionarily Conserved and Associate with AGO Proteins to Recognize Specific RNA Targets.” doi:10.1186/s12915-014-0078-0.

Kwon, Changhyuk, Hyosun Tak, Mina Rho, Hae Ryung Chang, Yon Hui Kim, Kyung Tae Kim, Curt Balch, Eun Kyung Lee, and Seungyoon Nam. 2014. “Detection of PIWI and piRNAs in the Mitochondria of Mammalian Cancer Cells.” *Biochemical and Biophysical Research Communications* 446 (1). Elsevier Inc.: 218–23. doi:10.1016/j.bbrc.2014.02.112.

Langgut, W., and H. Kersten. 1990. “The Deazaguanine-Derivative, Queuine, Affects Cell Proliferation, Protein Phosphorylation and the Expression of the Proto Oncogenes c-Fos and c-Myc in HeLa Cells.” *FEBS Letters* 265 (1-2): 33–36. doi:10.1016/0014-5793(90)80877-L.

Lee, Yong Sun, Yoshiyuki Shibata, Ankit Malhotra, and Anindya Dutta. 2009. “A Novel Class of Small RNAs: tRNA-Derived RNA Fragments (tRFs).” *Genes & Development* 23 (22): 2639–49. doi:10.1101/gad.1837609.

Liebers, Reinhard, Minoo Rassoulzadegan, and Frank Lyko. 2014. “Epigenetic Regulation by Heritable RNA.” *PLoS Genetics* 10 (4): e1004296. doi:10.1371/journal.pgen.1004296.

Lillycrop, Karen a, Emma S Phillips, Christopher Torrens, Mark a Hanson, Alan a Jackson, and Graham C Burdge. 2008. “Feeding Pregnant Rats a Protein-Restricted Diet Persistently Alters the Methylation of Specific Cytosines in the Hepatic PPAR Alpha Promoter of the Offspring.” *The British Journal of Nutrition* 100 (2): 278–82. doi:10.1017/S0007114507894438.

Lim, Jana P, and Anne Brunet. 2013. “Bridging the Transgenerational Gap with Epigenetic Memory.” *Trends in Genetics : TIG* 29 (3). Elsevier Ltd: 176–86. doi:10.1016/j.tig.2012.12.008.

Liu, Nian, Qing Dai, Guanqun Zheng, Chuan He, Marc Parisien, and Tao Pan. 2015. “N6-Methyladenosine-Dependent RNA Structural Switches Regulate RNA–protein Interactions.” *Nature* 518 (7540). Nature Publishing Group: 560–64. doi:10.1038/nature14234.

Liu, Wei-Min, Ronald T K Pang, Philip C N Chiu, Benancy P C Wong, Kaiqin Lao, Kai-Fai Lee, and William S B Yeung. 2012. “Sperm-Borne microRNA-34c Is Required for the First Cleavage Division in Mouse.” *Proceedings of the National Academy of Sciences of the United States of America* 109 (2): 490–94. doi:10.1073/pnas.1110368109.

Lumey, L H, Aryeh D Stein, Henry S Kahn, and J A Romijn. 2009. “Lipid Profiles in Middle-Aged Men and Women after Famine Exposure during Gestation : The Dutch Hunger Winter Families Study 1 – 4.” doi:10.3945/ajcn.2008.27038.1.

Lumey, L H, Aryeh D Stein, Henry S Kahn, Karin M van der Pal-de Bruin, G J Blauw, Patricia a Zybert, and Ezra S Susser. 2007. “Cohort Profile: The Dutch Hunger Winter Families Study.” *International Journal of Epidemiology* 36 (6): 1196–1204. doi:10.1093/ije/dym126.

Lykke-andersen, Karin, Michael J Gilchrist, Joanna B Grabarek, Partha Das, Eric Miska, and Magdalena Zernicka-goetz. 2008. “Maternal Argonaute 2 Is Essential for Early Mouse Development at the Maternal-Zygotic Transition” 19 (October): 4383–92. doi:10.1091/mbc.E08.

Maden, B E, M E Corbett, P a Heeney, K Pugh, and P M Ajuh. 1995. “Classical and Novel Approaches to the Detection and Localization of the Numerous Modified Nucleotides in Eukaryotic Ribosomal RNA.” *Biochimie* 77 (1-2): 22–29. http://www.ncbi.nlm.nih.gov/pubmed/7599273.

Manolio, Teri a, Francis S Collins, Nancy J Cox, David B Goldstein, Lucia a Hindorff, David J Hunter, Mark I McCarthy, et al. 2009. “Finding the Missing Heritability of Complex Diseases.” *Nature* 461 (7265). Nature Publishing Group: 747–53. doi:10.1038/nature08494.

Marks, T, and W R Farkas. 1997. “Effects of a Diet Deficient in Tyrosine and Queuine on Germfree Mice.” *Biochemical and Biophysical Research Communications* 230 (2): 233–37. doi:10.1006/bbrc.1996.5768.

Martin, M. 2011. “Cutadapt Removes Adapter Sequences from High-Throughput Sequencing Reads.” *EMBnet.journal* 17 (1).

Martinez, Fernando Jose, Jeong Ho Lee, Ji Eun Lee, Sandra Blanco, Elizabeth Nickerson, Stacey Gabriel, Michaela Frye, Lihadh Al-Gazali, and Joseph G Gleeson. 2012. “Whole Exome Sequencing Identifies a Splicing Mutation in NSUN2 as a Cause of a Dubowitz-like Syndrome.” *Journal of Medical Genetics* 49 (6): 380–85. doi:10.1136/jmedgenet-2011-100686.

Metzker, Michael L. 2010. “Sequencing Technologies - the next Generation.” *Nature Reviews. Genetics* 11 (1). Nature Publishing Group: 31–46. doi:10.1038/nrg2626.

Meyer, Kate D, Yogesh Saletore, Paul Zumbo, Olivier Elemento, Christopher E Mason, and Samie R Jaffrey. 2012. “Resource Comprehensive Analysis of mRNA Methylation Reveals Enrichment in 3 0 UTRs and near Stop Codons.” *Cell* 149 (7). Elsevier Inc.: 1635–46. doi:10.1016/j.cell.2012.05.003.

Motorin, Y, S Muller, I Behm-Ansmant, and C Branlant. 2007. “Identification of Modified Residues in RNAs by Reverse-Transcription Based Methods.” *Methods in Enzymology* 425: 21–53.

Motorin, Yuri, and Mark Helm. 2011. “RNA Nucleotide Methylation.” doi:10.1002/wrna.79.

Motorin, Yuri, Frank Lyko, and Mark Helm. 2010. “5-Methylcytosine in RNA: Detection, Enzymatic Formation and Biological Functions.” *Nucleic Acids Research* 38 (5): 1415–30. doi:10.1093/nar/gkp1117.

Müller, Martin, Mark Hartmann, Isabelle Schuster, Sebastian Bender, Kathrin L. Thüring, Mark Helm, Jon R. Katze, Wolfgang Nellen, Frank Lyko, and Ann E. Ehrenhofer-Murray. 2015. “Dynamic Modulation of Dnmt2-Dependent tRNA Methylation by the Micronutrient Queuine.” *Nucleic Acids Research*, no. 14: gkv980. doi:10.1093/nar/gkv980.

Ng, Sheau-Fang, Ruby C Y Lin, D Ross Laybutt, Romain Barres, Julie a Owens, and Margaret J Morris. 2010. “Chronic High-Fat Diet in Fathers Programs B-Cell Dysfunction in Female Rat

Offspring." *Nature* 467 (7318). Nature Publishing Group: 963–66. doi:10.1038/nature09491.

Nigita, Giovanni, Dario Veneziano, and Alfredo Ferro. 2015. "A-to-I RNA Editing: Current Knowledge Sources and Computational Approaches with Special Emphasis on Non-Coding RNA Molecules." *Frontiers in Bioengineering and Biotechnology* 3 (March): 37. doi:10.3389/fbioe.2015.00037.

Ogawa, M. 1993. "Differentiation and Proliferation of Hematopoietic Stem Cells." *Blood* 81 (11): 2844–53. doi:10.1182/blood-2001-12-1234.

Okano, M, S Xie, and E Li. 1998. "Dnmt2 Is Not Required for de Novo and Maintenance Methylation of Viral DNA in Embryonic Stem Cells." *Nucleic Acids Research* 26 (11): 2536–40. http://www.pubmedcentral.nih.gov/articlerender.fcgi?artid=147598&tool=pmcentrez&rendertype=abstract.

Ostermeier, G Charles, David J Dix, David Miller, Purvesh Khatri, and Stephen A Krawetz. 2002. "Mechanisms of Disease Spermatozoal RNA Profiles of Normal Fertile Men," 772–77.

Ostermeier, G Charles, David Miller, John D Huntriss, Michael P Diamond, and Stephen A Krawetz. 2004. "Delivering Spermatozoan RNA to the Oocyte." *Nature* 429 (6988): 1 p following 154; discussion 2 p following 154. doi:10.1038/nature02603.

Ott, G, and H Kersten. 1985. "Differential Turnover of tRNAs of the Queuosine Family in Dictyostelium Discoideum and Its Possible Role in Regulation." *Biological Chemistry Hoppe-Seyler* 366 (1): 69–76.

Padilla, S L, a M Howe, and J P Boldt. 1988. "Effects of Charcoal-Extracted Serum as a Growth Medium Supplement on in Vitro Development of Mouse Embryos." *Journal of in Vitro Fertilization and Embryo Transfer : IVF* 5 (5): 286–89. doi:10.1007/BF01132179.

Painter, R C, C Osmond, P Gluckman, M Hanson, D I W Phillips, and T J Roseboom. 2008. "Transgenerational Effects of Prenatal Exposure to the Dutch Famine on Neonatal Adiposity and Health in Later Life." *BJOG : An International Journal of Obstetrics and Gynaecology* 115 (10): 1243–49. doi:10.1111/j.1471-0528.2008.01822.x.

Peng, Hongying, Junchao Shi, Ying Zhang, He Zhang, Shangying Liao, Wei Li, Li Lei, et al. 2012a. "A Novel Class of tRNA-Derived Small RNAs Extremely Enriched in Mature Mouse Sperm." *Cell Research*, 1–4. doi:10.1038/cr.2012.141.

Phalke, Sameer, Olaf Nickel, Diana Walluscheck, Frank Hortig, Maria Cristina Onorati, and Gunter Reuter. 2009. "Retrotransposon Silencing and Telomere Integrity in Somatic Cells

of Drosophila Depends on the Cytosine-5 Methyltransferase DNMT2." *Nature Genetics* 41 (6): 696–702. doi:10.1038/ng.360.

Phizicky, Eric M, and Anita K Hopper. 2010. "tRNA Biology Charges to the Front." *Genes & Development* 24 (17): 1832–60. doi:10.1101/gad.1956510.

Raddatz, Günter, Paloma M Guzzardo, Nelly Olova, Marcelo Rosado Fantappié, Markus Rampp, Matthias Schaefer, Wolf Reik, Gregory J Hannon, and Frank Lyko. 2013. "Dnmt2-Dependent Methylomes Lack Defined DNA Methylation Patterns." *Proceedings of the National Academy of Sciences of the United States of America* 110 (21): 8627–31. doi:10.1073/pnas.1306723110.

Rai, Kunal, Stephanie Chidester, Chad V Zavala, Elizabeth J Manos, Smitha R James, Adam R Karpf, David a Jones, and Bradley R Cairns. 2007. "Dnmt2 Functions in the Cytoplasm to Promote Liver, Brain, and Retina Development in Zebrafish." *Genes & Development* 21 (3): 261–66. doi:10.1101/gad.1472907.

Rassoulzadegan, Minoo, Valérie Grandjean, Pierre Gounon, Stéphane Vincent, Isabelle Gillot, and François Cuzin. 2006a. "RNA-Mediated Non-Mendelian Inheritance of an Epigenetic Change in the Mouse." *Nature* 441 (7092): 469–74. doi:10.1038/nature04674.

Reyniers, J. P., J. R. Pleasants, B. S. Wostmann, J. R. Katze, and W. R. Farkas. 1981. "Administration of Exogenous Queuine Is Essential for the Biosynthesis of the Queuosine-Containing Transfer RNAs in the Mouse." *Journal of Biological Chemistry* 256 (22): 11591–94.

Rodgers, Ali B, Christopher P Morgan, Stefanie L Bronson, Sonia Revello, and Tracy L Bale. 2013. "Paternal Stress Exposure Alters Sperm microRNA Content and Reprograms Offspring HPA Stress Axis Regulation." *The Journal of Neuroscience : The Official Journal of the Society for Neuroscience* 33 (21): 9003–12. doi:10.1523/JNEUROSCI.0914-13.2013.

Russell WMS, Burch KL. 1992. "The Principles of Humane Experimental Technique." *UFAW, London*, Available from: http://altweb. jhsph.edu/.

Schaefer, Matthias, and Frank Lyko. 2010a. "Solving the Dnmt2 Enigma." *Chromosoma* 119 (1): 35–40. doi:10.1007/s00412-009-0240-6.

Schaefer, Matthias, Tim Pollex, Katharina Hanna, and Frank Lyko. 2009. "RNA Cytosine Methylation Analysis by Bisulfite Sequencing" 37 (2). doi:10.1093/nar/gkn954.

Schaefer, Matthias, Tim Pollex, Katharina Hanna, Francesca Tuorto, Madeleine Meusburger, Mark Helm, and Frank Lyko. 2010a. "RNA Methylation by Dnmt2 Protects Transfer RNAs against Stress-Induced Cleavage Service RNA Methylation by Dnmt2 Protects Transfer RNAs against Stress-Induced Cleavage," 1590–95. doi:10.1101/gad.586710.

Seisenberger, Stefanie, Julian R Peat, and Wolf Reik. 2013. “Conceptual Links between DNA Methylation Reprogramming in the Early Embryo and Primordial Germ Cells.” *Current Opinion in Cell Biology* 25 (3). Elsevier Ltd: 281–88. doi:10.1016/j.ceb.2013.02.013.

Sen, Arko, Nicole Heredia, Marie-Claude Senut, Susan Land, Kurt Hollocher, Xiangyi Lu, Mary O. Dereski, and Douglas M. Ruden. 2015. “Multigenerational Epigenetic Inheritance in Humans: DNA Methylation Changes Associated with Maternal Exposure to Lead Can Be Transmitted to the Grandchildren.” *Scientific Reports* 5 (January). Nature Publishing Group: 14466. doi:10.1038/srep14466.

Shanmugam, Raghuvaran, Jacob Fierer, Steffen Kaiser, Mark Helm, Tomasz P Jurkowski, and Albert Jeltsch. 2015. “Cytosine Methylation of tRNA-Asp by DNMT2 Has a Role in Translation of Proteins Containing Poly-Asp Sequences.” *Cell Discovery* 1 (June): 15010. doi:10.1038/celldisc.2015.10.

Siard, T. J., K. B. Jacobson, and W. R. Farkas. 1991. “Queuine Metabolism and Cadmium Toxicity in Drosophila Melanogaster.” *Biofactors* 3 (1): 41–47.

Sobala, Andrew, and Gyorgy Hutvagner. 2013. “Small RNAs Derived from the 5 ’ End of tRNAs Can Inhibit Protein Translation in Human Cells,” no. April: 1–11.

Song, Rui, Grant W Hennig, Qiuxia Wu, Charlie Jose, Huili Zheng, and Wei Yan. 2011. “Male Germ Cells Express Abundant Endogenous siRNAs.” *Proceedings of the National Academy of Sciences of the United States of America* 108 (32): 13159–64. doi:10.1073/pnas.1108567108.

Squires, Jeffrey E, Hardip R Patel, Marco Nousch, Tennille Sibbritt, David T Humphreys, Brian J Parker, Catherine M Suter, and Thomas Preiss. 2012. “Widespread Occurrence of 5-Methylcytosine in Human Coding and Non-Coding RNA.” *Nucleic Acids Research* 40 (11): 5023–33. doi:10.1093/nar/gks144.

Suh, Nayoung, and Robert Blelloch. 2011. “Small RNAs in Early Mammalian Development: From Gametes to Gastrulation.” *Development (Cambridge, England)* 138 (9): 1653–61. doi:10.1242/dev.056234.

Svoboda, Petr, and Matyas Flemr. 2010. “The Role of miRNAs and Endogenous siRNAs in Maternal-to-Zygotic Reprogramming and the Establishment of Pluripotency.” *EMBO Reports* 11 (8): 590–97. doi:10.1038/embor.2010.102.

Tam, Oliver H, Alexei a Aravin, Paula Stein, Angelique Girard, Elizabeth P Murchison, Sihem Cheloufi, Emily Hodges, et al. 2008. “Pseudogene-Derived Small Interfering RNAs Regulate Gene Expression in Mouse Oocytes.” *Nature* 453 (7194): 534–38. doi:10.1038/nature06904.

Teerds, K J, D G De Rooij, F F Rommerts, I van der Tweel, and C J Wensing. 1989. “Turnover Time of Leydig Cells and Other Interstitial Cells in Testes of Adult Rats.” *Archives of Andrology* 23 (2): 105–11. doi:10.3109/01485018908986831.

Thomson, D. W., K. a. Pillman, M. L. Anderson, D. M. Lawrence, J. Toubia, G. J. Goodall, and C. P. Bracken. 2014. “Assessing the Gene Regulatory Properties of Argonaute-Bound Small RNAs of Diverse Genomic Origin.” *Nucleic Acids Research* 43 (1): 470–81. doi:10.1093/nar/gku1242.

Tobi, Elmar W, P Eline Slagboom, Jenny van Dongen, Dennis Kremer, Aryeh D Stein, Hein Putter, Bastiaan T Heijmans, and L H Lumey. 2012. “Prenatal Famine and Genetic Variation Are Independently and Additively Associated with DNA Methylation at Regulatory Loci within IGF2/H19.” *PloS One* 7 (5): e37933. doi:10.1371/journal.pone.0037933.

Torres, Adrian Gabriel, David Piñeyro, Liudmila Filonava, Travis H. Stracker, Eduard Batlle, and Lluis Ribas de Pouplana. 2014. “A-to-I Editing on tRNAs: Biochemical, Biological and Evolutionary Implications.” *FEBS Letters* 588 (23). Federation of European Biochemical Societies: 4279–86. doi:10.1016/j.febslet.2014.09.025.

Trapnell, Cole, David G Hendrickson, Martin Sauvageau, Loyal Goff, John L Rinn, and Lior Pachter. 2013. “Differential Analysis of Gene Regulation at Transcript Resolution with RNA-Seq.” *Nature Biotechnology* 31 (1). Nature Publishing Group: 46–53. doi:10.1038/nbt.2450.

Trapnell, Cole, Lior Pachter, and Steven L Salzberg. 2009. “TopHat: Discovering Splice Junctions with RNA-Seq.” *Bioinformatics (Oxford, England)* 25 (9): 1105–11. doi:10.1093/bioinformatics/btp120.

Tuorto, Francesca, Friederike Herbst, Nader Alerasool, Sebastian Bender, Oliver Popp, Giuseppina Federico, Sonja Reitter, Reinhard Liebers, Georg Stoecklin, Hermann-josef Gröne, Gunnar Dittmar, Hanno Glimm, and Frank Lyko. 2015. “The tRNA Methyltransferase Dnmt 2 Is Required for Accurate Polypeptide Synthesis during Haematopoiesis,” 1–13.

Tuorto, Francesca, Reinhard Liebers, Tanja Musch, Matthias Schaefer, Sarah Hofmann, Stefanie Kellner, Michaela Frye, Mark Helm, Georg Stoecklin, and Frank Lyko. 2012a. “RNA Cytosine Methylation by Dnmt2 and NSun2 Promotes tRNA Stability and Protein Synthesis.” *Nature Structural & Molecular Biology*, no. August. Nature Publishing Group: 1–7. doi:10.1038/nsmb.2357.

Waddington, C. H. 1942. “The Epigenotype. 1942.” *Endeavour*, 18–20. doi:10.1093/ije/dyr184.

Walser, Claudia B, and Howard D Lipshitz. 2011. “Transcript Clearance during the Maternal-to-Zygotic Transition.” *Current Opinion in Genetics & Development* 21 (4). Elsevier Ltd: 431–43. doi:10.1016/j.gde.2011.03.003.

Warnecke, Peter M, Clare Stirzaker, Jenny Song, Christoph Grunau, John R Melki, and Susan J Clark. 2002. “Identification and Resolution of Artifacts in Bisulfite Sequencing” 27: 101–7.

Watanabe, Toshiaki, Shin-ichi Tomizawa, Kohzoh Mitsuya, Yasushi Totoki, Yasuhiro Yamamoto, Satomi Kuramochi-Miyagawa, Naoko Iida, et al. 2011. “Role for piRNAs and Noncoding RNA in de Novo DNA Methylation of the Imprinted Mouse Rasgrf1 Locus.” *Science (New York, N.Y.)* 332 (6031): 848–52. doi:10.1126/science.1203919.

Watanabe, Toshiaki, Yasushi Totoki, Atsushi Toyoda, Masahiro Kaneda, Satomi Kuramochi-Miyagawa, Yayoi Obata, Hatsune Chiba, et al. 2008. “Endogenous siRNAs from Naturally Formed dsRNAs Regulate Transcripts in Mouse Oocytes.” *Nature* 453 (7194): 539–43. doi:10.1038/nature06908.

Weaver, Ian C G, Nadia Cervoni, Frances A Champagne, Ana C D Alessio, Shakti Sharma, Jonathan R Seckl, Sergiy Dymov, Moshe Szyf, and Michael J Meaney. 2004. “Epigenetic Programming by Maternal Behavior” 7 (8): 847–54. doi:10.1038/nn1276.

Wilkinson, D G. 1998. *In Situ Hybridization: A Practical Approach*.

Xi, Yuanxin, and Wei Li. 2009. “BSMAP: Whole Genome Bisulfite Sequence MAPping Program.” *BMC Bioinformatics* 10 (January): 232. doi:10.1186/1471-2105-10-232.

Yadlapalli, Swathi, and Yukiko M Yamashita. 2013. “Chromosome-Specific Nonrandom Sister Chromatid Segregation during Stem-Cell Division.” *Nature* 498 (7453). Nature Publishing Group: 251–54. doi:10.1038/nature12106.

Yamasaki, Satoshi, Pavel Ivanov, Guo Fu Hu, and Paul Anderson. 2009. “Angiogenin Cleaves tRNA and Promotes Stress-Induced Translational Repression.” *Journal of Cell Biology* 185 (1): 35–42. doi:10.1083/jcb.200811106.

Yuan, Shuiqiao, Daniel Oliver, Andrew Schuster, Huili Zheng, and Wei Yan. 2015a. “Breeding Scheme and Maternal Small RNAs Affect the Efficiency of Transgenerational Inheritance of a Paramutation in Mice.” *Scientific Reports* 5: 9266. doi:10.1038/srep09266.

Zaborske, John M., Vanessa L. Bauer DuMont, Edward W. J. Wallace, Tao Pan, Charles F. Aquadro, and D. Allan Drummond. 2014. “A Nutrient-Driven tRNA Modification Alters Translational Fidelity and Genome-Wide Protein Coding across an Animal Genus.” *PLoS Biology* 12 (12): e1002015. doi:10.1371/journal.pbio.1002015.

Zemach, Assaf, Ivy E Mcdaniel, Pedro Silva, and Daniel Zilberman. 2010. “Genome-Wide Evolutionary Analysis of Eukaryotic DNA Methylation” 11928 (May 2008).

Acknowledgements

I feel privileged to have been able to carry out my PhD project in Prof. Dr. Frank Lyko's lab at the DKFZ. I would first of all like to thank Frank for this great opportunity and also for his continuous support, advice, and supervision throughout my project, and most of all for always taking time for my inquiries.

*****

I have also had the pleasure of working with Dr. Francesca Tuorto, who has relentlessly given her all to motivate me, assist me, and pitch me promising experiments. A heartfelt thank you goes to you!

*****

I would like to thank Prof. Dr. Frank Lyko, PD Dr. Dieter Weichenhan, and Dr. Brian Luke for being members of my TAC.

*****

My sincere thank you goes to Prof. Dr. Frank Lyko, to Dr. Brian Luke, to Dr. Sylvia Erhardt, and to Dr. Tamás Fischer for taking the time to be my examiners.

*****

I am grateful for all the lively discussions and great tips and hints I got from Francesca, Mark, Sim, Dr. Matthias Schäfer, Prof. Dr. Jon Katze, and many others. Thank you Mark, Sim, and Francesca for reading everything from random thoughts to rough drafts and final versions.

*****

I am truly indebted to my colleagues and friends in lab. You made me feel welcome, supported me, and gave me a wonderful working environment. I especially thank Laura and Nader for support.

*****

I thank my incredible friends and my family for fueling me with motivation and love. I thank Mark, Sim, Derek, Asrar, and Phivos for being absolute legends. I thank Lukas, my good ol' Captain Ben, my little Captain Lille, Michi, Manu, and Judy. I thank my grandparents, Mom, Dad, Regina, Jakob – you are my rock solid foundation and my safe haven.

*****

I dedicate this thesis to the ones who make my world go 'round – my family and friends.